THE JOURNAL
OF
CHEMICAL PHYSICS

VOLUME 16, NUMBER 6 JUNE, 1948

The Photo-Chemical Decomposition of Acetone at 3130A*

LEON M. DORFMAN AND W. ALBERT NOYES, JR.
Department of Chemistry, University of Rochester, Rochester, New York

(Received March 15, 1948)

The photo-chemical decomposition of gaseous acetone in light of 3130A has been investigated at 26°C under conditions of high acetone pressure and low absorbed light intensities. The ratio C_2H_6/CO has been found to decrease substantially below unity at sufficiently low absorbed intensities, under which condition methane has been found as a major product, exceeding the amount of ethane at very low intensities. A kinetic analysis of these data has shown that only a free radical process for the formation of ethane and methane suffices to explain the experimental observations. The energy of activation for the reaction of a methyl radical with an acetone molecule to form methane has been determined as $E=6.5$ kcal./mole.

ALTHOUGH many investigations of the photo-chemical decomposition of acetone have been reported, completely unequivocal conclusions regarding several aspects of this reaction remain impossible. Particularly in the region of "banded absorption" about 3000A and above, the need for more data to permit an evaluation of the excited molecule mechanism proposed by Spence and Wild[1] was apparent.

Previous workers[2] have reported that the ratio of ethane to carbon monoxide in the products approaches a lower limiting value of unity with decreasing absorbed intensity and with increasing pressure of acetone. Differences in the experimental values of the C_2H_6/CO ratio reported by Spence and Wild[1] and by Herr and Noyes[2] led to a reinvestigation of the intensity dependence of the acetone decomposition. Davis[3] has reported recently that the amount of methane formed at temperatures over 100°C may be quite large, and Spence and Wild[1] have shown that methane formation may be quite important at high pressures even at room temperature. A complete survey of the literature through 1946 has been made by Davis.[4]

This paper presents the results of experiments in which the absorbed intensity has been carried to a considerably lower range than has normally been employed in the photochemical decomposition of acetone.

EXPERIMENTAL

Two types of mercury arc lamp were used as the source of radiation: a Hanovia U A30 A2 medium pressure arc; a General Electric Company AH-6 high pressure arc. The filters used to provide monochromatic illumination with 3130A have been described.[5] The equations for the

* This work was supported by Contract N6onr-241, Task I, with the Office of Naval Research, United States Navy.

[1] R. Spence and W. Wild, J. Chem. Soc., 352 (1937); 590 (1941).

[2] D. S. Herr and W. A. Noyes, Jr., J. Am. Chem. Soc. 62, 2052 (1940).

[3] W. Davis, Jr., J. Am. Chem. Soc., in press.

[4] W. Davis, Jr., Chem. Rev. 40, 201 (1947).

[5] R. E. Hunt and W. Davis, Jr., J. Am. Chem. Soc. 69, 1415 (1947).

TABLE I.

Run no.	Temperature °C	Pressure mm	Absorbed intensity q/sec./cc $\times 10^{-12}$	Fraction of gaseous products CO	C_2H_6	CH_4	$\frac{C_2H_6}{CO}$	$\frac{\Phi_{CH_4}}{\Phi_{C_2H_6}^{\frac{1}{2}}}$
8*	26.6	158.7	3.74	0.398	0.450	0.152	1.13	0.0834
7*	27.8	153.6	3.68	0.487	0.401	0.112	0.82	0.0665
2a, b	25.5	153.0	0.610	0.402	0.383	0.215	0.95	0.165
1	25.9	155.2	0.311	0.449	0.328	0.223	0.73	0.189
3	26.5	159.5	0.194	0.427	0.293	0.279	0.69	0.289
6	26.1	158.7	0.114	0.416	0.210	0.374	0.51	0.437

* AH-6 arc.

TABLE II.

Run no.	Temperature °C	Pressure mm	Absorbed intensity q/sec./cc $\times 10^{-12}$	Fraction of gaseous products CO	C_2H_6	CH_4	$\frac{\Phi_{CH_4}}{\Phi_{C_2H_6}^{\frac{1}{2}}}$
9*	121.9	117.4	2.86	0.500	0.297	0.204	0.529
4b	121.2	107.2	0.203	0.434	0.114	0.458	2.07
4a	121.8	107.4	0.201	0.407	0.101	0.492	2.43
11	123.2	123.2	0.0875	0.439	0.077	0.485	2.66
12	122.9	115.1	0.0743	0.402	0.067	0.531	3.22

* AH-6 arc.

calculation of absorbed intensity have been presented in detail.[6,7]

The light intensity was reduced where necessary, by inserting in the light path additional filters of Corning No. 9863 glass, and, in the run with the lowest absorbed intensity, by interposing a thin-blown Pyrex window.

The photo-chemical decomposition of acetone itself was used as an actinometer, since it has been shown by various workers[2,8] that the quantum yield of carbon monoxide in this photolysis is unity at temperatures slightly in excess of 100°C.

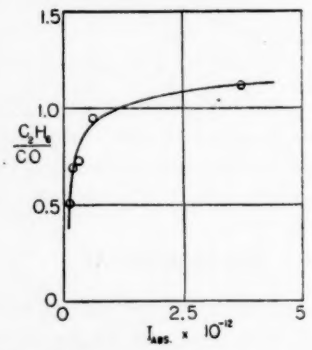

FIG. 1. The effect of absorbed intensity (quanta/cm³/sec. in the light beam) on the ratio of ethane to carbon monoxide during photo-chemical decomposition of acetone at 26°C and pressure of 156 mm. $\lambda = 3130$A.

The reaction vessel consisted of a cylindrical quartz cell, 200 mm in length and 22 mm in inside diameter. The light beam obtained from the U A30 A2 arc was parallel with a diameter of 15 mm, and consequently provided an illuminated volume of 35.4 cc. The AH-6 arc provided a slightly divergent beam with an incident cross section of 1.97 cm² and an emergent cross section of 2.39 cm² and, hence, an illuminated volume of 43.6 cc. The absorbed light intensity is expressed in quanta per second per cm³ of illuminated volume. It has been assumed that the absorbed intensity is uniform over the entire path length. The inaccuracy in this assumption is serious only at high percentage absorption.

Reagent acetone was purified by distillation in a 35-plate column, the middle third being retained, then dried over anhydrous copper sulfate. The gaseous products, CO, CH_4, and C_2H_6 were completely removed at -135°C using a Ward apparatus and Toepler pump. The products were analyzed by combustion on a hot platinum wire and in some experiments by combustion on hot copper oxide as well. These methods have been described by various authors.[2,7,9]

[6] R. E. Hunt and T. L. Hill, J. Chem. Phys. **15**, 111 (1947).
[7] W. Davis, Jr. and W. A. Noyes, Jr., J. Am. Chem. Soc. **69**, 2153 (1947).
[8] J. A. Leermakers, J. Am. Chem. Soc. **56**, 1899 (1934); C. A. Winkler, Trans. Faraday Soc. **31**, 761 (1935).
[9] W. M. Manning, J. Am. Chem. Soc. **56**, 2589 (1934).

RESULTS AND DISCUSSION

The results which are recorded in the following tables are for runs which have been carried out at sufficiently high acetone pressures to ensure that wall reactions play only a negligible role. The homogeneity of the elementary reactions which occur is accepted as the basis for the theoretical considerations which follow. The validity of this assumption is established by the curves for C_2H_6/CO as a function of pressure obtained by Herr and Noyes[2] and by the work of Howland and Noyes.[10] The value of this ratio falls off sharply below 60 mm, but undergoes no profound change as the acetone pressure is increased above 100 mm.

Table I consists of the runs at room temperature, in which the absorbed intensity has been varied over a 32-fold range. Table II contains the runs carried out at 122°C, in which the absorbed light intensity has been varied 38-fold.

As may be seen in Table I, the value of the ratio C_2H_6/CO falls well below unity with decreasing absorbed intensity, and does not have a lower limiting value of unity as has previously been supposed. The curve of this quantity as a function of absorbed intensity is shown in Fig. 1. Similarly, a plot of C_2H_6/CO against acetone pressure would seem to result in a family of curves, each member of which approaches a lower limit as the pressure is increased. This lower limit for each individual member depends upon the intensity parameter, and falls well below unity at low intensities. This is shown in Fig. 2.

Methane becomes an important product at low intensities, and, in fact, at sufficiently low values of absorbed intensity, exceeds the amount of ethane in the products. It is clear then that the conclusion reached by Spence and Wild,[1] that at high pressures the single step decomposition of an activated molecule to form ethane and carbon monoxide is the most important process, cannot be correct.

Ethane may be formed by the recombination of methyl radicals:

$$CH_3+CH_3=C_2H_6;\ k_1(CH_3)^2. \qquad (1)$$

At the high experimental pressures used, this reaction is homogeneous. Methane may be formed by the removal of a hydrogen atom from acetone by a methyl radical:

$$CH_3+CH_3COCH_3=CH_4+CH_2COCH_3;\ k_2(CH_3)(CH_3COCH_3). \qquad (2)$$

If reactions (1) and (2) represent the sole modes of formation of ethane and methane, respectively, the quantum yields of these products will be related by the following equation:

$$\Phi_{CH_4}/\Phi_{C_2H_6}^{\frac{1}{2}}=(k_2/k_1^{\frac{1}{2}})(\text{Acetone}/I_a^{\frac{1}{2}}). \qquad (3)$$

Figure 3 shows a plot of $\Phi_{CH_4}/\Phi_{C_2H_6}^{\frac{1}{2}}$ as a function of $(Ac)/I_a^{\frac{1}{2}}$. The curve which results, a straight line through the origin, establishes the validity of reactions (1) and (2).

The acetonyl radicals may be disposed of by the formation of methyl ethyl ketone:[11]

$$CH_3+CH_2COCH_3=CH_3CH_2COCH_3;\ k_3(CH_3)(CH_2COCH_3), \qquad (4)$$

and by their combination to form acetonyl

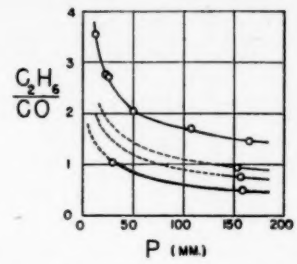

FIG. 2. The effect of pressure on the ratio of ethane to carbon monoxide during the photo-chemical decomposition of acetone at 26°C. The upper curve is from Herr and Noyes.[2]

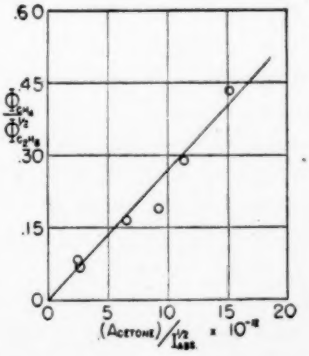

FIG. 3. A plot of Eq. (3) at 26°C.

[10] J. J. Howland, Jr. and W. A. Noyes, Jr., J. Am. Chem. Soc. 66, 974 (1944).

[11] A. O. Allen, J. Am. Chem. Soc. 63, 708 (1941).

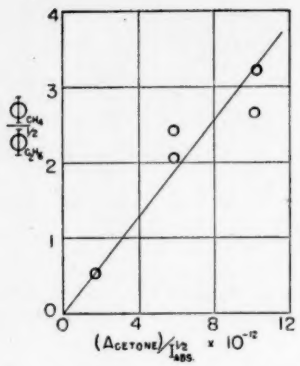

FIG. 4. A plot of Eq. (3) at 122°C.

acetone:

$$CH_2COCH_3+CH_2COCH_3 = (CH_2COCH_3)_2;\ k_4(CH_2COCH_3)^2. \quad (5)$$

This compound has been identified by Rice, Rodowskas, and Lewis[12] as a product in the reaction of methyl radicals with acetone at 350°C.

The slope of the straight line in Fig. 3 gives $k_2/k_1^{\frac{1}{2}}=2.70\times10^{-14}$ at 26°C. Figure 4 gives $k_2/k_1^{\frac{1}{2}}=3.19\times10^{-13}$ at 122°C. Writing $k_2=a_2e^{-E_2/RT}$ and $k_1=a_1e^{-E_1/RT}$, these values may be used to calculate $E_2-\frac{1}{2}E_1=5700$ cal. per mole. The $T^{\frac{1}{2}}$ factor in the pre-exponential term has been taken into account in this calculation. Taking the value of Cunningham and Taylor[13] for reaction (1), $E_1<1.5$ kcal./mole, gives

$$E_2=6500 \text{ calories per mole.}$$

This value is only slightly lower than the value of 7.1 kcal. mole obtained by Allen.[11]

[12] F. O. Rice, E. L. Rodowskas, and W. R. Lewis, J. Am. Chem. Soc. **56**, 2497 (1934).
[13] J. P. Cunningham, and H. S. Taylor, J. Chem. Phys. **6**, 359 (1938).

THE JOURNAL OF CHEMICAL PHYSICS VOLUME 16, NUMBER 6 JUNE, 1948

Thermodynamic Properties of the Internal Rotator. Double Minimum with Attractive Forces

J. O. HALFORD
Department of Chemistry, University of Michigan, Ann Arbor, Michigan

(Received March 22, 1948)

A previously outlined general method of calculating thermodynamic properties for an unsymmetrical internal rotation is applied to a double minimum with attractive forces, for which the potential energy has two maxima at the same height and two minima at different heights. The entropy is lower than that of the system of two equal potential valleys or that for a single valley, and can be lower than the former by as much as $R\ln 2$ when the potential barriers are high. This decrease tends to disappear in the region of close approach to free rotation, when the barriers are lower than RT. For very high potential barriers, if one of two equal minima is raised, the system acquires the properties of a simple harmonic oscillator.

IN a recent paper[1] it was shown that graphical old quantum-theory action integrals could be used to obtain mean positions of the energy levels of the symmetrical internal rotator from which the contributions of the internal rotation to the thermodynamic properties could be closely approximated. More recently[2] a scheme has been proposed for applying the old quantum theory when the rotation is not symmetrical. By assuming for the potential energy function a succession of linked sections of simple cosine curve, it is possible to use the graphical integrations carried out for the symmetrical rotator to evaluate the properties of the unsymmetrical system. The results of these integrations are contained in a table (Table II, reference 2) showing ρ, a quantum-number index, as a function of E/V, the ratio of the energy to the barrier height when the zero of energies is placed at the bottom of the potential valley. For a rotation or vibration through the region above one or more potential minima, a new quantum-

[1] J. O. Halford, J. Chem. Phys. **15**, 645 (1947).
[2] J. O. Halford, J. Chem. Phys. **16**, 410 (1948).

number index $\Re$ is given by the equation

$$\Re=\sum(\rho_i/a_i)(V_i/V_0)^{\frac{1}{2}}/2=r/[Q_f(V_0/RT)^{\frac{1}{2}}] \quad (1)$$

in which r is the quantum number, Q_f is the limiting partition function for free rotation, ρ_i is taken from the table at the selected value of E_i/V_i at which $\Re$ is sought, $a_i=a_0V_0/V_i$, and $\sum 1/a_i=2$ for the complete rotational cycle. The summation includes two terms for each potential valley in which, or above which, the vibration or rotation occurs. A relation between $\Re$ and E/V_0 is then set up, which by Eq. (1) permits the selection of ratios E/V_0 for any assigned set of quantum numbers r.

The establishment of the quantum-number index as a function of E/V_0 by the old quantum theory can be done in only one way for a given potential energy function. There is some latitude of choice, however, in the selection of quantum numbers for the representative mean positions of the energy levels, and this latitude will lead to uncertainties in the thermodynamic properties under certain limiting conditions. In calculations with the symmetrical rotator, it is possible to find the rules of assignment which will reproduce properties calculated by more rigorous methods.[1,3] When the rotator is unsymmetrical, however, there is no more rigorous solution available for comparison, and it becomes necessary to assume that an assignment of quantum numbers consistent with experience acquired with the symmetrical rotator will yield accurate results. When this experience cannot be applied unequivocally, the positions of some of the states will be in doubt.

For this reason, and because the method is an approximation based upon a postulate of limited validity, there will be regions of the variables V_i, T, and Q_f, in which accurate thermodynamic properties cannot be calculated. This is true to some degree of any method of evaluating these properties, and the practical question for any one method is whether molecules exist that have properties falling outside the region of accurate calculation.

The limitations of the proposed approximation are not obvious from superficial examination, but they should become apparent as the attempt to apply the method is made. The chosen approach to an understanding of these limits has been first, to find the conditions necessary for the accurate calculation of the known properties of the symmetrical rotator, second, to apply the general method for the unsymmetrical rotator to a double minimum with repulsive forces for which two unequal potential maxima occur between minima at the same level, and third, to study the double minimum with attractive forces where the maxima are at the same height but one minimum lies above the other. The first two of these studies appear in earlier publications. The third is the basis for the present paper.

The conditions sufficient to reproduce the n-fold symmetrical rotator properties are:

(1) Each nth rotational pair, as identified by the quantum numbers of the limiting free rotator, is counted.

(2) Quantization is performed over the entire rotational cycle and half the vibrational cycle. The vibrational states are placed at the positions $r\pm\frac{1}{4}$, the rotational states at $r\pm V/4E$, where r is an integer, V is the barrier height, and E is the energy at the mean position r.

(3) When a pair of states is split across the potential maximum, the upper component is so placed that the mean quantum number is an integer.

(4) When fewer than three states lie below the maximum, they are adjusted downward empirically to keep the partition function below its limiting value for free rotation.

With suitable modifications, but without essential changes, these conditions are applicable to the double minimum with repulsive forces:

(1) All states as identified by their quantum numbers in the free rotation limit are counted.

(2) For quantization over the whole rotational cycle and half the vibrational cycles, the states are placed at $r\pm\frac{1}{4}$ below the lower maximum, at $r\pm(\frac{1}{4}+V_2/4E)$ between the maxima and at $r\pm(V_1+V_2)/4E$ in the rotational region. Here V_1 is the higher barrier. Below the lower maximum the states have double weight.

(3) The average position of the pairs is again maintained at integral values of the quantum number.

(4) When fewer than three vibrational states occur within a potential valley, below the lower

[3] K. S. Pitzer and W. D. Gwinn, J. Chem. Phys. **10**, 428 (1942).

TABLE I. Thermodynamic properties of the double minimum internal rotator with attractive forces (cal./mole/degree).

V_1 / RT	V_2 / V_1	$1/Q_f$	0.05		0.10			0.20			0.30			0.40		
		$-F/T$	H/T	S	$-F/T$	H/T	S	$-F/T$	H/T	S	$-F/T$	H/T	S	$-F/T$	H/T	S
1	1	5.25	1.58	6.83	4.03	1.42	5.45									
	¾	5.11	1.74	6.84	3.88	1.59	5.47									
	½	5.03	1.80	6.83	3.78	1.68	5.46		X			X			X	
	¼	5.04	1.78	6.82	3.77	1.67	5.44									
	0	5.17	1.66	6.83	3.88	1.58	5.45									
4	1	3.96	1.86	5.82	2.90	1.58	4.48	2.09	1.12	3.21						
	¾	3.36	2.40	5.76	2.27	2.11	4.38	1.41	1.72	3.14						
	½	3.26	2.30	5.57	2.06	2.11	4.17	1.20	1.69	2.89		X			X	
	¼	3.44	2.12	5.56	2.26	1.93	4.19	1.27	1.58	2.85						
	0	3.79	2.02	5.81	2.58	1.86	4.44	1.51	1.58	3.09						
9	1	3.20	1.58	4.78	2.28	1.20	3.47	1.68	0.66	2.34	1.50	0.36	1.86			
	¾	2.20	2.03	4.22	1.22	1.67	2.89	0.55	1.15	1.70	0.34	0.84	1.18			
	½	2.32	1.79	4.11	1.27	1.44	2.71	0.52	0.96	1.48	0.25	0.63	0.88		X	
	¼	2.58	1.66	4.24	1.50	1.48	2.98	0.66	1.04	1.70	0.34	0.72	1.06			
	0	2.96	1.81	4.77	1.82	1.58	3.41	0.90	1.20	2.10	0.50	0.89	1.40			
16.	1	2.76	1.40	4.16	1.96	0.94	2.90	1.52	0.39	1.91				1.39	0.06	1.45
	¾	1.59	1.57	3.16	0.70	1.18	1.87	0.22	0.61	0.83				0.05	0.22	0.26
	½	1.82	1.53	3.54	0.89	1.15	2.09	0.28	0.62	0.99		X		0.04	0.15	0.19
	¼	2.09	1.60	3.69	1.09	1.27	2.36	0.40	0.76	1.16				0.07	0.24	0.32
	0	2.44	1.69	4.13	1.38	1.41	2.79	0.58	0.94	1.52				0.14	0.39	0.53

maximum, they are adjusted downward empirically by means of the same equation that was used for the symmetrical rotator. The adjustment is made separately, however, for each of the two unequal sides of the valley, and the mean of the two adjustments so obtained is applied.

For the double minimum with attractive forces it is no longer possible to meet all these conditions clearly:

(1) The number of states counted, in relation to the free rotator, is the same as for the double minimum with repulsive forces.

(2) This condition is met in the same manner as before.

(3) If the number of states below the potential maxima is even, the lowest rotational state will be the upper component of a pair, but there is no way to identify one of the vibrational states as the lower component. The scale of quantum numbers for the rotational region, however, can be projected below the potential maxima, and, if the rotational component is set at $r+\frac{1}{4}$, the location will be consistent with that used in the two cases previously considered. The effect of errors made by considerable shifts in the position of this state is negligible in all of the calculations summarized below.

(4) Downward adjustment for fewer than three states in the more shallow valley cannot be made by the empirical equation heretofore used because this equation would place the last state, as the lesser potential barrier approached zero, incorrectly at exactly the position of the potential maxima. It is found, however, within the limits of Table I that the adjustment can be neglected without introducing serious errors. The energies of the states in question are such that they may be lowered, by amounts larger than the empirical corrections previously made, without significant effects upon the thermodynamic properties.

It works out, then, that some doubt exists about the representative mean positions of the energy states in shallow valleys or immediately above the potential maxima. A limitation is thus placed upon the accurate application of the proposed approximate method for calculating the thermodynamic properties of the general unsymmetrical internal rotator, but from the cases thus far considered it appears that errors from these sources will not seriously interfere, in general, with the use of the method. At least there should be many potential energy functions for real molecules which will permit accurate evaluations by the scheme under consideration.

As a first step in resolving the questions just raised it would be useful to have a way to identify

each state of the hindered rotator with an individual level of the limiting free rotator system. Such an identification appears to have meaning because below any energy for which the effect of the hindering potential is negligible, the number of states is independent of the detail of the potential energy curve. If the restricting potential is slowly diminished, whether the relative positions of the maxima are maintained or not, the levels will rise in the valleys and escape into the rotational region, finally fitting themselves into the free rotator system of states. Presumably, then, each level of a restricted rotator could be labeled according to the place it would take in free rotation if the barrier were removed.

The identification can be made for the symmetrical rotator or for the unsymmetrical rotator with equivalent valleys that are identical or reflecting in character. When the two valleys are different, however, the labeling of the states is not clearly indicated. If the barrier system is diminished to zero without changing its shape, the levels will retain, at least approximately, their relative positions on the scale of energies. If, however, one barrier is first removed by raising a minimum, the levels in one valley will be poured into the neighboring valley in inverse order, and, when the second barrier is subsequently diminished, will retain this new order into the free rotation limit.

It appears, then, that there is no way to determine what limit is approached in the single minimum system by a state in the secondary valley as this valley is eliminated by raising its minimum. Likewise, for a rotational doublet divided across the potential maximum, it is not clear which vibrational state is a component of the pair. By trial, the location $r-\frac{1}{4}$, which follows from the position of the upper component at $r+\frac{1}{4}$, is a weighted mean of the positions of the uppermost states in the two valleys.

For the double minimum with attractive forces, calculations of the free energy $(-F/T)$, the heat content (H/T), and the entropy (S) have been made for five barrier ratios (V_2/V_1) at each of several representative combinations of the variables $1/Q_f$ and V_1/RT. The results are summarized in Table I. When the barriers are equal, the properties are taken from the tables of Pitzer and Gwinn at $2/Q_f$, V/RT, and the entropy and free energy $(-F/T)$ are increased by $R\ln 2$, with R taken to be 1.9869. For $V_2=0$, the single minimum limit, the values are taken directly from the tables at $1/Q_f$, V/RT. For each of the remaining three barrier ratios the relation between $\mathfrak{R}$ and E/V_1 has been set up and interpreted according to Eq. (1) to obtain the permitted values of the ratio E/V_1 for use in determining the thermodynamic properties. In this connection, the energy ratios for the two valleys are related according to the equation

$$E_2/V_2=1-(V_1/V_2)(1-E_1/V_1). \qquad (2)$$

When $V_1=RT$ the entropy is for practical purposes independent of the barrier ratio V_2/V_1. At higher values of V_1/RT, however, the entropy decreases as the barrier ratio is lowered by raising one of two equal minima, and the property passes through a minimum before the second valley disappears at $V_2/V_1=0$. The maximum entropy decrease becomes more pronounced as $1/Q_f$ or V_1/RT is increased, and would, in the limit, reach $R\ln 2$, or 1.38 for high values of V_1/RT for which the populations of excited states had become negligible. It appears that for real systems with V_1/RT of the order of 5, the entropy might be lower by as much as 0.5 cal./mole/degree than that for two equal potential valleys.

We may go continuously from the case of equal valleys to the single minimum limit either by lowering a maximum, or, as in the problem now under consideration, by raising a minimum. In the former case the entropy passes through a maximum, in the latter through a minimum. The extreme range of entropy values for the double minimum, with both attractive and repulsive forces considered, is of the order of 1.5 entropy units and approaches 500 cal. on the energy scale at room temperature.

Again, as in the system with repulsive forces, the heat content passes through a maximum and a minimum with changing barrier ratio, but the minimum tends to disappear at the lower values of V_1/RT.

It is of some practical interest that at $V_1=RT$ the entropy remains invariant between the limits

of the single minimum and the equal double minimum system. This is true for the intermediate situations produced either by lowering a maximum or raising a minimum. In other words, if the conditions are such that the entropy is the same in the limits, it will not change appreciably during the transition from one limit to the other by either of the two routes thus far considered. It is probably true that at still lower values of V_1/RT, with V_1 the higher potential barrier, the entropy will remain the same for all variations of the double minimum system produced by raising a minimum or lowering a maximum.

This conclusion will certainly be valid for all three thermodynamic properties in the region of close approach to free rotation, where for a given moment of inertia the differences between symmetrical systems are determined solely by the symmetry number. It must also be true that the invariant character will extend to higher values of V_1/RT for the entropy than for the free energy or heat content per degree. At low potential barriers the properties are largely determined by the location of states having energies less than RT, and for such states a disturbance of position tends to affect the free energy and heat content in opposite directions. Consequently, an increase in the barrier height which disturbs mainly states having energies less than RT will produce relatively little change in the entropy. Although there appears to be no rigorous method of demonstrating how far up the V_1/RT scale the invariance will go, it seems safe to assume that below any given level the constancy will improve. The invariance found at $V_1=RT$ can therefore be assumed to hold for $V_1<RT$ without much danger of error. For the double minimum, for $V_1 \lesssim RT$, the entropy deficiency below free rotation is thus taken to be independent of the barrier ratio, and may be obtained from the tables for the symmetrical rotator as determined by the higher of the potential barriers. It becomes unnecessary to use the method outlined here in the region of lowest values of V_1/RT, where uncertainties in the representative location of states could lead to inaccurate results.

In the region of high potential barriers relative to RT, the system acts like two harmonic oscillators at equilibrium, having a number of states placed at higher levels than their positions in either the single or the equal double minimum limit. This tends to decrease both the summations which enter into the three thermodynamic properties and will cause all of these properties to pass through minima between the two limits. This tendency persists, in the free energy $(-F/T)$ and the entropy, into regions far removed from the harmonic oscillator limit.

THE JOURNAL OF CHEMICAL PHYSICS VOLUME 16, NUMBER 6 JUNE, 1948

The Intrinsic Viscosities and Diffusion Constants of Flexible Macromolecules in Solution

JOHN G. KIRKWOOD
Gates and Crellin Laboratories, California Institute of Technology, Pasadena, California

AND

JACOB RISEMAN*
Baker Laboratory, Cornell University, Ithaca, New York

(Received February 16, 1948)

A theory of the intrinsic viscosities and translational diffusion constants of flexible macromolecules is developed on the basis of the random coil model with hindered internal rotation. Proper account is taken of the hydrodynamic interaction of the monomer units of the molecule and of inhibited flow through the chain. The theory leads to results qualitatively similar to those obtained by Debye on the basis of a molecular model consisting of a sphere containing a uniform distribution of resisting points. However, significant quantitative differences between the two theories are found.

I. INTRODUCTION

ALTHOUGH the intrinsic viscosities and diffusion constants of rigid macromolecules of ellipsoidal shape have received adequate theoretical interpretation, the manner in which these properties are related to molecular structure has until recently remained obscure and incompletely understood in the case of flexible macromolecules in solution, for example, linear high polymers and possibly some of the fibrous proteins. Staudinger's law,[1] requiring proportionality between the intrinsic viscosity and the first power of the molecular weight, received theoretical confirmation for linear polymers of the random coil structure at the hands of Kuhn,[2] Huggins,[3] and Kramers.[4] Nevertheless, the failure of the Staudinger relation as a quantitative law became evident from experimental efforts to calibrate intrinsic viscosity measurements by means of more direct and reliable molecular weight determinations. It was found empirically that the intrinsic viscosity could be represented over limited ranges of molecular weight in the form KM^{α} with an exponent α varying from 0.5 to 1.0, according to the structure of the polymer and the molecular weight range considered.

The reason for the failure of the theory of Kuhn, Huggins, and Kramers at high molecular weights has recently been pointed out by Debye.[5] In the KHK theory, the hydrodynamic interaction of the monomer units of the flexible polymer chain is neglected, and each chain element is supposed to offer the same resistance to the flow of the solvent that it would offer if the other chain elements were not present to perturb the flow in its neighborhood. Actually, the peripheral elements of the chain must perturb the flow in the neighborhood of the interior elements in such a manner that they are partially shielded from hydrodynamic interaction with the exterior fluid. At high molecular weights, the hydrodynamical shielding of the interior elements may become so effective that their contribution to the resistance offered by the molecule to the external fluid flow is negligibly small.

To describe the retarded flow through a polymer chain, Debye[5,6] and Brinkman[7] have independently investigated a molecular model consisting of a sphere containing a uniformly distributed system of resisting points equal in number to the number of monomer units of the molecule. Debye obtains qualitative agreement with the experimental observation that the exponent α in the formula must decrease from 1.0 to 0.5 as the molecular weight increases.

* Present address: Institute for High Polymer Research, Polytechnic Institute of Brooklyn, Brooklyn, New York.

[1] H. Staudinger, *Die Hochmolecularen Organischen Verbindungen* (Verlag Julius Springer, Berlin, 1932).
[2] W. Kuhn, Zeits. f. physik. Chemie **A161**, 1 (1932).
[3] M. L. Huggins, J. Phys. Chem. **43**, 439 (1939).
[4] H. A. Kramers, J. Chem. Phys. **14**, 415 (1946).
[5] Debye, reports to the Office of Rubber Reserve, Reconstruction Finance Corporation, October 10, 1946.
[6] P. Debye, Phys. Rev. **71**, 486 (1947).
[7] H. C. Brinkman, Physica **13**, 447 (1947).

In the present article, we describe an investigation of the retarded flow through a polymer chain which is based upon the more realistic random coil model. The method and model are employed to determine the intrinsic viscosities and the translational diffusion constants of flexible macromolecules. Results qualitatively similar to those of Debye are obtained. We believe our theory to be quantitatively more reliable, since it is based on a more accurate model of the polymer chain than that of Debye.

II. SPECIFICATION OF THE MODEL AND DESCRIPTION OF INHIBITED FLUID FLOW THROUGH THE POLYMER CHAIN

We base our theory of fluid flow through a linear polymer molecule, $(CHX)_{2n+1}$, on the familiar random coil model. The skeletal carbon atoms are numbered from $-n$ to $+n$ and are connected by $2n$ bond vectors $\mathbf{b}_l$ of length b_0 directed from skeletal atom $l-1$ to atom l. The internal configuration of the chain is specified by coordinates φ_l, the angles between the planes of successive bond pairs $(\mathbf{b}_{l-1}, \mathbf{b}_l)$ and $(\mathbf{b}_l, \mathbf{b}_{+1})$. The degree of polymerization, $2n$ for large n is denoted by z and is equal to M/M_0 where M and M_0 are the respective molecular weights of polymer and monomer unit, CHX. We assume internal rotation around each bond $\mathbf{b}_l$ with a hindering torque having $\varphi_l=0$ as a plane of symmetry. A more general torque can be used without undue complication, if desired.

For the model described, we obtain the following average values, asymptotically valid as the number of bonds between the monomer units l and s becomes large,

$$\begin{aligned}
&\langle \mathbf{R}_{ls}^2\rangle_{Av} = |l-s|b^2,\\
&\langle \mathbf{R}_{0l}^2\rangle_{Av} = (3l^2+n^2)b^2/6n,\\
&\langle \mathbf{R}_{0l}\cdot\mathbf{R}_{0s}\rangle_{Av} = (1/12n)\{3(l^2+s^2)\\
&\qquad -6n|l-s|+2n^2\}b^2,
\end{aligned} \tag{1}$$

where R_{ls} is the distance between chain elements l and s, and $\mathbf{R}_{0l}$ is the position of chain element l relative to the molecular center of mass. Also, if the distance R_{ls} is assumed to be normally distributed, we have

$$\langle 1/\mathbf{R}_{ls}\rangle_{Av} = (6/\pi)^{\frac{1}{2}}(1/b|l-s|^{\frac{1}{2}}), \tag{2}$$

where the effective bond length b is given by

$$\begin{aligned}
b = &[(1+\langle\cos\varphi\rangle_{Av})/(1-\langle\cos\varphi\rangle_{Av})]\\
&\times[(1-\cos\gamma)/(1+\cos\gamma)]b_0,
\end{aligned} \tag{3}$$

where γ is the fixed skeletal bond angle, equal to the tetrahedral angle for a carbon skeleton and $\langle\cos\varphi\rangle_{Av}$ is the mean value of the cosine of the angle between successive bond planes. In the case of free rotation $\langle\cos\varphi\rangle_{Av}$ vanishes. For the completely extended chain $\langle\cos\varphi\rangle_{Av}$ is equal to unity and the asymptotic formulas of Eqs. (1), (2), and (3) cease to be valid. The average values presented will be used later in the analysis.

When a polymer molecule is placed in fluid of low molecular weight in which there is a velocity field $\mathbf{v}_0(\mathbf{R})$, the flow is perturbed by the resistance offered by each monomer unit. If $\mathbf{v}_l$ is the velocity the fluid would possess at the point of location of chain element l, if that element were absent and $\mathbf{u}_l$ is the velocity of that element, a force $\mathbf{F}_l$

$$\mathbf{F}_l = -\zeta\mathbf{w}_l, \quad \mathbf{w}_l = \mathbf{v}_l - \mathbf{u}_l \tag{4}$$

is exerted on the fluid by chain element l, where ζ is a friction constant characteristic of the fluid and the structure of the monomer unit CHX. The perturbation $\mathbf{v}'$ at a point $\mathbf{R}_l$ from the locus of application of the force $\mathbf{F}_l$ is conveniently calculated by a formula advanced by Oseen.[8]

$$\begin{aligned}
\mathbf{v}'(\mathbf{R}_l) &= \mathbf{T}(\mathbf{R}_l)\cdot\mathbf{F}_l\\
&= (1/8\pi\eta_0 R_l)[\mathbf{F}_l+\mathbf{R}_l(\mathbf{R}_l\cdot\mathbf{F}_l)/R_l^2]\\
\mathbf{T}(\mathbf{R}_l) &= (1/8\pi\eta_0 R_l)\{1+(\mathbf{R}_l\mathbf{R}_l/R_l^2)\},
\end{aligned} \tag{5}$$

where η_0 is the viscosity coefficient of the solvent fluid and the tensor $\mathbf{T}$ is expressed in dyadic form. The Oseen formula will be used in two ways, first to determine the perturbation in the flow at the point of location of chain element l, produced by the other elements of the same molecule, and then the aggregate perturbation of flow produced by all elements at a specified distance from the molecular center of gravity.

The fluid velocity $\mathbf{v}_l$ at the point of location of element, calculated as the sum of the unperturbed velocity $\mathbf{v}_l^0$ existing in the solvent in the absence of the polymer molecule and the summed

[8] See Burgers, Chap. III; Second Report on Viscosity and Plasticity of the Amsterdam Academy of Sciences, Nordemann 1938.

Oseen perturbations from all other chain elements s, by means of Eqs. (4) and (5), is

$$\mathbf{v}_l=\mathbf{v}_l^0-\zeta\sum_{\substack{s=-n\\ \pm l}}^{+n}\mathbf{T}_{ls}\cdot\mathbf{w}_s$$
$$\mathbf{T}_{ls}=(1/8\pi\eta_0R_{ls})\{1+(\mathbf{R}_{ls}\mathbf{R}_{ls}/R_{ls}^2)\}, \tag{6}$$

where R_{ls} is the distance between elements l and s in a specified internal configuration of the molecule. If the velocities $\mathbf{u}_l$ are specified, the forces $\mathbf{F}_l$ exerted by the chain elements on the fluid are determined by the set of linear equations,

$$\mathbf{F}_l=-\zeta(\mathbf{v}_l^0-\mathbf{u}_l)-\zeta\sum_{\substack{s=-n\\ \pm l}}^{+n}\mathbf{T}_{ls}\cdot\mathbf{F}_s \qquad -n\leqslant l\leqslant+n. \tag{7}$$

The perturbation in the flow $\mathbf{v}'$ produced by the molecule as a whole at a point $\mathbf{R}$ from its center of mass is again given by the Oseen formula as

$$\mathbf{v}'(\mathbf{R})=\frac{1}{8\pi\eta_0}\sum_{l=-n}^{+n}\left\{\frac{\mathbf{F}_l}{|\mathbf{R}-\mathbf{R}_{0l}|}+\frac{(\mathbf{R}-\mathbf{R}_{0l})(\mathbf{R}-\mathbf{R}_{0l})\cdot\mathbf{F}_l}{|\mathbf{R}-\mathbf{R}_{0l}|^3}\right\}. \tag{8}$$

Equations (7) and (8) form the basis of the theories of viscosity and diffusion to be presented in the following sections. The intrinsic viscosities and diffusion constants of polymer molecules are expressed in terms of sum of mean values of products of the forces $\mathbf{F}_l$ and internal coordinates $\mathbf{R}_{0s}$, averaged over all internal configurations of chain. Equations (7) are then employed to formulate systems of linear equations for the pertinent mean values. For large n, the systems of linear equations may be replaced by asymptotically valid integral equations, which are then solved.

III. THE INTRINSIC VISCOSITY

In determining the intrinsic viscosity we have the choice of two methods. We may either calculate a dissipation function associated with the frictional resistance of flow through the polymer chain, or we may calculate the perturbation in flow at the boundaries of a fluid in a state of stationary viscous flow, produced by the introduction of a polymer molecule. The latter method proves to be the most convenient and direct in our case.

We suppose that before the introduction of the solute molecules, the low molecular weight solvent is in a state of stationary two-dimensional viscous flow between parallel plane boundaries. When a polymer molecule is introduced into the system, the center of gravity acquires a mean velocity equal to the local velocity of the solvent and the molecule acquires mean internal and external angular velocities which adjust average torques to the value, zero. If ϵ is the rate of strain and $\mathbf{e}_x$, $\mathbf{e}_y$, $\mathbf{e}_z$ are unit vectors defining a coordinate system with origin in the molecular center of gravity with $\mathbf{e}_x$ parallel to the stream lines of the unperturbed flow and $\mathbf{e}_y$ perpendicular to the plane boundaries, the unperturbed fluid velocity at the point of location of chain element l is given by

$$\mathbf{v}_l^0=\dot{\epsilon}(\mathbf{R}_{0l}\cdot\mathbf{e}_y)\mathbf{e}_x. \tag{9}$$

The average internal torques are made to vanish by average internal angular velocities, $\langle\dot{\varphi}_l\rangle_{Av}=0$, and the average external torque caused by viscous drag is made to vanish by an average angular velocity in the z direction of $\dot{\epsilon}/2$. Thus, with the neglect of fluctuations in the angular velocities, we may write for the velocities $\mathbf{u}_l$ of the elements of the chain

$$\mathbf{u}_l=(\dot{\epsilon}/2)(\mathbf{e}_z\times\mathbf{R}_{0l}), \tag{10}$$

and Eqs. (7) for the forces of frictional resistance exerted on the fluid become

$$\mathbf{F}_l=-\frac{\zeta\dot{\epsilon}}{2}[\mathbf{e}_x(\mathbf{R}_{0l}\cdot\mathbf{e}_y)+\mathbf{e}_y(\mathbf{R}_{0l}\cdot\mathbf{e}_x)] -\zeta\sum_{\substack{s=-n\\ \pm l}}^{+n}\mathbf{T}_{ls}\cdot\mathbf{F}_s; \quad -n\leqslant l\leqslant+n. \tag{11}$$

When the velocity perturbation of Eq. (8), depending upon the forces $\mathbf{F}_l$, is expanded in spherical harmonics and averaged over all internal configurations of the chain, one obtains at distances large relative to the linear dimensions of the chain,

$$\langle\mathbf{v}'\rangle_{Av}=-(3\zeta G\dot{\epsilon}/4\pi\eta_0R^5)(\mathbf{R}\cdot\mathbf{e}_x)(\mathbf{R}\cdot\mathbf{e}_y)\mathbf{R},$$
$$G=-\frac{1}{\zeta\dot{\epsilon}}\sum_{l=-n}^{+n}\langle(\mathbf{R}_{0l}\cdot\mathbf{e}_x)(\mathbf{R}_{0l}\cdot\mathbf{e}_y)\rangle_{Av}. \tag{12}$$

Following the method employed by Burgers[8] in the analysis of the intrinsic viscosity of rigid macromolecules, we sum the contributions $\langle \mathbf{v}' \rangle_{Av}$ at the parallel plane boundaries produced by all solute molecules contained between the planes and find that at constant shearing stress, the velocity gradient is reduced by an amount leading to the following expression for the intrinsic viscosity,

$$[\eta] = \lim_{c \to 0} [(\eta - \eta_0)/\eta_0 c], \qquad [\eta] = N\zeta G/100 M\eta_0, \tag{13}$$

where c is the solute concentration in grams per 100 ml, M the molecular weight, and N Avogadro's number.

In order to determine the average values contributing to the function G, we define quantities $\varphi_{ll'}$ by the relation,

$$\langle (\mathbf{F}_l \cdot \mathbf{e}_y)(\mathbf{R}_{0l'} \cdot \mathbf{e}_x) \rangle_{Av} = -(nb^2\zeta\dot{\epsilon}/9)\varphi_{ll'}, \tag{14}$$

where the average values over internal configurations of the chain are to be taken with the equilibrium distribution, unperturbed by the flow, since we are interested here only in the Newtonian approximation to the flow at small rates of strain. The intrinsic viscosity, Eq. (13), may then be expressed in the form

$$[\eta] = (N\zeta b^2 M/3600\eta_0 M_0^2) F, \qquad F = \frac{1}{n} \sum_{l=-n}^{+n} \varphi_{ll}. \tag{15}$$

For large n, the sum defining F may be replaced by the integral

$$F = \int_{-1}^{+1} \varphi(x,x)\,dx, \qquad \varphi_{ll'} = \varphi(x,y), \qquad x = l/n, \quad y = l'/n. \tag{16}$$

In order to obtain the functions $\varphi_{ll'}$, we multiply both sides of Eq. (11) by $(\mathbf{R}_{0l'} \cdot \mathbf{e}_x)\mathbf{e}_y$, average both sides, and use the last of Eqs. (11) for the averages of the inhomogeneous parts, with the result,

$$\varphi_{ll'} = f_{ll'} - (9\zeta/nb^2\dot{\epsilon}) \sum_{\substack{s=-n \\ \pm l}}^{+n} \langle (\mathbf{e}_x \cdot \mathbf{R}_{0l'})(\mathbf{e}_y \cdot \mathbf{T}_{ls} \cdot \mathbf{F}_s) \rangle_{Av}, \qquad -n \leqslant l \leqslant +n, \qquad -n \leqslant l' \leqslant +n, \tag{17}$$

$$f_{ll'} = \{3(l^2 + l'^2) - 6n|l - l'| + 2n^2\}/8n^2.$$

At this point, we introduce the approximation,

$$\langle (\mathbf{e}_x \cdot \mathbf{R}_{0l'})(\mathbf{e}_y \cdot \mathbf{T}_{ls} \cdot \mathbf{F}_s) \rangle_{Av} = \langle (\mathbf{e}_x \cdot \mathbf{R}_{0l'})(\mathbf{e}_y \cdot \langle \mathbf{T}_{ls} \rangle_{Av} \mathbf{F}_s) \rangle_{Av}$$
$$\langle \mathbf{T}_{ls} \rangle_{Av} = (1/6\pi\eta_0)\langle 1/R_{ls} \rangle_{Av} = 1[(6\pi^3)^{\frac{1}{2}}|l - s|^{\frac{1}{2}} b\eta_0]^{-1}, \tag{18}$$

where Eqs. (2) and (5) have been used to calculate $\langle \mathbf{T}_{ls} \rangle_{Av}$. Equations (17) and (18) yield the following set of linear equations for the quantities $\varphi_{ll'}$,

$$\varphi_{ll'} = f_{ll'} - \frac{\lambda}{n^{\frac{1}{2}}} \sum_{\substack{s=-n \\ \pm l}}^{+n} \frac{\varphi_{sl'}}{|l - s|^{\frac{1}{2}}}, \qquad \lambda = [\zeta/(12\pi^3)^{\frac{1}{2}} b\eta_0](M/M_0)^{\frac{1}{2}}, \tag{19}$$

which for large n are asymptotically approximated by the integral equations,

$$\varphi(x,y) = f(x,y) - \lambda \int_{-1}^{+1} \varphi(t,y)/(|x - t|)^{\frac{1}{2}} dt, \qquad f(x,y) = [3(x^2 + y^2) - 6|x - y| + 2]/8, \qquad x = l/n; \quad y = l'/n. \tag{20}$$

The accuracy of the approximation, Eq. (18), depends upon the magnitude of the fluctuation,

$$\langle (\mathbf{e}_x \cdot \mathbf{R}_{0l'})(\mathbf{e}_y \cdot [\mathbf{T}_{ls} - \langle \mathbf{T}_{ls} \rangle_{Av}] \cdot \mathbf{F}_s) \rangle_{Av},$$

the estimation of which is a difficult problem, which we will not undertake in the present article. Refinement of the present theory would have to be based upon an investigation of the fluctuation.

The integral equation, Eq. (20), can be solved by expansion of $\varphi(x,y)$ in a Fourier series of the

form,**

$$\varphi(x,y)=\sum_{\substack{k=-\infty\\ \pm 0}}^{+\infty}\frac{f_k(y)e^{i\pi kx}}{1+\lambda(2/|k|)^{\frac{1}{2}}},\qquad(21)$$

$$f_k(y)=(3/4\pi^2k^2)e^{-i\pi ky}+(-1)^k(3iy/4\pi|k|).$$

The calculation of the function F of Eqs. (15) and (16) with the aid of Eq. (21) yields,

$$[\eta]=(N\zeta b^2/3600\eta_0M_0)zF(\lambda_0z^{\frac{1}{2}}),$$

$$\lambda_0=[\zeta/(6\pi^3)^{\frac{1}{2}}\eta_0b],$$

$$F(x)=(6/\pi^2)\sum_{k=1}^{\infty}\frac{1}{k^2}\frac{1}{1+x/(k)^{\frac{1}{2}}},\qquad(22)$$

$$z=M/M_0$$

as the final formula for the intrinsic viscosity.

It is instructive to examine the behavior of the function $F(\lambda_0z^{\frac{1}{2}})$ for large and small values of the reduced molecular weight

$$\lim_{\lambda_0z^{\frac{1}{2}}\to 0}F(\lambda_0z^{\frac{1}{2}})=1,$$

$$\lim_{\lambda_0z^{\frac{1}{2}}\to\infty}\lambda_0z^{\frac{1}{2}}F(\lambda_0z^{\frac{1}{2}})=1.588.\qquad(23)$$

From Eqs. (22) and (23), we observe that as $z\to 0$ the intrinsic viscosity approaches proportionality to the first power of the molecular weight, the result of the theories of Kuhn, Huggins, and Kramers, in which the hydrodynamic interaction of the elements of the polymer chain is neglected. For large molecular weights, the intrinsic viscosity approaches proportionality to the square root of the molecular weight, the result of the theory of Debye. However, the limiting value of $[\eta]/z^{\frac{1}{2}}$ as $z\to\infty$ differs from that of Debye's by a factor of about 0.46. This discrepancy is doubtless to be attributed to the failure of Debye's model, a sphere of uniformly distributed centers of hydrodynamic resistance, adequately to represent the random coil molecule for any molecular weight. We therefore believe our theory to be more reliable from the quantitative standpoint.

The curve $[\eta]=kz^{\alpha}$ which is tangent to the log-log plot of Eq. (22) at a particular value of z possesses an exponent α given by

$$\alpha=1+\tfrac{1}{2}(d\log F(x)/d\log x),$$

$$x=\lambda_0z^{\frac{1}{2}}.\qquad(24)$$

** See Appendix I.

TABLE I.

x	$F(x)$	$xF(x)$	$\alpha(x)$
0	1.0	0	1.0
0.1	0.925	0.092	0.963
0.2	0.861	0.172	0.932
0.3	0.806	0.242	0.905
0.4	0.759	0.304	0.882
0.5	0.717	0.358	0.862
0.6	0.679	0.407	0.845
0.7	0.646	0.452	0.829
0.8	0.616	0.493	0.815
0.9	0.588	0.529	0.802
1.0	0.564	0.564	0.791
1.5	0.467	0.700	0.746
2.0	0.400	0.800	0.715
2.5	0.350	0.875	0.691
3.0	0.312	0.936	0.674
3.5	0.281	0.984	0.660
4.0	0.256	1.024	0.647
4.5	0.236	1.062	0.638
5.0	0.218	1.090	0.632
10	0.126	1.260	0.583
20	0.070	1.400	0.562
	0	1.588	0.500

As z increases from zero to infinity, α decreases monotonically from 1.0 to 0.5, so that the empirical representation of $[\eta]$ by a power law over a limited range of molecular weights should yield an exponent with a value between 0.5 and 1.0, in agreement with observed behavior in such treatment of experimental data.

At a specified molecular weight, the intrinsic viscosity, given by Eq. (22), is determined by the friction constant ζ of a monomer unit and the effective bond length b of the chain. For large values of z, $[\eta]$ becomes independent of ζ and b may be determined by the relation

$$b^3=\frac{2267M_0}{(6\pi^3)^{\frac{1}{2}}N}\lim_{z\to\infty}\frac{[\eta]}{z^{\frac{1}{2}}}.\qquad(24)$$

Thus b may be determined from experimental data by plotting $[\eta]/z^{\frac{1}{2}}$ against $z^{-\frac{1}{2}}$, say, and extrapolating the resulting curve to obtain the intercept on the $[\eta]/z^{\frac{1}{2}}$ axis. The friction constant, ζ, may be calculated from b and λ_0 as $(6\pi^3)^{\frac{1}{2}}\eta_0b\lambda_0$. In order to determine the parameter λ_0 from experimental data, a value of $\alpha(\lambda_0z^{\frac{1}{2}})$ is obtained for a convenient intermediate value of z from the slope of a log-log plot of $[\eta]$ against z. Then from a table or graph of $\alpha(x)$ *versus* x, a value of $\lambda_0z^{\frac{1}{2}}$ is read off and divided by the given value of $z^{+\frac{1}{2}}$ to yield λ_0.

To facilitate the use of Eq. (22) and the determination of the parameters b and ζ from

experimental data, $F(x)$, $xF(x)$, and $\alpha(x)$ are presented in Table I as functions of x at convenient intervals between 0.0 and 20.0, a range sufficiently large for most purposes.

As a test of Eq. (22) we have analyzed measurements of the intrinsic viscosities of polystyrene fractions, ranging from 20,000 to 1,500,000 in molecular weight, in two solvents, benzene and butanone, made by Ewart and Gingey[9] in the Research Laboratory of the United States Rubber Company. Although for application to polystyrene the theory should properly be generalized for two types of monomer unit, the present theory has been used with an average monomer weight M_0 of 52, the average of that of CH_2- and C_6H_5-CH-. The parameters b and ζ were determined in each solvent by the methods described and the results are presented in Figs. 1 and 2. We observe that in both solvents, Eq. (22) represents the experimental data with a very satisfactory accuracy. The constants b and ζ derived from the data are presented in Table II. In the last column of Table II are tabulated the mean values of $\langle\cos\varphi\rangle_{Av}$, calculated from the experimental values of b by means of Eq. (3). From the values of $\langle\cos\varphi\rangle_{Av}$, we conclude that in both solvents the polystyrene molecule is much more extended than a simple random coil molecule of the same molecular weight, possessing free internal rotation around each bond. Thus a polystyrene molecule in benzene of molecular weight, $M=10^6$, is calculated to have a root mean square length,

$$R_0 = z^{\frac{1}{2}}b = 1125\text{A},$$

approximately four times the root mean square length of the freely rotating random coil of the same molecular weight. Parallel evidence is provided by the asymmetry of light scattering by polymers in solution. In an informal communication, Professor Debye estimates by this method an R_0 for polystyrene of molecular weight 10^6 in benzene to be about 1000A, in good agreement with our value. In order to demonstrate the sensitivity of the intrinsic viscosity to the parameter b, we have plotted as the dotted curve of Fig. 1, the values of $[\eta]$ calculated by Eq. (22) and a value of b corresponding to $R_0=1000$A at $M=10^6$. The agreement with experiment is still fair, but not excellent.

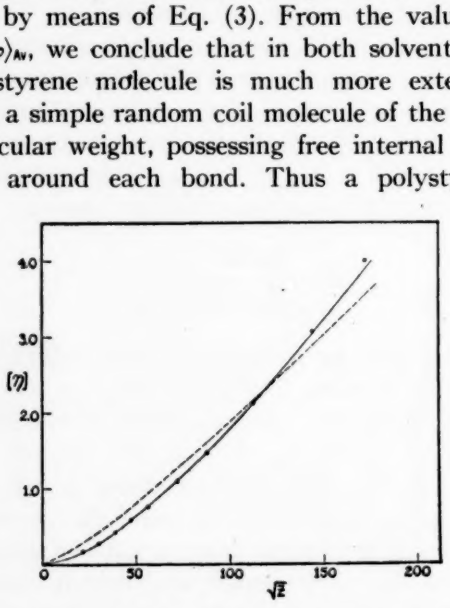

FIG. 1. The intrinsic viscosity of polystyrene in benzene plotted as a function of the square root of the degree of polymerization. Solid curve, theory; circles experimental values; dotted curve, theory with modified value of b.

[9] Ewart and Gingey, unpublished data. We are indebted to Professor Debye for calling our attention to these measurements and to Dr. Ewart for his kind permission to discuss them in this publication.

The values of the friction constants ζ require little comment except the remark that they are of the expected order of magnitude. The representative linear dimension of the monomer unit would be calculated to be about an order of magnitude too small, if estimated by Stokes law and the macroscopic viscosity of the solvent. This circumstance is not surprising and is best interpreted as additional evidence for the failure of Stokes law on the molecular scale.

The fact that b is smaller in butanone than in benzene is of some interest. It can be qualitatively understood if one supposes that butanone, being a polar solvent, exerts thermodynamic forces on the non-polar polystyrene molecule, acting to produce a less extended configuration and less contact with solvent molecules than in benzene. Although such forces cannot accurately be represented by additional hindering torques around individual bonds, their effect would be in the same direction as additional hindering torques decreasing the value of $\langle\cos\varphi\rangle_{Av}$.

It is evident that without empirical calibration by other methods, measurements of intrinsic viscosity cannot be used to determine molecular

TABLE II. Constants of the polystyrene molecule.

Solvent	$b(A)$	$10^{10}\zeta$(g/sec.)	$\langle\cos\varphi\rangle_{Av}$
Benzene	8.12	1.3	0.87
Butanone	5.20	3.9	0.70

weight, since the intrinsic viscosity depends not only upon molecular weight but also on structural parameters of the polymer molecule. However, when the molecular weight is known, such structural parameters may be estimated from the intrinsic viscosity with the aid of the present theory. In this manner significant information relative to the internal configuration of the chain may be obtained and the effective bond length b, or the length of the statistically independent units of the chain in a given solvent may be determined.

IV. THE TRANSLATIONAL DIFFUSION CONSTANT

We consider a polymer molecule, the center of gravity of which is in motion with mean velocity $\mathbf{u}$, relative to the solvent in which it is immersed. The friction constant Ξ of the entire molecule is then defined by the relation,

$$\langle \mathbf{F} \rangle_{Av} = \Xi \mathbf{u}, \quad \langle \mathbf{F} \rangle_{Av} = -\sum_{l=-n}^{+n} \langle \mathbf{F}_l \rangle_{Av}, \tag{25}$$

where $\langle \mathbf{F} \rangle_{Av}$, the mean force exerted by the fluid on the molecular center of gravity is the sum of the mean forces $-\langle \mathbf{F}_l \rangle_{Av}$ exerted by the individual monomer units, averaged over all internal configurations of the chain. The translational diffusion constant D may be calculated from the Einstein relation,

$$D = kT/\Xi, \tag{26}$$

when the friction constant Ξ is known.

In order to determine the mean forces $\langle \mathbf{F}_l \rangle_{Av}$, we return to Eq. (7), average both sides over internal configurations of the chain, and set $\langle \mathbf{v}_l^0 - \mathbf{u}_l \rangle_{Av}$ equal to $\mathbf{u}$, obtaining

$$\langle \mathbf{F}_l \rangle_{Av} = -\zeta \mathbf{u} - \zeta \sum_{\substack{s=-n \\ \pm l}}^{+n} \langle \mathbf{T}_{ls} \cdot \mathbf{F}_s \rangle_{Av}. \tag{27}$$

If, as in the theory of viscosity, we write

$$\langle \mathbf{T}_{ls} \cdot \mathbf{F}_s \rangle_{Av} = \langle \mathbf{T}_{ls} \rangle_{Av} \cdot \langle \mathbf{F}_s \rangle_{Av} + \langle (\mathbf{T}_{ls} - \langle \mathbf{T}_{ls} \rangle_{Av}) \cdot \mathbf{F}_s \rangle_{Av} \tag{28}$$

and neglect the fluctuation, we obtain the following set of linear equations for the $\langle \mathbf{F}_l \rangle_{Av}$,

$$\langle \mathbf{F}_l \rangle_{Av} = -\zeta \mathbf{u} - (\lambda/n^{\frac{1}{2}}) \sum_{\substack{s=-n \\ \pm l}}^{+n} [\langle \mathbf{F}_s \rangle_{Av} / |l-s|^{\frac{1}{2}}]. \tag{29}$$

Defining functions ψ_l by the relation,

$$\langle \mathbf{F}_l \rangle_{Av} = -\zeta \psi_l \mathbf{u} \tag{30}$$

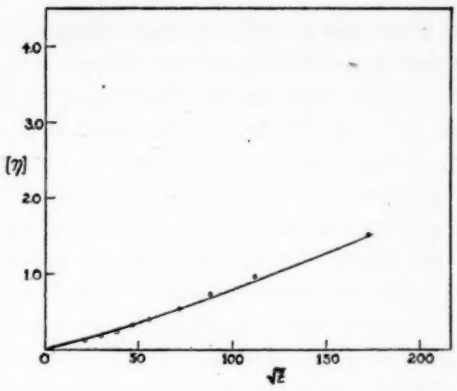

FIG. 2. The intrinsic viscosity of polystyrene in butanone, plotted as a function of the square root of the degree of polymerization z. Solid curve, theory; circles, experimental values.

and replacing Eqs. (29) by the asymptotic integral equation, we obtain

$$\psi(x) = 1 - \lambda \int_{-1}^{+1} [\psi(t)/(|x-t|)^{\frac{1}{2}}] dt; \tag{31}$$

$$x = l/n,$$

which differs from Eq. (20) of the theory of viscosity only in the inhomogeneous part. From Eqs. (25) and (30) we observe that the friction constant Ξ for the molecule as a whole is given by

$$\Xi = (M\zeta/2M_0) \int_{-1}^{+1} \psi(x) dx. \tag{32}$$

If $\psi(x)$ is expanded in the Fourier series,

$$\psi(x) = \sum_{k=-\infty}^{+\infty} \psi_k e^{i\pi kx}, \tag{33}$$

we see that

$$\Xi = \zeta \psi_0 z, \quad z = M/M_0, \tag{34}$$

where ψ_0 is the constant term in the Fourier expansion, which is shown in Appendix I to have the value

$$\psi_0 = 1/[1 + 8\lambda/3\sqrt{2}]. \tag{35}$$

Thus we obtain

$$\Xi = z\zeta/[1 + (8\lambda_0/3)z^{\frac{1}{2}}], \quad \lambda_0 = \zeta/(6\pi^3)^{\frac{1}{2}}\eta_0 b \tag{36}$$

as the final expression for the friction constant. The corresponding expressions for the diffusion and sedimentation constants are

$$\begin{aligned} D &= [1 + (8\lambda_0/3)z^{\frac{1}{2}}](kT/z\zeta), \\ S &= [1 + (8\lambda_0/3)z^{\frac{1}{2}}][1 - v\rho]/z\zeta, \end{aligned} \tag{37}$$

where v is the partial specific volume of the solute and ρ the density of the solvent.

We remark that the friction constant of the flexible macromolecule, proportional to the molecular weight for small z, becomes asymptotically proportional to the square root of the molecular weight for large z. This result has also been obtained by Bueche,[10] using the Debye model, and equations identical with Eqs. (36) and (37) have been obtained by Hermans[11] on the basis of a less detailed analysis, which did not yield a theoretical interpretation of the constant $8\lambda_0/3$.

An experimental test of Eqs. (36) and (37) is being deferred until reliable data on both the intrinsic viscosity and sedimentation constant of the same specimens of a carefully fractionated polymer are available.

In conclusion, we wish to thank Dr. Mark Kac of Cornell University for suggesting a method of solution of the integral equations (20) and (31).

APPENDIX I: SOLUTION OF THE INTEGRAL EQUATIONS

The integral equations (20) and (21) are both of the form,

$$\varphi(x)=f(x)-\lambda\int_{-1}^{+1}[\varphi(t)/(|x-t|)^{\frac{1}{2}}]dt, \quad \text{(A1)}$$

where for brevity we have suppressed the parameter y upon which φ and f depend in Eq. (20). In order to solve Eq. (A1), we represent the kernel, $|x-t|^{-\frac{1}{2}}$, in the following form:

$$1/(|x-t|)^{\frac{1}{2}}=[1/(\pi)^{\frac{1}{2}}]\int_{-\infty}^{+\infty}e^{-|x-t|\beta^2}d\beta, \quad \text{(A2)}$$

which we wish to substitute in Eq. (A1) and interchange the order of integration, a procedure which is permissible only if the integral

$$\varphi_0=\tfrac{1}{2}\int_{-1}^{+1}\varphi(x)dx$$

vanishes. As a preliminary step, we therefore define a new function,

$$\varphi^*(x)=\varphi(x)-\varphi_0,$$
$$\varphi_0=\tfrac{1}{2}\int_{-1}^{+1}\varphi(x)dx, \quad \text{(A3)}$$

the integral of which does vanish, and find that $\varphi^*(x)$ satisfies the equation,

$$\varphi^*(x)=f^*(x)-\lambda\int_{-1}^{+1}[\varphi^*(t)/(|x-t|)^{\frac{1}{2}}]dt,$$
$$f^*(x)=f(x)-\varphi_0\mu(x), \quad \text{(A4)}$$
$$\mu(x)=1+2\lambda(1+x)^{\frac{1}{2}}+2\lambda(1-x)^{\frac{1}{2}}.$$

Substitution of Eq. (A2) into Eq. (A4) and inversion of the order of integration yields

$$\varphi^*(x)=f^*(x)-[\lambda/(\pi)^{\frac{1}{2}}]\int_{-\infty}^{+\infty}g(x,\beta)d\beta,$$
$$g(x,\beta)=\int_{-1}^{+1}e^{-|x-t|\beta^2}\varphi^*(t)dt. \quad \text{(A5)}$$

The second of Eqs. (A5) is an integral equation equivalent to the following differential equation,

$$\frac{\partial^2 g}{\partial x^2}=\beta^4 g-2\beta^2\varphi^*, \quad \text{(A6)}$$

a result which may be verified by differentiating (A5) twice with respect to x. We now solve the pair of equations,

$$\varphi^*(x)=f^*(x)-\frac{\lambda}{(\pi)^{\frac{1}{2}}}\int_{-\infty}^{+\infty}g(x,\beta)d\beta,$$
$$\partial^2 g/\partial x^2=\beta^4 g-2\beta^2\varphi^*, \quad \text{(A7)}$$

by the Fourier series:

$$\varphi^*(x)=\sum_{k=-\infty}^{+\infty}\varphi_k{}^*e^{i\pi kx},$$
$$g(x,\beta)=\sum_{k=-\infty}^{+\infty}g_k(\beta)e^{i\pi kx}. \quad \text{(A8)}$$

From the second of Eqs. (A7), we obtain

$$g_k(\beta)=2\beta^2\varphi_k{}^*/(\pi^2k^2+\beta^4), \quad \text{(A9)}$$

and from the first of Eqs. (A7),

$$\varphi_k{}^*=f_k{}^*-[\lambda\varphi_k{}^*/(\pi)^{\frac{1}{2}}]\int_{-\infty}^{+\infty}g_k(\beta)d\beta. \quad \text{(A10)}$$

[10] A. Bueche (unpublished communication).
[11] J. J. Hermans, Rec. Trav. Chim. des Pays Bas **63**, 219 (1944).

Substitution of (A9) into (A10) yields

$$\varphi_k^* = f_k^* - [2\lambda\varphi_k^*/(\pi)^{\frac{1}{2}}]\int_{-\infty}^{+\infty} \times[\beta^2 d\beta/(\pi^2k^2+\beta^4)]; \quad k\neq 0,$$
$$\int_{-\infty}^{+\infty}[\beta^2 d\beta/(\pi^2k^2+\beta^4)] = (\pi/2|k|)^{\frac{1}{2}}; \quad k\neq 0, \tag{A11}$$
$$\varphi_k^* = f_k^*/[1+\lambda(2/|k|)^{\frac{1}{2}}]; \quad k\neq 0.$$

Since by definition, Eq. (A3), φ_0^* vanishes, f_k^* must also vanish, and

$$\varphi_0 = f_0/\mu_0,$$
$$\mu_0 = \tfrac{1}{2}\int_{-1}^{+1}\mu(x)dx = 1+(8\sqrt{2}/3)\lambda, \tag{A12}$$

and the constant term in the Fourier series for $\varphi(x)$ is determined. Writing f_k^* as $f_k - \varphi_0\mu_k$, we obtain from Eqs. (A8), (A11), and (A12) the following Fourier series for $\varphi(x)$:

$$\varphi(x) = \frac{f_0}{1+8\sqrt{2}\lambda/3} + \sum_{k=-\infty,\pm 0}^{+\infty} \times[(f_k-\mu_k f_0/\mu_0)/(1+\lambda(2/|k|)^{\frac{1}{2}})]e^{i\pi kx},$$
$$\mu_k = \tfrac{1}{2}\int_{-1}^{+1}[1+2\lambda(1+x)^{\frac{1}{2}} + 2\lambda(1-x)^{\frac{1}{2}}]e^{-i\pi kx}dx, \tag{A13}$$
$$f_k = \tfrac{1}{2}\int_{-1}^{+1} f(x)e^{-i\pi kx}dx,$$

which is the desired solution of Eq. (A1), employed in the foregoing theories of viscosity and diffusion.

THE JOURNAL OF CHEMICAL PHYSICS VOLUME 16, NUMBER 6 JUNE, 1948

Intrinsic Viscosity, Diffusion, and Sedimentation Rate of Polymers in Solution

P. DEBYE AND A. M. BUECHE

(Received March 2, 1948)

Intrinsic viscosity, diffusion and sedimentation rate of polymers in solution is calculated by a generalization of Einstein's theory for impermeable spheres. For the coiled polymer molecule a sphere is substituted which hinders the liquid flow through its interior only to a degree depending on the average density in space of the polymer molecule in solution. The amount of shielding of the liquid flow which is introduced in this way determines the exponent in the customary exponential relation between intrinsic viscosity, diffusion, or sedimentation rate and molecular weight. This relation is shown to have only the merits of an interpolation formula. It is shown how the dimensions of the molecular coil can be derived from the experimental data on viscosity, and these dimensions are compared with those derived from interference measurements. The point is stressed that the relation between intrinsic viscosity and molecular weight is rather indirect and depends essentially on the type of polymer molecule under consideration. In most cases polymer molecules are decidedly stiffer and therefore cover a larger space in solution than would be expected from models with free rotation around bonds.

IN the preceding paper Kirkwood and Riseman refer to some theoretical calculations concerning intrinsic viscosity of Debye and similar calculations of Bueche concerning diffusion and sedimentation. Since these papers are not readily available* it seems appropriate, in order to facilitate a comparison of the different lines of attack, to present here the main features of the theoretical approach as conceived by one of the authors of this paper.**

If the mutual interaction of the beads of a

* The theory of viscosity was the subject of a report to the Office of Rubber Reserve presented in a meeting in Chicago, Oct. 31 and Nov. 1, 1946. A later report of A. M. Bueche dealt with sedimentation and diffusion. A paper containing the results concerning intrinsic viscosity as well as diffusion and sedimentation was submitted to Section 11 of the eleventh International Congress of Pure and Applied Chemistry (London: July 17th–24th, 1947). This paper has not yet been printed. Two short notes appeared, one in Phys. Rev. **71**, 486 (1947), the other in the Jan.–April issue of the Record of Chemical Progress, 1947.

** Calculations along the same line were made independently by H. C. Brinkman, Proc. Amsterdam Acad. **50**, No. 6 (1947); App. Sci. Res. **A1**, 27 (1947). Brinkman's results coincide with ours.

pearl string, which is substituted for a linear chain molecule with more or less free rotation, is neglected, the intrinsic viscosity is represented by the following relation:***

$$[\eta]=\frac{1}{36}\frac{f/\eta}{m}R^2. \tag{1}$$

$[\eta]$ is the intrinsic viscosity expressed in cc/gr (which is 100 times the value expressed in customary units); f the friction factor of one bead, defined in such a way that in order to drag one single bead through the liquid with a velocity v a force fv is needed; η is the viscosity of the solvent, m the mass of one bead, and R^2 the average square of the distance between the two ends of the chain. Since R^2 is proportional to the degree of polymerization, the relation confirms Staudinger's rule.

I

The assumption that the interaction can be neglected obviously cannot be accepted. As a matter of fact, each individual bead will move in a velocity field which deviates from the original undisturbed field because of the superposition of the disturbances caused by all the other beads. The situation is analogous to a case in which a dielectric medium is placed in an electric field and in which we find that in a point in the dielectric the field is distorted because of the disturbances caused by the polarization of all the other parts of the medium. In an attempt to formulate this idea such that care is taken of the essential features and at the same time the mathematical complications are reduced to a minimum, Debye comes to the following scheme.

In a homogeneous liquid, considered incompressible and with a viscosity η, the velocity $\bar{v}$ can be determined from the fundamental equations

$$\eta\,\mathrm{curl}\,\mathrm{curl}\bar{v}+\mathrm{grad}p=0,\quad \mathrm{div}\bar{v}=0, \tag{2}$$

in which p denotes the pressure. The first equation merely expresses that equilibrium exists between the frictional force on an element of volume and the force caused by local variations in pressure. As soon, however, as parts of the polymer molecule are situated in the element of volume under consideration, we have to take account also of the frictional force between the beads and the liquid. If we call the relative velocity of the liquid with respect to the molecule at the point in question, $\bar{v}_r$, the average value of this force acting on the liquid in an element of volume $d\tau$ will be

$$-\nu f\bar{v}_r d\tau,$$

provided the average number of beads contained in $d\tau$ is $\nu d\tau$. Adding this force to the forces already considered in (2) we arrive at a new set of equations, namely,

$$\eta\,\mathrm{curl}\,\mathrm{curl}\bar{v}+\nu f\bar{v}_r+\mathrm{grad}p=0,\quad \mathrm{div}\bar{v}=0. \tag{3}$$

From the statistics of the chain molecule we know the bead density ν as a function of the distance from the center of gravity. For the relative velocity $\bar{v}_r$ we can substitute the actual velocity of the liquid $\bar{v}$ minus a velocity $\bar{v}_0$ corresponding to the proceeding and rotating molecule. In this way the problem of finding the velocity of the liquid everywhere, inside and outside of the space occupied in the average by the polymer molecule, is now reduced to finding the appropriate solution of the set of Eqs. (3). And, of course, as soon as we know this velocity distribution, the additional heat developed due to the immersion of one polymer molecule can be found, and the intrinsic viscosity can be calculated along familiar lines.

The main point to consider before proceeding with the solution of Eq. (3) is the average density in space of the beads. From a consideration of the statistics of the chain it is found that this density is a maximum around the center of gravity of the polymer molecule, and with increasing distance r of this point ν decreases gradually. The function $F(r)$ which represents this density has a shape which resembles a Gaussian probability curve. At this stage I have not considered it worth while to go ahead and solve our problem using the exact representation of the density. It is more than probable that the essential features of the final result will depend only in minor details on the exact form of $F(r)$. Instead I propose to substitute as a picture for the average space occupied by the polymer molecule a sphere of radius R_s in which the bead density ν is supposed to be constant throughout,

*** P. Debye, J. Chem. Phys. **14**, 636 (1946).

whereas outside of this sphere $\nu=0$. If N is the total number of beads of the string, we then have inside the sphere

$$\nu=(3/4\pi)(N/R_s^3). \quad (4)$$

In this formulation we have to find solutions of Eq. (3), one for the outside of the sphere of radius R_s with $\nu=0$, another for the inside with ν equal to the constant value given by Eq. (4). The constants appearing in these solutions have to be adjusted in such manner that at large distances we have the original undisturbed velocity distribution. At the surface of the sphere the velocities inside and outside must be the same as well as the stresses.

The mathematical method which leads to this goal is a generalization of a method derived by *G. Kirchhoff*, formerly used by *A. Einstein* in his well-known but simpler problem of calculating the effect of a number of immersed *impermeable* spheres on the over-all viscosity.†

The angular velocity of the whole molecule can be left indeterminate at the outset, but using the condition, as in the simpler case in which no interaction was considered, that the average total torque on the molecule must be zero, it turns out that just as before this angular velocity still is equal to half the gradient of the velocity of the liquid.

Accepting the form which has now been given to the problem, it is readily seen that apart from the number of beads, N, only two constants each of the dimension of a length enter into it. The first is, of course, the radius R_s of the substituted spherical space occupied in the average by the polymer molecule. The second is a length L defined by the relation

$$1/L^2=\nu(f/\eta), \quad (5)$$

in which ν is the bead density according to Eq. (4). I would like to call L the "*shielding length*" for the following reason. Consider a much simpler case in which a liquid is flowing free in the x direction with a velocity having a gradient α in the z direction everywhere above the plane $z=0$, whereas below this plane the flow is hindered by an accumulation of beads, distributed with constant density ν. Using Eq. (3), we find that in this latter part, that is for negative values of z, the velocity v_x decreases exponentially and is proportional to $\exp(z/L)$. The lower part of the medium is therefore shielded by the accumulated effect of the beads, and the distance in this part over which the velocity decreases by a factor $1/e$ is our shielding length L. I understand that the same formulation as expressed by Eq. (3) is used by engineers in discussing the flow of water through sand.

The advantage of using the approximation of constant bead density in our problem of the rotating sphere is that all the functions which have to be introduced as solutions of the equations can be expressed by elementary functions. By a queer coincidence the fundamental equation which has to be satisfied is of the same type as that describing the potential around an ion in a strong electrolyte.

Skipping now all further mathematical details, the final result for the intrinsic viscosity appears in the following form:

$$[\eta]=(\Omega_s/M)\phi(\sigma)\cdots\sigma=R_s/L. \quad (6)$$

$\Omega_s=(4\pi/3)R_s^3$ is the spherical volume occupied by the sphere substituted for the polymer molecule, M is its actual mass, and $\phi(\sigma)$ is a function of a number $\sigma=R_s/L$, which I would like to call the "shielding ratio."†† This function is represented by Eq. (7):

$$\phi(\sigma)=\frac{5}{2}\frac{(1+(3/\sigma^2)-(3/\sigma)\operatorname{cotgh}\sigma)}{1+(10/\sigma^2)(1+(3/\sigma^2)-(3/\sigma)\operatorname{cotgh}\sigma)}. \quad (7)$$

For small values of the shielding ratio σ we have

$$\phi(\sigma)=\sigma^2/10[1-(2/35)\sigma^2+\cdots]. \quad (8)$$

Substituting the first approximation of ϕ for small values of σ in Eq. (6) and remembering the definition of ν and L as expressed by Eqs. (4) and (5), we find in the limit for $\sigma=0$

$$[\eta]=1/10(f/\eta m)R_s^2. \quad (8')$$

This relation should be compared with Eq. (1), which was derived directly (without using the approximation of the substituted sphere with constant bead density) for the case of infinitely small shielding effect. If we do this we see that in

† A. Einstein, Ann. d. Physik (4) **19**, 289 (1906); **34**, 591 (1911).

†† The intrinsic viscosity is again expressed in cc/g.

order to obtain coincidence we should take $R_s^2/10$ equal $R^2/36$, and this means that the diameter $2R_s$ of our spherical volume should be taken equal to $1.054R$. This diameter is therefore very nearly equivalent to R, the square root of the average square of the distance between ends of the chain.

For large values of the shielding ratio we have

$$\phi(\sigma)=5/2[1-(3/\sigma)-\cdots], \tag{9}$$

and

$$[\eta]=5/2(\Omega_s/M)=5/2(\Omega_s/Nm). \tag{9'}$$

This is Einstein's relation for rigid impenetrable spheres, as it should be.

It is of interest to observe that the important features which determine the intrinsic viscosity are *not* primarily concerned with the molecular weight. They are, as seen from (6): firstly, the specific volume of the material of the polymer molecule as distributed over the average space occupied by this molecule in the liquid; secondly, the shielding ratio σ. However, if we know the structure of the molecule we can connect both these quantities with the degree of polymerization N (or the molecular weight). So for linear chains we know that R or R_s is proportional to $N^{\frac{1}{2}}$, and we see immediately from (8') and (9') that in this case we can find anything between proportionality with N to proportionality with $N^{\frac{1}{2}}$ depending on the shielding ratio. However, if the chain is not linear, if, for instance, the molecule is highly cross-linked, a very different dependence on the molecular weight will prevail. Under such circumstances we can have very high molecular weights combined with relatively small intrinsic viscosities.

It remains to be seen how the customary formula for the intrinsic viscosity with an exponent of the molecular weight between 1 and $\frac{1}{2}$ has to be interpreted.

If we assume a linear chain ($R_s \sim N^{\frac{1}{2}}$) and draw according to Eq. (6) a curve for the intrinsic viscosity as a function of the degree of polymerization, we will find that it begins proportional to N and that its slope gradually decreases with increasing N until for very large N we end up with a proportionality to $N^{\frac{1}{2}}$. At any point of this curve for a given value $N=N_0$ we can approximate the curve by its tangent, representing it by the linear function

$$[\eta]=\alpha+\beta(N-N_0) \tag{10}$$

with two constants α and β. This would be the usual procedure. But of course this procedure is arbitrary inasmuch as we decided arbitrarily on the outset that a linear approximation was what we wanted to use. We can just as well decide that in the vicinity of $N=N_0$ we want to approximate the curve by an expression of the form

$$[\eta]=AN^{\epsilon} \tag{10'}$$

with two other constants A and ϵ. If we take the logarithm on both sides of (10'), we see that the meaning of this second form of approximation is to draw a curve for $\log[\eta]$ as a function of $\log N$ and to approximate this new curve by its tangent. Fundamentally and from a purely mathematical point of view, there is no difference between the two procedures, but in our special case the exponential approximation according to (10') has a peculiar advantage. We know that our formula, as well as any other formula which might be proposed, makes $[\eta]=0$ for $N=0$. The exponential approximation formula (10') does this also, automatically, whereas the linear approximation (10) does not. In this way it turns out that the exponential approximation has really 3 points in common with the actual curve, whereas the linear approximation has only 2. We will therefore expect that the exponential approximation will not usually deviate much from the actual curve over a large range of values N. This is actually what is observed. We have here before us a case in which a special formula fits the experimental data very well, and still it would be wrong to conclude that its special form has any fundamental importance.

From what has been said about the meaning of the exponential approximation, it follows immediately that *for a linear chain*

$$\epsilon=\frac{d\log[\eta]}{d\log N}=\frac{N}{[\eta]}\frac{d[\eta]}{dN}=\frac{1}{2}+\frac{1}{4}\frac{\sigma\, d\phi}{\phi\, d\sigma}. \tag{11}$$

To every value N of the degree of polymerization belongs a definite exponent ϵ, which can be calculated from (11) as a function of the shielding ratio σ. The following table gives corresponding

values of the shielding ratio σ, the function ϕ (which for reasons apparent from Eq. (6) is called the volume factor), and the exponent ϵ.

In order to illustrate the use of this table, we can take some measurements of R. H. Ewart on polystyrene in benzene. Ewart represents his results by the interpolation formula

$$[\eta]=7.54\cdot 10^{-3}\,(MW)^{0.783} \tag{12}$$

in which the intrinsic viscosity is measured in cc/g. and MW indicates the customary molecular weight. The measurements covered a range from $MW=50000$ to $MW=800000$. The average molecular weight of this interval (the average being taken in the logarithmic diagram) is $MW=200000$. We will assume that the exponent 0.783 corresponds exactly to this average MW. Now assuming that polystyrene is a linear polymer, we find by interpolation in Table I that $\epsilon=0.783$ corresponds to $\sigma=3.92$ and $\phi=0.836$. At the same time Ewart's relation (12) gives for $MW=200000$ the value $[\eta]=107$ cc/g. From Eq. (6) it follows that the specific volume of the polymer substance within the substituted sphere is $\Omega_s/M=128$ cc/g. Since we know the mass of the polymer molecule, we now can calculate the volume Ω_s and the diameter $2R_s$ of this sphere and find $2R_s=431$A. If we decide that the relation $2R_s=1.054R$, which holds for the limiting case $\sigma=0$, can be used, we will conclude that for a linear polystyrene molecule in benzene of $MW=200000$ the root mean square distance between ends $R=409$A, which is 3 times as large as the theoretical value of a C−C chain with absolutely free rotation.

TABLE I. (Linear polymers) $[\eta]=(\Omega_s/M)\phi$.

Shielding ratio σ	Volume factor ϕ	Exponent ϵ
0	0	1.000
1	0.0947	0.973
2	0.327	0.910
3	0.600	0.839
4	0.857	0.778
5	1.07	0.731
6	1.25	0.693
7	1.40	0.664
8	1.52	0.642
9	1.62	0.625
10	1.70	0.611
15	1.96	0.569
20	2.10	0.549
∞	2.50	0.500

II

A. M. Bueche has applied the same line of reasoning to the problem of diffusion and sedimentation. If a polymer molecule is dragged through a liquid with the velocity v, a force Fv will have to be applied. The friction constant F is the essential quantity in sedimentation experiments, the diffusion constant D follows from Einstein's relation

$$D=kT/F. \tag{13}$$

For the friction constant F Bueche finds

$$F=6\pi\eta R_s\psi(\sigma) \tag{14}$$

in which ψ is again a function of the shielding ratio σ analogous to ϕ. It is defined by the relation

$$\psi(\sigma)=\frac{(1-(1/\sigma)Tgh\sigma)}{1+(3/2\sigma^2)(1-(1/\sigma)Tgh\sigma)}. \tag{15}$$

For small σ we have

$$\psi=(2/9)\sigma^2[1-(4/15)\sigma^2+\cdots], \tag{16}$$

which leads in the limiting case $\sigma=0$ to

$$F=Nf, \tag{16'}$$

remembering the definition of the shielding length L by Eq. (5). This is exactly what has to be expected since, if we neglect all interaction, the force on N beads is N times as large as that on a single bead.

For large σ we have

$$\psi(\sigma)=1-(1/\sigma)-\cdots, \tag{17}$$

which leads to Stokes' formula

$$F=6\pi\eta R_s. \tag{17'}$$

TABLE II. (Linear polymer) $F=6\pi\eta R_s\psi$.

Shielding ratio σ	Volume factor ψ	Exponent ϵ
0	0.000	1.000
1	0.176	0.899
2	0.432	0.752
3	0.600	0.661
4	0.701	0.610
5	0.770	0.574
8	0.858	0.544
10	0.890	0.532
∞	1.000	0.500

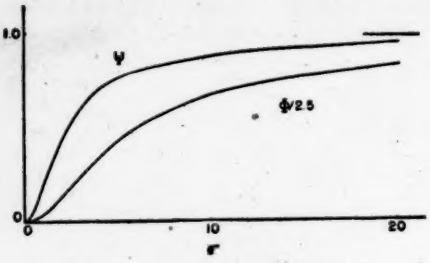

FIG. 1. Volume factor Φ and radius factor Ψ as functions of the shielding ratio σ.

Again as in the case of the intrinsic viscosity, the friction constant F can be represented by an exponential formula of the type

$$F=AN^{\epsilon}$$

over a limited range of molecular weights and again there will exist a one-to-one correspondence between ϵ and σ, according to the relation

$$\epsilon=\frac{1}{2}+\frac{1}{4}\frac{\sigma\, d\psi}{\psi\, d\sigma}. \tag{18}$$

Table II contains corresponding values of the shielding ratio σ, the "radius factor" ψ, and the exponent ϵ for the case of linear polymers. In Fig. 1 the two functions $\phi/2.5$ and ψ are shown plotted as functions of the shielding ratio σ.

III

We now have two theoretical representations of the intrinsic viscosity and two of the friction constant, one type attributable to Kirkwood and Riseman, which we will indicate by the letters K.R., and one type discussed in this paper to be indicated by the letters D.B.

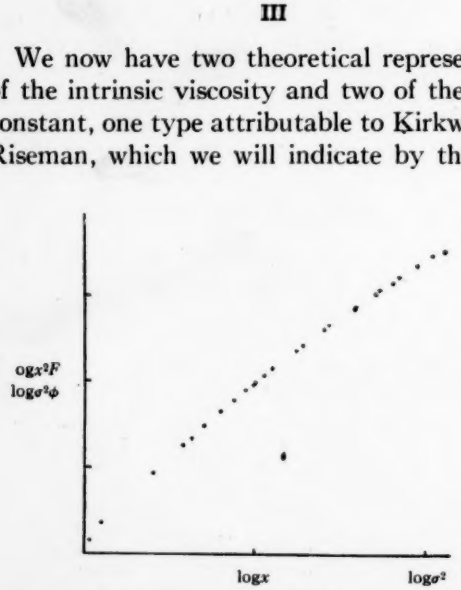

FIG. 2. Comparison of the Kirkwood-Riseman representation of intrinsic viscosity with that of Debye-Bueche. Circles for K.R., cross for D.B.

In making the calculations of the K.R. type a pearl string with small beads is substituted for the polymer and it is assumed that the links connecting the beads do not experience any friction. The very interesting mathematical treatment cannot be carried out quite rigorously; interchanges of averaging processes have to be introduced. In the calculations of the D.B. type a permeable sphere is substituted for the polymer, and its permeability is connected with the monomer number in the polymer. Once the problem has been formulated mathematically, it is solved rigorously.

The question now arises as to which of the two types of representation is better as compared with the experimental facts. Confirming our attention to the intrinsic viscosity alone, K.R. as well as D.B. are satisfied with the performance in the few examples for which sufficiently accurate data are available. It seems, therefore, that we should ask how much difference exists between the two types when each of them is used to represent a definite set of experimental values.

In the K.R. case the intrinsic viscosity is represented by a formula of the type

$$[\eta]=Ax^2F(x), \quad x=BN^{\frac{1}{2}}, \tag{19}$$

in which A and B are adjustable constants and N is the degree of polymerization. The function F and the variable x are those used in the K.R. paper. In the D.B. case the intrinsic viscosity is represented by a formula of the type

$$[\eta]=A^*\sigma^2\phi(\sigma), \quad \sigma^2=B^*N^{\frac{1}{2}}, \tag{19'}$$

with two adjustable constants A^* and B^*. The function ϕ and the variable σ are those used in this paper.

A comparison of the two types can most easily be carried out, without any reference to specific experimental values, by plotting on one sheet of paper $\log(x^2F)$ as a function of $\log x$, and on another transparent sheet $\log(\sigma^2\phi)$ as a function of $\log\sigma^2$. After superimposing the two sheets, the transparent sheet is moved until the two curves are estimated to coincide as well as possible, always keeping the corresponding axes of the two sheets parallel. This has been done using the

F values from the K.R. table and the ϕ values from the D.B. table. The result of this superposition is represented in Fig. 2, the circles are K.R. points, the crosses D.B. points. The length of the decades is indicated on the axes. Since the horizontal axis covers 2 decades, which means a factor 10^4 in the degree of polymerization, and the vertical axis comprises 3 decades, which means a factor 10^3 in the intrinsic viscosity, it seems that only one conclusion can be drawn. Both types of representation show such exceedingly small deviations from each other that with proper adjustment of the constants, A and B in the one case, A^* and B^* in the other, no preference can be given to either. It is, of course, still possible that a set of experimental data may deviate, but if it does so, we have to expect that these deviations will be just as serious in the one case as in the other.

We now come to the interpretation of the constants in terms of the fundamental molecular quantities. One of these quantities is the friction factor of the monomer: ζ in the K.R. paper, f in the D.B. paper. The four authors agree that no theory exists which links this factor adequately with the structure of the monomer and that an attempt to represent it by a Stokes sphere turns out to be very unsatisfactory indeed. The other quantity appears in two forms, in the K.R. theory it is the root mean square distance R of the ends of the linear chain, in the D.B. theory it is the diameter $2R_s$ of the substituted sphere. In this last case a comparison with the R value of a linear chain can only be made for the limiting case of small shielding and then it is found that $2R_s = 1.054R$. It is evident that further progress can only be made if the R value can be determined by some other independent method. As such we now have the interference method based on the difference of the intensity of the light scattered by the solution in different directions,††† for which in appropriate cases also the dependence of the scattered intensity on the wave-length of the light can be substituted. The theory of the interference effect is decidedly more reliable than a theory of viscosity can ever expect to be.

Three sets of dissymmetry measurements performed on polystyrene are known to us. Reducing the experimental sets of data which have been obtained with polymers of different molecular weights to a common molecular weight of 10^6, the following values of R in A units have been found: Doty for polystyrene in toluene 1080, Ewart for polystyrene in carbon tetrachloride 1050, Bueche for polystyrene in benzene 1110. I believe that the very close agreement is accidental to some degree. In the K.R. paper R is found from viscosity measurements equal to 1125, in this paper we found as a result from our discussion of one set of measurements 914. It seems, therefore, that the experimental evidence from light scattering favors the K.R. representation. However, viscosity measurements of Bueche on the same samples on which he measured the light scattering, discussed according to the D.B. schedule, lead to $R = 1030$. Taking the average of all the values without any preference and disregarding the use of different solvents in the interference measurements, since all 3 liquids are good solvents, we arrive at $R = 1050$. As far as the experimental evidence goes we have to conclude that we do not yet have a clear-cut case.

There is general agreement about the one point that polystyrene is much more extended than we would calculate from the usual formula in which free rotation is assumed, since this formula leads to $R = 300$ which is 3.5 times smaller than the average experimental value.

Another final point has to be considered which happens to be in favor of the D.B. treatment. The K.R. treatment is restricted to a linear chain. Many of the polymers may be branched or cross-linked. If this is so or if we do not definitely know from the beginning that the polymer is linear, the substitution of the sphere of the D.B. treatment seems to be indicated.

††† P. Debye, J. Phys. a. Coll. Chem. **51**, 18 (1947).

Infra-Red Vibrations in NaCl*

JORDAN J. MARKHAM**
Brown University, Providence, Rhode Island

(Received November 4, 1947)

A detailed calculation has been made of the propagation properties of the lattice vibrations in NaCl. The phase velocity, the group velocity, displacement angle (angle between the particle displacement and the direction of propagation), and the displacement ratio were calculated as a function of wave-length for three directions of propagation. In these calculations, Born's theory was used. The crystal has a low pass (acoustical) and at times overlapping upper band (optical). At the lowest frequency the waves are simply elastic ones. As the frequency increases, the structure exhibits strong dispersion. In the limit of shortest wave-length, the group velocity approaches zero. The optical branch is highly dispersive at all frequencies. The group velocity is negative (on the single-zone scheme), and approaches zero at both the short and long wave-length limits. Generally, for both branches at the short wave-length limit the particle displacement lines up along the direction of nearest neighbors. Exceptions to this occur for propagation along some highly symmetrical direction.

INTRODUCTION

ONE may approach the vibrations of solids from two points of view. The simpler method considers a crystalline solid to be an anisotropic continuum. The second treats it as a system of coupled vibrating particles. In the one-dimensional case, the first method corresponds to the problem of the continuous vibrating string, while the second method is analogous to the treatment of the loaded string. One would expect the simpler method to give correct results only for wave-lengths long compared with the distance between neighboring particles.

The purpose of this paper is to make a detailed theoretical study of the normal modes of vibrations in NaCl using Born's theory of ionic crystals. Particular study is made of wave transmission through the crystal. The phase and group velocities, the displacement angle (angle between the particle displacement and the direction of propagation) and the displacement ratio (ratio of the displacement of the sodium ion to the chlorine ion) are calculated for several directions of propagation. Detailed calculations of the propagation properties of waves through highly simplified ideal crystals have been made by various authors. These are well summarized by Brillouin.[1] To the author's knowledge no one has made actual calculations of the sort referred to here for real crystals. The present calculations use Kellermann's[2] equations relating the wave vector to the frequency. Kellermann gives an integrated picture of all the vibrations and particularly their relation to the specific heat problem. Here we consider the individual waves in detail and study more of their properties than are given in reference 2. It is hoped that these calculations will permit some generalizations regarding the properties of waves of this type.

We may briefly summarize the properties of the waves as found from the calculations on ideal crystals.[1]

(1) In general, there are two classes of waves for a crystal with more than one type of particle. The lower branches (acoustical) behave similarly to an elastic wave at the lower frequency. At the high frequencies, when the wave-length becomes of the order of the distance between particles, these waves become dispersive. The higher branches (optical) are dispersive at all frequencies.

(2) The crystal behaves essentially as a filter made of a combination of a low pass band and a series of upper pass bands.

(3) Since the waves are dispersive, the energy is propagated with the group velocity. For a linear crystal, it becomes zero at the short wave-

* Part of a dissertation presented to the faculty of the Graduate School of Brown University in candidacy for the degree of Doctor of Philosophy.

** Now at the University of Pennsylvania, Philadelphia, Pennsylvania.

[1] Brillouin, *Wave Propagation in Periodic Structures* (McGraw-Hill Book Company, Inc., New York, 1946), Chapters IV, V, and VI.

[2] E. W. Kellermann, Phil. Trans. **A238**, 513 (1940).

length limit (on the reduced zone scheme).[3] In a two-dimensional crystal the group velocity decreases with decreasing wave-length but does not necessarily go to zero at the limit.[4]

(4) Now consider the displacement of the particles as the wave travels through the crystal. Again, for the long wave-lengths in the diatomic chain the acoustical branch behaves similarly to a continuum. At the short wave-length limit, however, only the heavier particles are displaced. In the optical branch, at the long wave-length limit the particles vibrate 180° out of phase, while at the short wave-length limit only the light particles vibrate. In the two-dimensional crystal, in general, the waves are not pure transverse or pure longitudinal, but are quasi-longitudinal—when the angle between the wave vector and the particle displacement is less than 45°—or quasi-transverse. At the short wave-length limit the displacements line up along the direction of nearest neighbors.

GENERAL EQUATIONS FOR VIBRATION WITHIN IONIC CRYSTALS

This paper follows Kellermann's technique in obtaining the equations for the normal modes in an ionic crystal. To calculate this, the classical (Born) model of an ionic crystal is used. The basic assumption is that only central forces act between the ions and that these can be divided into two types. The first is the Coulomb force and the second is a short-range repulsive force.

Let us assume that our crystal has n^3 cells and p particles per cell. Then the position vector of the Kth particle in the lth cell is given by

$$\mathbf{r}_K{}^l = \mathbf{a}^l + \mathbf{r}_K, \tag{1}$$

where $\mathbf{r}_K$ is the vector from the origin of a cell to the Kth particle in the same cell, and $\mathbf{a}^l$ is the vector from the origin of the crystal to the origin of the lth cell. Further, we denote the potential energy due to the interaction between the K'th particle in the l'th cell and the Kth particle in the lth cell by $\varphi_{KK'}{}^{l-l'}$. If one of the l's is omitted when this expression appears in a summation, it means that one of the particles is in the original cell. Thus the total potential energy of the crystal is

$$\Phi = \tfrac{1}{2} \sum_{KK'} \sum_{ll}{}' \varphi_{KK'}{}^{l-l'}. \tag{2}$$

The prime on the second sum means that we omit the term for which $l=l'$ when $K=K'$.

To simplify the analysis, it is necessary to assume an explicit type of vibration. Following Born and von Kármàn we assume that the displacement of the particle from its equilibrium position is:

$$\mathbf{u}_K{}^l = \mathbf{U}_K \exp\{-i\omega t + 2\pi i \mathbf{s}\cdot\mathbf{r}_K{}^l\}, \tag{3}$$

where $\mathbf{U}_K$ is the displacement amplitude, which is independent of the position of the cell, ω is the angular frequency, and $\mathbf{s}$ is the wave vector. The exact method of specifying the $\mathbf{s}$ vector has been a subject of lengthy discussion in recent years between Raman and Born. In the author's opinion, the Born condition has a sounder theoretical basis and gives a better agreement with experiment.[5,6] As a consequence of the Born-von Kármàn periodic boundary condition for the lattice, it follows for NaCl (reduced zone scheme) that:

$$\mathbf{s} = (1/2r_0)\{q_x, q_y, q_z\}. \tag{4}$$

TABLE I. Additional binding coefficients for cut No. 1 $q_x = 2q_y$; $q_z = 0$.

q_z	$C(11; xx)(v/e^2)$	$C(11; yy)(v/e^2)$	$C(11; zz)(v/e^2)$	$C(12; xx)(v/e^2)$	$C(12; yy)(v/e^2)$	$C(12; zz)(v/e^2)$	$C(11; xy)(v/e^2)$	$C(12; xy):(v/e^2)$
0.2	−5.544	1.586	3.949	6.405	−1.820	− 4.581	−4.905	4.647
0.3	−5.154	1.502	3.653	7.030	−1.975	− 5.063	−4.734	4.204
0.5	−4.033	1.353	2.690	8.765	−2.216	− 6.520	−4.090	2.975
0.6	−3.363	1.334	2.033	9.687	−2.250	− 7.436	−3.529	2.322
0.7	−2.665	1.370	1.319	10.506	−2.091	− 8.424	−2.831	1.663
0.9	−1.342	1.538	−0.192	11.278	−1.006	−10.275	−1.016	0.491

[3] F. Seitz, *Modern Theory of Solids* (McGraw-Hill Book Company, Inc., New York, 1940), p. 117.
[4] Reference 1, p. 121ff.
[5] E. W. Kellermann, Proc. Roy. Soc. **A178**, 17 (1941); M. Blackman, Proc. Phys. Soc. London **54**, 377 (1942). The second paper gives a summary of data. B. Dayal, Proc. Ind. Acad. **A19**, 182 (1944).
[6] For reference to recent work on the connection between Born's theory of vibrations and the Raman effect see E. Gross and A. Stehanov, Nature **159**, 474 (1947) and references given there.

TABLE II. Summary of data for cut No. 1.

q_x	$\nu^{(1)}\times10^{-12}$ sec^{-1}	$v^{(1)}\times10^{-6}$ (cm/sec)	$u^{(1)}\times10^{-6}$ (cm/sec)	$\rho^{(1)}$	$\delta_{Na}{}^{(1)}$	$\delta_{Cl}{}^{(1)}$	$\nu^{(2)}\times10^{-12}$ sec^{-1}	$v^{(2)}\times10^{-6}$ (cm/sec)	$u^{(2)}\times10^{-6}$ (cm/sec)	$\rho^{(2)}$	$\delta_{Na}{}^{(2)}$	$\delta_{Cl}{}^{(2)}$
0.2	9.33	2.347		−1.57[a]	180.5°	0.6°	4.49	1.129		−1.58[a]	270.6°	90.4°
0.3	9.01	1.511	−0.19	−1.60	181.1°	1.2°	4.42	0.742		−1.64	271.6°	90.6°
0.4	8.58	1.079	−0.24	−1.67	181.9°	2.3°	4.34	0.547		−1.75	273.1°	89.9°
0.5	8.07	0.813	−0.28	−1.77	182.7°	3.5°	4.28	0.431	average	−1.99	277.6°	82.5°
0.6	7.48	0.628	−0.30	−1.93	183.2°	4.7°	4.34	0.365	−0.004	−1.30	310.1°	16.1°
0.7	6.88	0.494	−0.31	−2.27	182.8°	6.1°	4.62	0.332		−0.79	320.4°	1.0°
0.8	6.25	0.395	−0.29	−3.01	180.3°	8.2°	4.74	0.298		−0.80	307.3°	−2.2°
0.9	5.73	0.320	−0.20	−8.28	172.0°	18.0°	4.69	0.262		−1.09	270.7°	−6.9°
1.0	5.44	0.274	0[b]	−13.0[c]	153.4°	153.4°	4.63	0.233		$-\infty$[b]	243.4°	—

q_x	$\nu^{(3)}\times10^{-12}$ sec^{-1}	$v^{(3)}\times10^{-6}$ (cm/sec)	$u^{(3)}\times10^{-6}$ (cm/sec)	$\rho^{(3)}$	$\nu^{(4)}\times10^{-12}$ sec^{-1}	$v^{(4)}\times10^{-6}$ (cm/sec)	$u^{(4)}\times10^{-6}$ (cm/sec)	$\rho^{(4)}$	$\delta_{Na}{}^{(4)}$	$\delta_{Cl}{}^{(4)}$
0.2	4.60	1.157		−1.57[a]	1.75	0.440	0.42	0.98[a]	− 3.9°	−4.2°
0.3	4.65	0.779		− 1.62	2.55	0.427	0.38	0.96	− 3.8°	−4.8°
0.4	4.71	0.593		− 1.71	3.25	0.408	0.32	0.92	− 2.5°	−5.9°
0.5	4.81	0.484		− 1.80	3.82	0.385	0.22	0.85	3.9°	−9.0°
0.6	4.90	0.411	average	− 2.04	4.15	0.348	0.09	1.38	68.8°	140.0°
0.7	5.00	0.359	−0.04	− 2.55	4.19	0.301	0.03	2.25	82.4°	132.7°
0.8	5.14	0.323		− 3.53	4.28	0.269	0.06	2.40	81.3°	149.6°
0.9	5.30	0.296		− 5.73	4.41	0.246	0.02	1.43	76.0°	163.2°
1.0	5.44	0.274		−13.0[c]	4.38	0.220	0[b]	0.12[d]	−26.6°	153.4°

q_x	$\nu^{(5)}\times10^{-12}$ sec^{-1}	$v^{(5)}\times10^{-6}$ (cm/sec)	$u^{(5)}\times10^{-6}$ (cm/sec)	$\rho^{(5)}$	$\delta_{Na}{}^{(5)}$	$\delta_{Cl}{}^{(5)}$	$\nu^{(6)}\times10^{-12}$ sec^{-1}	$v^{(6)}\times10^{-6}$ (cm/sec)	$u^{(6)}\times10^{-6}$ (cm/sec)	$\rho^{(6)}$
0.2	1.04	0.262	0.26	0.97[a]	85.9°	86.0°	0.97	0.245	0.25[e]	1.01[a, f]
0.3	1.54	0.259	0.25	0.94	85.4°	85.7°	1.47	0.246	0.25[e]	0.95
0.4	2.02	0.254	0.22	0.88	84.9°	85.5°	1.97	0.248	0.26	0.91
0.5	2.43	0.245	0.21	0.80	84.0°	85.7°	2.48	0.250	0.26	0.84
0.6	2.85	0.239	0.19	0.65	80.8°	84.9°	2.99	0.251	0.24	0.75
0.7	3.18	0.229	0.15	0.46	76.0°	84.8°	3.45	0.247	0.22	0.63
0.8	3.44	0.216	0.11	0.27	63.8°	83.9°	3.85	0.242	0.18	0.46
0.9	3.63	0.203	0.08	0.14	43.2°	79.4°	4.17	0.233	0.13	0.28
1.0	3.74	0.188	0[b]	0[b]		63.4°	4.38	0.220	0[b]	0.12[d]

[a] Strictly speaking, the displacement ratio is a complex number since the displacements are not 180° apart.
[b] Estimated value from graph.
[c] This value is unreliable. It may be ∞.
[d] This value is unreliable. It may be zero.
[e] The author does not believe that $u^{(6)}$ exceeds $v^{(6)}$ for the same value of q_x.
[f] The author does not believe that $\rho^{(6)}$ actually exceeds unity.

The expression on the right means the vector whose x component is given by $q_x/2r_0$, etc. As is the custom, we have selected the x, y, and z axes to lie along the direction of nearest neighbors, which are r_0 apart. The restrictions on the q's are

$$|q_x|+|q_y|+|q_z|\leqslant 1.5;\quad |q_x|\leq 1;\quad |q_y|\leq 1;\quad |q_z|\leq 1. \quad (5)$$

Strictly speaking, only specific values of the q's are allowed, since the crystal has only $3pn^3-6$ degrees of freedom, but since n is very large, we may consider the points to be dense and select arbitrary values of $\mathbf{s}$.

Now with the use of Lagrange's equations it is possible to obtain the following expression relating the ω's to the $\mathbf{U}$'s,

$$\omega^2 m_K U_{Kx}+\sum_{K'}\sum_{y}(KK';xy)U_{Ky}=0: \quad (x, y=x, y, z), \quad (6)$$

where m_K is the mass of the Kth particle, and U_{Kx} is the x component of $\mathbf{U}_K$. We further define:

$$(KK';xy)=\sum_{l}(\varphi_{KK'}{}^{l})_{xy}\exp\{2\pi i\mathbf{s}\cdot\mathbf{r}_{KK'}{}^{l}\}, \quad (7)$$

$$(\varphi_{KK'}{}^{0})_{xy}=-\sum_{K'}\sum_{l}{}'(\varphi_{KK'}{}^{l})_{xy}. \quad (8)$$

The subscripts x and y in (7) and (8) imply partial differentiation with respect to x and y. In order to obtain Eq. (6), one uses Taylor's theorem and neglects higher order terms. $(KK';xy)$ is called a binding coefficient.

Formally the evaluation of the ω's and $\mathbf{U}$'s is identical with the problem of finding eigenvalues of a matrix.[7] Explicit expressions must, of course,

[7] R. A. Frazer, W. J. Duncan, and H. R. Collar, *Elementary Matrices* (Cambridge University Press, Teddington, 1938).

be given for the binding coefficients. We shall not go into that lengthy phase of the problem.[2]

Kellermann estimates his error in the binding coefficients to be 1 to 2 percent. In the present calculations a fixed number of terms were carried in the expansion for the binding coefficients. Only in one case was the leading omitted term greater than 1 percent of the binding coefficient; this occurred for the smallest (absolute) coefficient (see Table I). In general, the leading omitted term was much less. The accuracy in calculating the frequency is about the same as Kellermann's. Of course, in calculating some of the other quantities, e.g., group velocity, such an accuracy cannot be expected. Errors of 5 percent or greater are possible in the group velocity values presented in the tables.

Kellermann's primary interest was in the frequency distribution function obtained by solving Eq. (6) and relating it to the specific heat problem by Einstein's equation. We shall here be interested in the U's as well as the frequency and relate them to the wave vector s.

CALCULATIONS ON NaCl

In evaluating the propagation properties of the wave, an arbitrary direction was selected, keeping the ratio of the vector components constant and varying the wave-length. The most general case (cut) considered corresponds to

$$q_x=2q_y; \quad q_z=0. \tag{9}$$

The wave vector is thus in the xy plane and makes an angle of 26° 34′ with the x axis. Admittedly, this is a rather specialized direction; it was selected to simplify the calculations. The wave-lengths were selected by letting q_x take on the values 0.2, 0.3, 0.4, $\cdots$0.9, 1.0. The wave-length is given by

$$\lambda=2r_0/(q_x^2+q_y^2+q_z^2)^{\frac{1}{2}}. \tag{10}$$

From a further development[2] of Eq. (7), the binding coefficients were calculated. Actually for four values of q_x—namely, $q_x=0$, 0.4, 0.8, and 1.0—the coefficients and the ω's have been calculated by Kellermann. In Table I, the Coulomb part for the new $\mathbf{q}$'s is given. This part of the coefficient depends only on the lattice structure and on the ionic charge. The superscript C refers to the Coulomb part of the binding coefficient given by Eq. (7), v is the cellular volume, and e is the charge on the electron. By adjusting the ratio of the cellular volume to the ionic charge, these coefficients can be used for any NaCl type of ionic crystal. The repulsive part of the coefficient is not given, since it can be calculated easily from the formulae found in Kellermann's paper. As a check, a few coefficients were recalculated. These values showed excellent agreement. Usually the difference was less than a tenth of a percent. Thus, Table I is really an extension of the second table found in Kellermann's paper.[8]

Once the coefficients are known, we may use Eq. (6) to calculate the ω's and the $\mathbf{U}$'s. From these values the summary table of the propagation properties (Table II) has been prepared. The phase velocity v, columns 3 and 9, is given by $v=\nu\lambda$, which can be put into the form

$$v=\frac{1}{\pi}\frac{r_0}{(q_x^2+q_y^2+q_z^2)^{\frac{1}{2}}}. \tag{11}$$

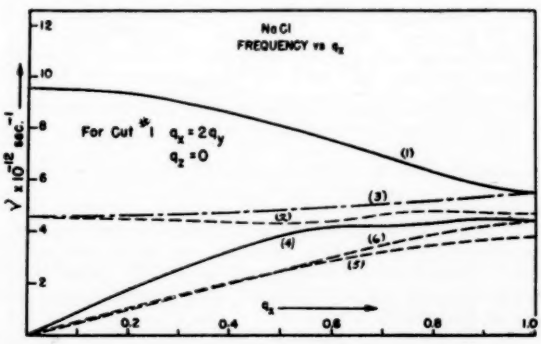

FIG. 1. Plot of frequency ν against the x component of the wave vector for cut No. 1.

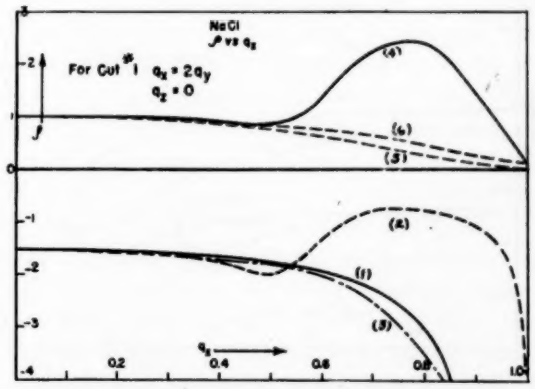

FIG. 2. Plot of displacement ratio against x component of the wave vector for cut No. 1.

[8] Reference 2, p. 537.

TABLE III. Additional binding coefficients for cut No. 2 $q_x \neq 0$; $q_y = q_z = 0$.

q_x	$C(11; xx)(v/e^2)$	$C(11; yy)(v/e^2)$	$C(12; xx)(v/e^2)$	$C(12; yy)(v/e^2)$
0.1	−8.290	4.161	8.540	−4.248
0.3	−7.581	3.790	9.626	−4.856
0.5	−6.412	3.209	11.646	−5.827
0.7	−5.207	2.603	13.628	−6.815
0.9	−4.444	2.211	14.876	−7.440

Note: $C(KK'; yy) = C(KK'; zz)$ and $C(KK'; xy) = 0$ for $x \neq y$.

The group velocity u (columns 4 and 10) is given by $\partial\nu/\partial|s|$, which was evaluated by numerical differentiation using Sterling's formula.[9] The other quantities—namely, ρ, the ratio of the displacement of the sodium ion to the chlorine ion; δ_{Na}, the angle between $\mathbf{q}$ and the displacement of the sodium ion, and the δ_{Cl}, were calculated by the use of simple trigonometry from the knowledge of the $\mathbf{q}$'s and the $\mathbf{U}$'s. The superscripts in the table refer to the various branches, as follows:

(1) Quasi-longitudinal wave—optical branch—displacement in the xy plane.
(2) Quasi-transverse wave—optical branch—displacement in the xy plane.
(3) Pure transverse wave—optical branch—displacement along z axis.
(4) Quasi-longitudinal wave—acoustical branch—displacement in the xy plane.
(5) Quasi-transverse wave—acoustical branch—displacement in the xy plane.
(6) Pure transverse wave—acoustical branch—displacement along z axis.

The branches (3) and (6) are pure transverse waves because we have selected a rather specialized case by letting $q_z = 0$. The results summarized in graphical form are in Figs. 1 to 4.

There is a definite perturbation in the ν *versus* q_x curves at about $q_x = 0.7$, which does not seem to be due to error or limit of accuracy in the calculations.*** These perturbations seem to indicate that the acoustical branch does not cross the optical branch. The curve reminds one of the shift in the frequencies of two oscillators when brought together, because of coupling. However, it is clear that this is not the identical situation, since here there is no coupling between the modes. The reason for the perturbation of the curves is not clear to the author.

At the long wave-length limit the wave behaves exactly as calculated by Lyddane and Herzfeld.[10] The optical branches at this limit approach two values. The lower value, which is doubly degenerate, represents a pure transverse wave, while the upper value corresponds to a non-degenerate, pure longitudinal wave. The acoustical frequencies approach zero, but they do not necessarily correspond to pure transverse or longitudinal waves. Further, Frohlich and Mott[11] have calculated the spread between the optical branches at the long wave-length limit. Their values agree with the values given here. Kellermann,[2] however, using Born's theory, predicts for the optical

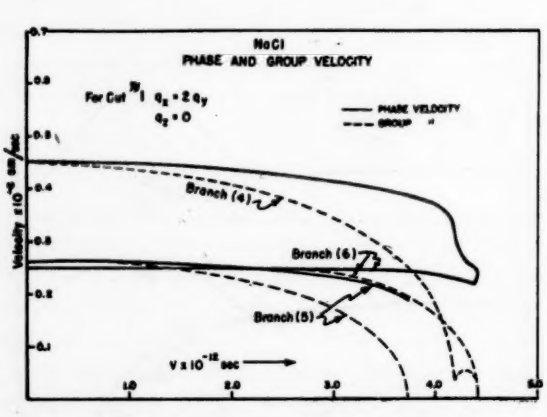

FIG. 3. Plot of velocity against frequency for the acoustic branch of cut No. 1.

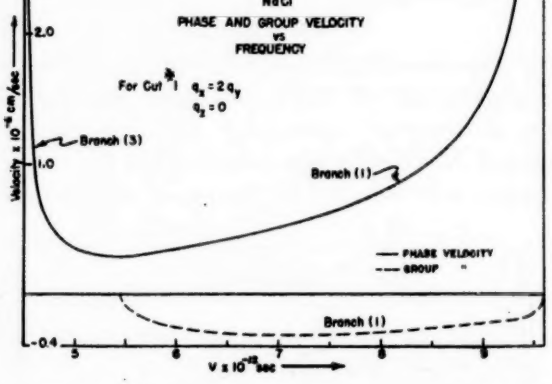

FIG. 4. Plot of velocity against frequency for the optical branch of cut No. 1.

[9] I. B. Scarborough, *Numerical Mathematical Analysis* (Johns Hopkins University Press, Baltimore, 1930).

*** It is believed that the perturbations are not due to inaccuracy in calculating because one would expect the largest perturbation to occur for wave (5), which is unperturbed, and the calculations were checked very carefully in this region.

[10] R. H. Lyddane and K. F. Herzfeld, Phys. Rev. **54**, 846 (1938).

[11] H. Frohlich and N. F. Mott, Proc. Roy. Soc. **A171**, 496 (1939).

TABLE IV. Summary of data for cut No. 2.

q_x	$\nu^{(1)}\times10^{-12}$ sec^{-1}	$v^{(1)}\times10^{-6}$ (cm/sec)	$u^{(1)}\times10^{-6}$ (cm/sec)	$\rho^{(1)}$	$\nu^{(2)}\times10^{-12}$ sec^{-1}	$v^{(2)}\times10^{-6}$ (cm/sec)	$u^{(2)}\times10^{-6}$ (cm/sec)	$\rho^{(2)}$
0.1	9.52	5.36		−1.55	4.55	2.56		−1.55
0.2	9.34	2.62	−0.14	−1.56	4.60	1.29		−1.55
0.3	9.02	1.69	−0.19	−1.60	4.63	0.869		−1.58
0.4	8.66	1.22	−0.23	−1.63	4.68	0.658	average	−1.64
0.5	8.21	0.925	−0.26	−1.72	4.73	0.532	−0.02	−1.70
0.6	7.75	0.727	−0.25	−1.86	4.79	0.449		−1.75
0.7	7.35	0.589	−0.22	−2.08	4.84	0.389		−1.83
0.8	6.97	0.490	−0.16	−2.43	4.89	0.344		−1.88
0.9	6.75	0.423	−0.08	−2.92	4.90	0.307		−1.94
1.0	6.68	0.376	0	−3.02	4.92	0.277		−1.96

q_x	$\nu^{(3)}\times10^{-12}$ sec^{-1}	$v^{(3)}\times10^{-6}$ (cm/sec)	$u^{(3)}\times10^{-6}$ (cm/sec)	$\rho^{(3)}$	$\nu^{(4)}\times10^{-12}$ sec^{-1}	$v^{(4)}\times10^{-6}$ (cm/sec)	$u^{(4)}\times10^{-6}$ (cm/sec)	$\rho^{(4)}$
0.1	0.83	0.463		1.00	0.29[a]			
0.2	1.62	0.457	0.44	0.99	0.86	0.241		1.01[b]
0.3	2.40	0.451	0.39	0.97	1.26	0.235	0.22	0.97
0.4	3.02	0.425	0.34	0.94	1.64	0.231	0.20	0.94
0.5	3.63	0.409	0.31	0.89	1.97	0.223	0.17	0.91
0.6	4.12	0.387	0.25	0.83	2.26	0.212	0.15	0.87
0.7	4.50	0.363	0.18	0.74	2.50	0.201	0.12	0.84
0.8	4.76	0.335	0.11	0.64	2.69	0.189	0.08	0.82
0.9	4.89	0.305	0.05	0.54	2.79	0.174	0.04	0.79
1.0	4.93	0.277	0	0.50	2.82	0.159	0	0.79

[a] Value unreliable.
[b] It is not likely that $\rho^{(4)}$ is really greater than one, thus points doubtless in error.

limit a single, triply degenerate value equal to the lower value of Lyddane and Herzfeld. The present author is not convinced by Kellermann's arguments for a single frequency. If Kellermann's value is correct, an abrupt discontinuity in the ν against q_x curve is required, which off-hand seems to have little physical justification. Kellermann gives a mathematical argument to show that there might be a discontinuity at the limit. Perhaps the discontinuity occurs for infinitesimal values of q, so small that the wave-length is longer than twice the crystal length, which is physically not permitted. This assumption would solve the problem, giving "physically" a double limit. The author has not gone into the problem sufficiently to know whether this assumption can be justified.

An examination of the ρ *versus* q_x curves shows that for the optical branches the displacements are inversely proportional to the masses of the particles at the long wave-length limit, again as calculated by Lyddane and Herzfeld and as one might expect from the one-dimensional case. Likewise, the acoustical branch behaves as in the one-dimensional case—i.e., the displacement between neighboring particles is almost the same and in phase. With decrease in wave-length, however, the curve shows somewhat peculiar behavior, with bends and humps. This is probably due to the perturbation mentioned above. At the short wave-length limit, ρ, whose values here are not too reliable, does not seem to go to zero or infinity for branches (1), (3), (4), and (6). This is in disagreement with what one might expect from the one-dimensional case. In Fig. 2, we have plotted ρ for the optical branch as a negative quantity, while ρ for the acoustical branch is assumed positive. Strictly speaking, this follows only for the long wave-length limit, since ρ is complex. At the short wave-length limit $\rho^{(1)}$ is positive (pure number) while $\rho^{(4)}$ is negative. We have not considered the sign for this value of q_x, since it would require that ρ cross the axis and become zero, which is untrue. Here, as in the two-dimensional case considered, at the short wave-length limit the displacement lines up along the x, y, and z axes.

The phase and group velocity curves show results similar to the one-dimensional case. The group velocity approaches zero at the short wave-length limit. Whether it actually reaches zero is not known from these calculations, since the numerical differentiation can only give a rough estimate of the final value. The fluctuation in the curves is, however, believed to be real. One can show from symmetry considerations[4] that the group velocity for the long wave-length limit is

zero for the optical branch. It is evident from these results that the group velocity is much lower than the phase velocity and is practically zero for the two optical transverse branches.

In another calculation the vector $\mathbf{q}$ was selected along the x axis. The basic properties of the wave are summarized in Tables III and IV. Here, in place of six branches, we obtain four pure waves, the transverse being doubly degenerate. The superscripts in the tables mean:

(1) Pure longitudinal wave—optical branch.
(2) Pure transverse wave—optical branch.
(3) Pure longitudinal wave—acoustical branch.
(4) Pure transverse wave—acoustical branch.

To save space, no plots of the results are given. The plots indeed are similar to Figs. 1 through 4, but there is no indication of perturbation between the modes—i.e., no humps. Filtration action definitely appears here but not between the acoustical and optical branches, only between the two optical branches. Here from symmetrical arguments one can show that at the zonal boundary the group velocity is zero. At the zonal boundary, however, both types of particles are vibrating. At the long wave-length limit these waves behave exactly as the previous ones.

One may obtain a similar table for the case $q_x=q_y=q_z$ directly from Kellermann's results. From symmetry this again leads to only four pure type waves. Here the displacements do not line up along the x, y, and z axes at the short wave-length limit. ρ, however, behaves exactly as in the one-dimensional case—i.e., at the short wave-length limit for the acoustical branch only the chlorine ion, the heavier, is displaced, while for the optical branch only the lighter sodium ion is displaced. Here again there is a gap between the upper longitudinal wave and the three lower branches, and the group velocity goes to zero at the zonal boundary.

CONCLUSION

It is hoped that these calculations will give a better understanding of the high frequency vibrations in ionic solids. Using the low frequency end of the calculation, it should be possible to check the acoustical velocities with experimental values when acoustic experimental technique permits measurements in the relevant frequency range. Dayal[12] has objected to Born's theory of specific heat on the ground that there is a difference between the velocity of thermal waves and acoustic waves. Without going into a complete theory of the heat transmission, one would certainly expect from these calculations that the thermal waves would be transmitted much more slowly because the medium is dispersive at the higher frequencies. If the thermal energy includes mainly higher frequency vibrations, then for this reason alone the heat will be transmitted at some average group velocity which is appreciably lower than the acoustical velocity. This provides at least a qualitative answer to Dayal. Actually, however, the process is much more complex since the diffusion of heat waves, here neglected, is the primary means of transmission.

The author would like to thank Professor R. B. Lindsay for valuable assistance and encouragement during the course of this work, which was undertaken while the author held a University Junior Fellowship at Brown University. Finally, thanks are due his wife, Lillian Markham, for assistance in preparing the manuscript and for encouragement while carrying on the research.

[12] B. Dayal, Proc. Ind. Acad. **A20**, 24 (1944).

Approximate Configurational Partition Functions for Certain Aggregates of Spherical Molecules

MANUEL F. MORALES AND JEAN BOTTS
Department of Physiology, Section of Mathematical Biophysics, University of Chicago, Chicago, Illinois

(Received January 28, 1948)

There are calculated by two different methods the number of ways in which i sites out of a total of n sites may be filled in such a manner that among the filled sites there will be p nearest neighbor pairs when the sites form certain regular spherical surface lattices: the contact points on any sphere in the cubic and hexagonal closest packings of spheres, and in the simple cubic packing of spheres. The use of these results in the treatment of a model of antibody-antigen combination is briefly indicated.

IN treating[1] a model of the reaction in which molecules of antibody, A, combine with molecules of antigen, G, (where A and G are assumed to be spherical and of approximately equal radius) according to the equations

$$A+A_{i-1}G\overset{K_i}{\rightleftarrows}A_iG; \quad i=1, 2, \cdots n, \qquad (1)$$

there arises the problem of estimating the contribution which interactions of A molecules on the same G surface make to the equilibrium constant, K_i. Because of the large size of the molecules involved and the short-range nature[2,3] of the forces giving rise to the intermolecular potential, it seems admissible to consider only interactions between antibody molecules which are adjacent to one another, i.e., nearest neighbors, on the surface of the antigen. We have for certain reasons assumed that the reactive sites of G form regular surface lattices corresponding to simple packings of spheres,[4] but these choices are here to be regarded as purely arbitrary. Given the surface lattice and the bond energies, E_{AG} and E_{AA}, the approximate configurational partition function of the ith aggregate is

$$Z_i^{(cfg)}=\exp(-iE_{AG}/kT) \times\sum_p W_i^{(p)}\exp(-pE_{AA}/kT), \qquad (2)$$

where $W_i^{(p)}$ is the number of ways in which i sites of the lattice can be filled in such a manner that among the i filled sites there are p nearest neighbor pairs. In the present paper we wish to give the $W_i^{(p)}$ for the three surface lattices corresponding to the contact points on any sphere in the (a) hexagonal closest packing of spheres, (b) cubic closest packing of spheres, and (c) simple cubic packing of spheres (Fig. 1), and to report briefly on the methods used in computing them. It may be mentioned that the equilibrium (1) is formally identical with that of ampholyte dissociation,[5] and that a problem in ampholyte equilibria analogous to the present one has been considered by Kirkwood.[6] The specific assumptions in Kirkwood's treatment, however, are (necessarily) quite different, e.g., the nearest neighbor approximation is not, in that case, available.

The calculation of the $W_i^{(p)}$ must be made for each of the lattices proposed; however, they are rather obvious for (c), and special discussion is necessary only for (a) and (b). Neither of two methods devised is elegant or rapid, but both are straightforward and lead to correct results verifiable by certain independent conditions (Appendix A). Moreover, there is a simple relation between $W_i^{(p)}$ and $W_{i'}^{(p')}$, $(i'=n-i)$, making it unnecessary to calculate $W_i^{(p)}$ for i greater than $n/2$ (Appendix B).

In the first method there are constructed for every i all the point clusters consistent with the

[1] Morales, Botts, and Hill, J. Am. Chem. Soc. (in print).
[2] Pauling, Campbell, and Pressman, Physiol. Rev. **23**, 203 (1943).
[3] That is, of the A-A forces. Whether or not the A-G forces are also "short-ranged" as is currently believed, is another matter, which has been brought into question by the recent work of A. Rothen (J. Biol. Chem. **168**, 75 (1947)). In principle, however, the outcome does not affect the validity of a treatment employing the bond energy concept.
[4] L. Pauling, *The Nature of the Chemical Bond* (Cornell University Press, Ithaca, 1940).
[5] See, for example, T. Teorell, J. Hyg. **44**, 227, 237 (1946).
[6] J. G. Kirkwood, in E. J. Cohn and J. T. Edsall's, *Proteins, Amino Acids and Peptides* (Reinhold Publishing Corporation, New York, 1943), pp. 290–294.

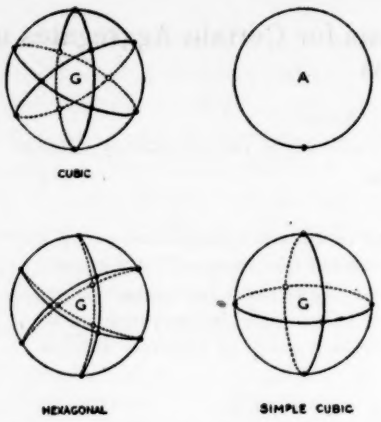

FIG. 1. Models for the surface lattice of reactive sites on the A and G molecules. The titles refer to packings of spheres discussed in the text.

lattice. This can be readily done, for when i is small, say 3, the possible clusters are evident from inspection. The clusters of 4 are then generated by linking a point to each of the points in each of the clusters of 3, paying attention to the restrictions imposed by the lattice. The clusters of 5 are generated in the same fashion by the clusters of 4, and so on.[7] Having at hand a table of clusters such as in Fig. 2, one may next consider the partitions of i written, say, in "dictionary" order (Table I). For example, when $i=4$ these are (4), (31), (22), (211), (1111). A partition such as (211) is to be identified with an arrangement in which two of the attached A's are nearest neighbors to each other, and two additional A's are nearest neighbors neither to each other nor to the doublet. Such an arrangement has one nearest neighbor pair, and the number of microscopically different ways in which it is attainable can be calculated by straightforward combinatory methods. There is, of course, only one cluster of two molecules. If we consider instead the partition (31), matters are slightly more involved because there exist three clusters of three points, one of which has three nearest neighbor pairs, while the remaining two each have two nearest neighbor pairs. The number of ways of attaining the three arrangements corresponding to (31) must, of course, be calculated separately, and later the numbers corresponding to the two arrangements having two nearest neighbor pairs are to be added. In computing the number of ways

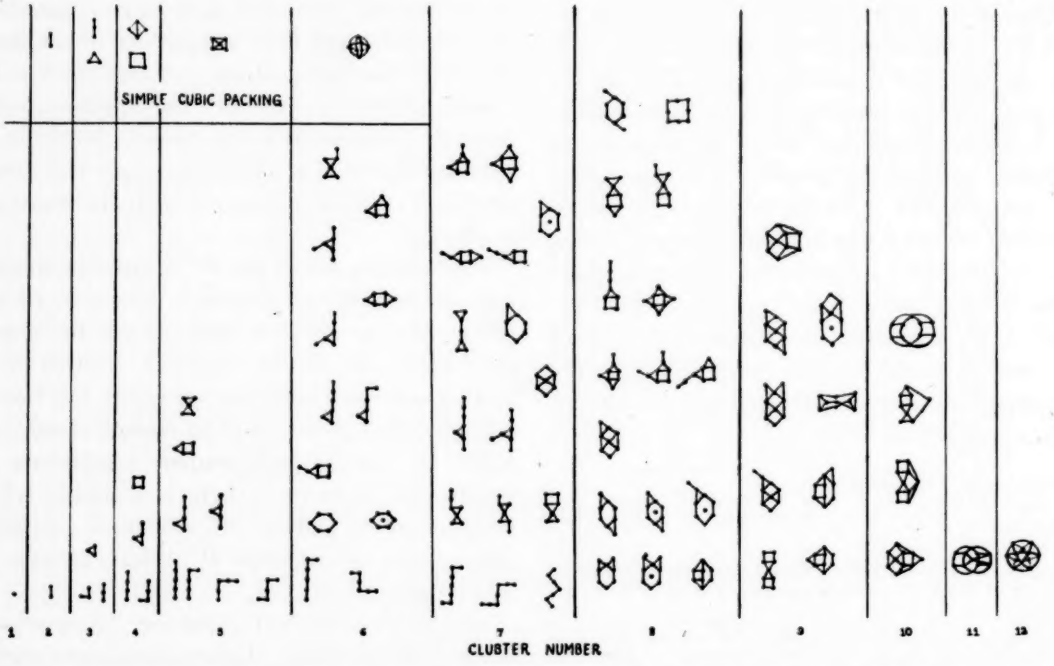

FIG. 2. Point clusters on the surface lattice consisting of the contact points on any sphere in the face-centered cubical arrangement of spheres (upper left inset: same, for simple cubic arrangement).

[7] This is essentially the same procedure which W. G. Schlecht (U. S. Geol. Survey Bull. No. 950, 1946) and P. Niggli (Helv. Chim. Acta **30**, 1562 (1947)) have used in finding the small clusters possible in regular infinite lattices. We are grateful to Professor Linus Pauling for calling these references to our attention.

in which a particular configuration may be attained, say one of those corresponding to the partition (ξ, η, ζ), it has been found convenient to calculate first the number of ways in which ξ may be obtained, and then to calculate the number of ways in which (η, ζ) may be obtained in what is designated as the subdomain complementary to ξ, i.e., a domain consisting of the original lattice minus ξ and all the points which are nearest neighbors to the points of ξ. In such a procedure the topologically equivalent stereographic projection (Fig. 3) of the spherical lattices may frequently be used to advantage.

In the second method the lattice is considered as composed of three rings, *I*, *II*, and *III* (Fig. 3), containing, respectively, three, six, and three sites. We shall denote by i_I, i_{II}, and i_{III} the number of filled sites in the corresponding rings; so $i=i_I+i_{II}+i_{III}$. In finding the $W_i^{(p)}$ it will be convenient first to find for all possible values of i_{II} the number of microscopically different ways in which i_{II} sites of ring *II* may be filled. The nearest neighbor pairs in ring *II* may be divided into two groups—those which share a nearest neighbor in, say, ring *I*, and those which do not. (It is necessary to make a distinction between these two groups when considering neighbor relations with the other two rings. The difference in calculations between lattices (a) and (b) depends only on this distinction.[8]) Accordingly, configurations in ring *II* having exactly one nearest neighbor pair may also be classified into two corresponding groups. If $W_{i_{II}}$ be written as

$$W_{i_{II}}=\sum_{\lambda_{II}} \lambda_{II} W_{i_{II}},$$

where $\lambda_{II} W_{i_{II}}$ is the number of ways of obtaining the λ_{II}th configuration on ring *II*, using i_{II} filled sites, then each $\lambda_{II} W_{i_{II}}$ can be multiplied by the number of ways in which each of the configurations, λ_I, are obtainable on ring *I*, i.e., by $\lambda_I W_{i_I}$. These products, $\lambda_{II} W_{i_{II}} \lambda_I W_{i_I}$, may be conveniently subdivided further, and classified according to the number of nearest neighbor pairs in the domain *I–II*, i.e., p_{I-II}. Since ring *I* cannot have a nearest neighbor in ring *III*, the classification for the combined configurations in *II–III* with respect to p_{II-III} is the same as that of configurations in *I–II* with respect to p_{I-II}. Therefore,

$$\sum_{\lambda_I} \sum_{\lambda_{II}} \sum_{\lambda_{III}} \lambda_I W_{i_I} \lambda_{II} W_{i_{II}} \lambda_{III} W_{i_{III}} = W_i^{(p)},$$

where it is understood that the summations extend only over configurations λ for which $i=i_I+i_{II}+i_{III}$, and for which $p_{I-II}+p_{II-III}-p_{II}=p$. A simplification in the foregoing calculations may be made by noting that each ring may itself be considered as a separate (1-dimensional) lattice. By a discussion similar to that of Appendix B, it may be shown that it is necessary to calculate $W_{i_{II}}$ only for $i_{II}=0, 1, 2, 3$, and W_{i_I} (or $W_{i_{III}}$) only for $i_I=0, 1$, since other configurations of filled sites have configurations of vacant sites among those just named. It is quite obvious that an analogous procedure could be applied to any spherical lattice divisible into parallel rings.

The application of either of the foregoing methods to lattices (a), (b), and (c) leads to the

TABLE I. Nearest neighbor partitions obtainable on the 12-point surface lattices consisting of the contact points on any sphere in the two closest packings of spheres.

Molecule	Cubic	Hexagonal
A_1G	(1)	(1)
A_2G	(2), (11)	(2), (11)
A_3G	(3), (21), (111)	(3), (21), (111)
A_4G	(4), (31), (22), (211), (1111)	(4), (31), (22), (211), (1111)
A_5G	(5), (41), (32), (311), (221)	(5), (41), (32), (221), (311), (2111)
A_6G	(6), (51), (42), (411), (33)	(6), (51), (42), (411), (33), (321), (222)
A_7G	(7), (61), (52), (43)	(7), (61), (52), (43)
A_8G	(8), (71)	(8), (71)
A_9G	(9)	(9)
$A_{10}G$	(10)	(10)
$A_{11}G$	(11)	(11)
$A_{12}G$	(12)	(12)

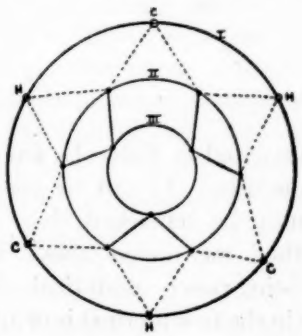

FIG. 3. Stereographic projection of the 12-point lattices. The pole is taken as the center of any triangle, a normal axis through the center of which is perpendicular to the plane of a great circle. Connections from ring *II* to the points marked "*C*" or ring *III* generate the "cubic lattice;" connections to points marked "*H*" generate the "hexagonal" lattice.

[8] In lattice (a) the nearest neighbor pairs in ring *II* which have a common nearest neighbor in ring *I* do not have a common nearest neighbor in ring *III*, whereas in lattice (b) they do.

TABLE IIa. The number of ways of filling i sites of a 12-point spherical surface lattice in such a manner that among the filled sites there will be p nearest neighbor pairs. Top entry for the "hexagonal" lattice; lower entry for the "cubic."

i ↓	p→ 0	1	2	3	4	5	6	7	8	9	10	11	12	13	14	15	16	17	20	24
1	12																			
	12																			
2	42	24																		
	42	24																		
3	44	120	48	8																
	44	120	48	8																
4	9	99	228	114	42	3														
	9	96	240	96	54															
5		6	90	276	276	102	42													
			108	264	264	120	36													
6				18	144	348	264	114	36											
					216	240	336	96	36											
7						6	90	276	276	102	42									
							108	264	264	120	36									
8									9	99	228	114	42	3						
									9	96	240	96	54							
9													44	120	48	8				
													44	120	48	8				
10																	42	24		
																	42	24		
11																			12	
																			12	
12																				1
																				1

TABLE IIb. Same as Table IIa for the "face-centered" lattice.

i ↓	p→ 0	1	2	3	4	5	8	12
1	6							
2	3	12						
3			12	8				
4					3	12		
5							6	
6								1

results summarized in Table II, from which the partition functions, (1) can be constructed directly. It may be remarked that whereas the second method mentioned above has the advantage of being purely analytical, the finding of the clusters in the first method is of additional use in the calculation of the moments of inertia for the various microscopic configurations of aggregates.

The specific application of these calculations to the equilibrium (1) is to be dealt with elsewhere,[1] but it may be of interest to note here that, generally speaking, the interaction of bonded A's is not likely to contribute negligibly to the equilibrium constants. For example, assuming that the surface lattice of sites on the antigen molecule is (c) and that there is a weak $A-A$ repulsion corresponding to a bond energy of $+kT$, one finds that by including such interactions there are introduced factors of 1, 1/5, and 1/328, respectively, into the constants K_1, K_3, and K_6.

APPENDIX A

Two conditions useful in checking the nearest neighbor tables constructed by the methods outlined above are, first, that $\sum_p W_i^{(p)} = n!/i!(n-i)!$ and, second, that $\sum_p pW_i^{(p)}$ is numerically the same for either lattice (a) or (b). The first of these conditions is self-evident, and the second will now be proved.

We can imagine that for each *microscopic* configuration obtainable in the domain consisting

of rings *II* and *III* we tabulate the corresponding number of nearest neighbor pairs, e.g., for the κth configuration there are $p_{II-III}^{(\kappa)}$ nearest neighbors.[9] The sum, $\sum_\kappa p_{II-III}^{(\kappa)}$, is, therefore, the total number of nearest neighbor pairs obtainable by this procedure. Now let us select one of these configurations, κ, arbitrarily except for the fact that in ring *II* there must not be exactly one nearest neighbor pair. Maintaining κ fixed on rings *II* and *III*, and assuming that the sites of ring *I* are in one of the two possible positions relative to the sites of *II–III*, we will now count the additional nearest neighbor pairs for each of the microscopic configurations possible on ring *I*, then sum these numbers to obtain $p_{II-III}^{(\kappa)}$. It is readily evident on diagramming this process that for this type of configuration, κ, $p_{I-II}^{(\kappa)}$—and, therefore, $p_{II-III}^{(\kappa)}+p_{I-II}^{(\kappa)}$—is the same regardless of the choice of lattice. It will be shown below that this is also true for the other type of κ, i.e., those in which there is exactly one nearest neighbor pair in ring *II*. Thus, in general, $\sum_\kappa (p_{II-III}^{(\kappa)}+p_{I-II}^{(\kappa)})$ is the same for the two lattices. But this sum is exactly $\sum_p pW^{(p)}$, and therefore our theorem will stand proved.

Let us consider a microscopic configuration on lattice (a) such that among the i_{II} there is exactly one nearest neighbor pair. Lattice (b) is now generated by rotating ring *I* (or *III*) through 60°, holding the other two rings fixed. If ring *I* is completely filled (or completely empty), $p_{I-II}^{(\kappa)}$ is numerically the same for both lattices. We therefore need consider configurations of ring *I* in which there is but one filled site. (Two filled sites are equivalent to one vacant site.) Corresponding to the three ways of filling a site in ring *I*, there are three microscopically different configurations possible in either lattice. If we imagine these configurations to be generated by allowing an antibody, A_I, to move successively into each of the three sites of ring *I*, it is clear that it will be nearest neighbor to each *A* of ring *II* once and only once for *either* lattice; $p_{I-II}^{(\kappa)}$ is therefore the same for either lattice.

[9] The remarks that follow are true when speaking either of a nearest neighbor pair of *filled* sites or of *vacant* sites; this makes it unnecessary to consider all cases of configurations of filled sites, since some of these are always expressible as configurations of vacant sites identical with configurations of filled sites already treated.

APPENDIX B

If τ is the total number of lattice segments (lines connecting together adjacent sites), $W_i^{(p)} = W_{n-1}^{(p')}$, where $p'=\tau+p-4i$. This symmetry makes it unnecessary to compute $W_i^{(p)}$ beyond $n/2$. The proof is as follows. We set p = number of segments connecting two filled sites, s = number of segments connecting a filled site and a vacant site, and v = number of segments connecting two vacant sites. Then,

$$p+s+v=\tau. \tag{3}$$

If (and only if) the number of sites connected to any site is the same for all sites—four in all cases here considered,

$$4i-2p=s. \tag{4}$$

Combining (3) and (4), we get

$$v=p+\tau-4i. \tag{5}$$

Equation (5) implies that, for a given i, *all* configurations which have the same p number will have the same v number; furthermore, if in (5) we substitute $k=n-i$, it also follows that, for a given k, all configurations which have the same v number have the same p number. We may now imagine that all filled sites are converted to vacant sites and vice versa; the theorem is thus proved, since the number of ways of getting all the former configurations of filled sites will be exactly equal to the number of ways of getting all the configurations after the exchange.

THE JOURNAL OF CHEMICAL PHYSICS VOLUME 16, NUMBER 6, JUNE, 1948

Kinetics of Emulsion Polymerization

WENDELL V. SMITH AND ROSWELL H. EWART
General Laboratories, United States Rubber Company, Passaic, New Jersey
(Received February 12, 1948)

As a basis for understanding emulsion polymerization, the kinetics of free radical reactions in isolated loci is discussed subject to the condition that the free radicals are supplied to the loci from an external source. Three cases of interest are considered: that in which the average number of free radicals per locus is small compared with unity, that in which this number approximates one-half, and that in which the number is large. Of these three possibilities, the second, in which the free radicals per locus approximate one-half, is by far the most interesting as it explains in a satisfactory manner the characteristic features of styrene emulsion polymerization. For this case the average rate of reaction per locus is independent of the size of the locus, since this rate is simply one-half the rate of polymerization of a single free radical. Thus the rate of emulsion polymerization, the concentration of monomer in the loci, and the number of loci present provide the information needed for calculating the chain propagation constant for the monomer.

A simplified treatment is given for approximating the number of reaction loci (polymer particles) produced in emulsion polymerization when the rate of polymerization per locus is constant (see case 2 above). The law obtained indicates that the number of particles should increase with the soap concentration (3/5ths power) and with the rate of formation of free radicals (2/5ths power), but should decrease with increasing rate of growth of the free radicals (−2/5ths power).

INTRODUCTION

ONE of the most interesting characteristics of emulsion polymerization is the production of high molecular weight polymer with simultaneous rapid rate of reaction. The most plausible current attempts to explain this consist in attributing an abnormally low value to the rate of mutual termination of growing free radicals due to the high viscosity of the polymerization locus (i.e., the swollen polymer particles).[1] However, a more attractive explanation is offered by a consideration of the kinetics of free radical reactions in isolated loci when the free radicals originate in a medium outside of the loci of reaction, or are generated by reaction of substances which come from the outside medium.

Harkins[2] has recently discussed the locus of the emulsion polymerization reaction and the function of the various phases present. His discussion may be briefly reviewed as follows. During emulsion polymerization there are four phases which play an integral role in the over-all process. The water phase normally contains the "catalyst," or more properly, chain initiator; it is probable that the initial formation of free radicals takes place here. Dispersed in the water phase are emulsified droplets of monomer; as long as these remain present, they serve to keep the other phases supplied with monomer. In the early stages of the reaction, soap micelles containing dissolved monomer are present; these serve as "generators" of polymer particles and they continue to serve this function until all the soap becomes adsorbed on the polymer-water interface produced by the polymerization. After polymerization has started, the fourth phase present consists of very small polymer particles which are swollen with monomer; these serve as the principal loci of polymerization.

Thus, the problem of the kinetics of emulsion polymerization is twofold. There is the problem of determining what factors govern the rate of polymerization in a single swollen polymer particle and also there is the problem of determining how many such polymer particles are formed. Part I of this discussion is concerned with the first, while Part II presents a simplified discussion of the factors determining the number of reaction loci produced in emulsion polymerization.

In Part I the rate of polymerization is discussed for three limiting cases in terms of the variables: rate of formation of free radicals, rate of escape of free radicals from reaction loci, rates of termination of free radicals in reaction loci and water solution, rate of polymerization of a

[1] J. H. Baxendale, M. G. Evans, and J. K. Kilham, J. Pol. Sci. **1**, 466 (1946); W. P. Hohenstein and H. Mark, J. Pol. Sci. **1**, 549 (1946).
[2] W. D. Harkins, J. Chem. Phys. **13**, 381 (1945); **14**, 47 (1946); and J. Am. Chem. Soc. **69**, 1428 (1947).

free radical in a reaction locus, size, and number of reaction loci (polymer particles).

Case 1 is that in which the number of free radicals per reaction locus is much less than unity. Under these conditions, if termination is chiefly in the water phase, the rate law obtained is similar to the oil phase law, but the initiation rate and termination constant are those for the water solution, also a new factor appears which is the ratio of free radicals in the reaction loci to those in the water phase. The rate, therefore, is independent of the size of the reaction loci. If termination is in the reaction loci, the law is identical with the oil phase law except that the termination constant is replaced by a quantity giving the probability of escape of a free radical from a reaction locus. Since this latter quantity does involve the interfacial area, the rate is dependent on the size of the reaction loci but not very greatly so.

Case 2 is that in which the number of free radicals per reaction locus approximates one-half. This is the case of outstanding interest, since its existence is responsible for the extraordinarily high rates of polymerization and high molecular weights obtainable by emulsion polymerization. The rate law is remarkably simple since it involves only the rate of polymerization of a free radical and the number of reaction loci present. This simplicity makes it possible to determine the chain propagation constants of polymerizing monomers by studying their rates of emulsion polymerization.

Case 3 covers the situation when the number of free radicals per reaction locus is large. The rate law obtained is exactly equivalent to the oil phase law, and hence does not depend on the size of the reaction loci.

PART I. FREE RADICAL REACTION IN ISOLATED LOCI

Consider a system consisting of 1 cc of an external medium (water solution) having suspended in it N isolated reaction loci (polymer particles), each of which has a volume v and an interfacial area a. Suppose that free radicals are initiated only in the external medium, then let the rate of entrance of free radicals into a single locus be

$$dn/dt=\rho'/N,$$

where ρ' is the over-all rate of entrance into all the N loci.

Having once entered a locus, suppose that a free radical continues to cause polymerization until its activity is destroyed or transferred out of the locus. Let the rate of transfer out of a locus be given by

$$dn/dt=-k_0a(n/v),$$

where k_0 is a specific rate constant for the event, n/v is the concentration of free radicals in a locus, and a is the interfacial area through which the transfer takes place. Suppose that destruction of free radicals takes place only by mutual termination so that the rate of destruction in a given locus is given by

$$dn/dt=-2k_tn[(n-1)/v],$$

where the factor of 2 arises from the fact that two free radicals are destroyed for each event of termination, k_t is the mutual termination specific reaction rate constant, and $(n-1)/v$ is the concentration of free radicals with which any of the n free radicals in a locus can react.

If these three events be the only ones which need be considered in determining the numbers of free radicals in the various reaction loci, then the N_0, N_1, $N_2\cdots N_n\cdots$ reaction loci containing 0, 1, 2, $\cdots n\cdots$ free radicals, respectively, will be related by the steady-state condition:

$$\begin{aligned}&N_{n-1}(\rho'/N)+N_{n+1}k_0a((n+1)/v)\\&\quad+N_{n+2}k_t[(n+2)(n+1)/v]\\&\quad=N_n\{(\rho'/N)+k_0a(n/v)+k_tn[(n-1)/v]\}.\end{aligned}\quad(1)$$

This equation states that the rate of formation of reaction loci characterized by containing n free radicals is just equal to the rate of disappearance of these loci.

Rather than obtaining a general solution of this recursion formula, which would appear to be difficult, a discussion is given of three limiting cases which are of interest.

Case 1. Number of Free Radicals per Particle Small Compared with Unity

If the free radicals have a high enough probability of being transferred out of a particle, then at any time only a small number of the particles will have free radicals in them. This condition

will be fulfilled when

$$\rho'/N \ll k_0 a/v.$$

Then of the various relations given by Eq. (1), it is only necessary to consider the first which approaches

$$N_1 k_0 a/v = N_0 \rho'/N.$$

But since

$$N_0 \cong N, \quad N_1 \cong \rho' v/k_0 a.$$

The number of free radicals in polymer particles is also very nearly equal to N_1, so if the rate of polymerization per free radical is $k_p(M)$ where k_p is the propagation constant and (M) is the monomer concentration in the particle, then the over-all rate of polymerization per cc of external medium (water solution) will be

$$dM/dt = k_p(M)(\rho' v/k_0 a). \tag{2}$$

An obvious alternative form for writing this equation is

$$dM/dt = k_p(M) V_p c_p, \tag{2a}$$

where V_p is the total volume of the polymer particles in 1 cc of water solution and c_p is the average concentration of free radicals in the particles.

Now termination of the free radicals may take place in either the water phase or the polymer particles. If termination is in the water phase, the rate law governing their disappearance may be written

$$dn/dt = -2k_t(c_w)^2,$$

where k_t is the termination constant and c_w is the concentration of free radicals in the water phase. When a steady state is attained, this rate will be equal to ρ, the rate of formation of free radicals per cc of water phase; thus

$$\rho = 2k_t(c_w)^2. \tag{3}$$

Under these conditions of rapid exchange of free radicals between water phase and polymer particles it is useful to use a partition coefficient, α, defined by

$$\alpha = c_p/c_w. \tag{4}$$

Then from Eqs. (2a), (3), and (4)

$$dM/dt = k_p(M) V_p \alpha (\rho/2k_t)^{\frac{1}{2}}. \tag{5}$$

Another quantity of interest is the average polymerizing lifetime of a free radical, which is a measure of the initiator efficiency. The average lifetime, τ_p, of a free radical in polymer particles is equal to the number of free radicals in polymer particles divided by the rate at which they are terminated or

$$\tau_p = [V_p c_p/2k_t(c_w)^2] = (V_p \alpha/2k_t c_w).$$

From Eq. (3) this becomes

$$\tau_p = [V_p \alpha/(2k_t \rho)^{\frac{1}{2}}]. \tag{6}$$

Thus under these conditions the rate of polymerization and initiator efficiency do not depend on the size of the polymer particles but only on their total volume.

If termination takes place in the polymer particles and if these particles are so small that termination takes place very rapidly every time two free radicals are in the same particle, then the rate of termination is simply two times the rate at which free radicals enter the polymer particles which already contain a free radical or

$$dn/dt = -2(\rho'/N)N_1 = -2[(\rho')^2/N](v/k_0 a). \tag{7}$$

Equating this to the rate of formation of free radicals, ρ, to obtain the steady state condition, solving for ρ' and substituting in Eq. (2) gives

$$dM/dt = k_p(M)(V_p \rho/2k_0 a)^{\frac{1}{2}}. \tag{8}$$

The mean polymerizing lifetime is approximately N_1 divided by the rate of termination; so from Eq. (7),

$$\tau_p = N/2\rho' = (V_p/2k_0 a \rho)^{\frac{1}{2}}. \tag{9}$$

To know which of the two terminations discussed will apply, it is necessary to make an assumption concerning the relationship between c_w and ρ'/N. The simplest assumption to make is that the rate of entrance of free radicals into a particle is just that given by the rate of diffusion of molecules from an infinite medium of concentration c_w into a particle of radius, r, having zero concentration of the molecules, this rate is

$$\rho'/N = 4\pi D r c_w,$$

where D is the diffusion constant of the molecules through the water phase. Then the rate of termination in the polymer particles will be given by Eq. (7) to be

$$dn/dt = -2N(4\pi D r c_w)^2(v/k_0 a).$$

If this is small compared with the rate of termination in the water phase, Eq. (3), then the water phase termination will apply. Thus water phase termination predominates when

$$k_t \gg V_p(4\pi D^2/k_0).$$

Case 2. Number of Free Radicals per Polymer Particle Approximately Equal to 0.5

Suppose that there is no readily available mechanism by which the activity of a free radical in a polymer particle can be transferred again to the water phase, then having once entered a polymer particle a free radical must remain there until another one comes in to terminate it. If, in addition, the probability of mutual termination of two free radicals in the same particle is large enough so that the average time necessary for them to terminate is small compared with the average time interval between successive entrances of free radicals into a particle, then the very simple situation exists in which approximately one-half the particles contain a single free radical and the other half contain none. This is much the most interesting case and is the one which appears to apply to the emulsion polymerization of styrene under normal conditions. The requirements for this case can be stated as

$$k_0(a/v) \ll \rho'/N < k_t/v. \tag{10}$$

In view of the importance of this case, a solution will be given to a higher approximation than the simple limiting law; however, this will be done only for the condition in which $k_0=0$ (this is probably closely approached in many unregulated polymerizations). Neglecting terms involving k_0, Eq. (1) becomes

$$N_{n-1}(\rho'/N)+N_{n+2}k_t[(n+2)(n+1)/v] = N_n\{(\rho'/N)+k_t n[(n-1)/v]\}. \tag{11}$$

For convenience, the quantity β may be defined as

$$\beta = k_t N/v\rho',$$

(from (10) $\beta>1$) then Eq. (11) may be written

$$N_{n-1}+N_{n+2}\beta(n+2)(n+1) = N_n[1+\beta n(n-1)]. \tag{12}$$

It is shown in Appendix I that a satisfactory approximation for this recursion formula when $\beta>1$ is

$$N_{n-1}/N_n = 1+\beta n(n-1). \tag{13}$$

From Eq. (12) when $n=0$

$$N_2 = N_0/2\beta.$$

When $n=1$

$$N_0+3\times 2N_3\beta = N_1.$$

But N_3 can be related approximately to N_2 by Eq. (13) so

$$N_3 = [N_0/2\beta(1+6\beta)],$$

and

$$N_1 = N_0(4+6\beta)/(1+6\beta).$$

This could be continued to obtain any degree of approximation desired.

So far as the rate of polymerization is concerned, the important thing is the total number of free radicals present in polymer particles; this is given by

$$n_T = 1N_1+2N_2+3N_3+\cdots nN_n\cdots,$$

while the total number of particles is

$$N = N_0+N_1+N_2+N_3+\cdots N_n\cdots.$$

From these relations and those given above, the total number of free radicals can be expressed as the series

$$n_T = (N/2)(1+1/\beta-1/3\beta^2+\cdots). \tag{14}$$

Thus, if β is sufficiently large, the total number of free radicals present will be very nearly equal to one-half the number of polymer particles.

Under these conditions, the rate of polymerization per cc of water solution is given by the remarkably simple expression

$$dM/dt = k_p(M)N/2. \tag{15}$$

The mean polymerizing lifetime, τ_p, will be $N/2\rho'$. Under normal polymerization conditions, some semiquantitative considerations indicate that practically every free radical produced will enter polymer particles; hence $\rho'=\rho$ and

$$\tau_p = N/2\rho. \tag{16}$$

The characteristic features of emulsion polymerization can now be easily interpreted. It is seen from Eq. (14) that the number of polymerizing free radicals will be nearly equal to half the number of particles. Since it is possible to have a large number of particles present (compared

with the concentration of free radicals normally present in oil phase polymerization), the fast rate of polymerization naturally follows. Also from Eq. (16) the average lifetime of a free radical increases with increase in number of particles; thus it is possible to have high rates of polymerization with simultaneous high molecular weights in emulsion polymerizations.

It may be pointed out that when the conditions characterizing this case are fulfilled, determinations of the over-all rate of polymerization, number of polymer particles, and concentration of monomer in the particles provide the data necessary to calculate the chain propagation constant by Eq. (15).

Case 3. Number of Free Radicals per Polymer Particle Large Compared With Unity

This situation will prevail when

$$\rho'/N \gg k_t/v.$$

This case is not of as much interest as case 2, but in view of its possible application to some "bead polymerizations," a brief discussion will be given.

For most purposes, it is not necessary to have the detailed knowledge of the distribution of free radicals which would be provided by a solution of the recursion formula (1). It will suffice to write down directly the steady-state condition as

$$\rho'/N = 2k_t(n^2/v). \tag{17}$$

This assumes that the system can be approximated by one in which all the particles contain the same number, n, of free radicals. This is, no doubt, a good approximation if n is large enough. Solving Eq. (17) for n gives

$$n = (v\rho'/2k_tN)^{\frac{1}{2}}.$$

So the over-all rate of polymerization per cc of water solution will be

$$dM/dt = k_p(M)(V_p\rho'/2k_t)^{\frac{1}{2}}, \tag{18}$$

and the polymerizing lifetime of a free radical will be

$$\tau_p = (V_p/2k_t\rho')^{\frac{1}{2}}. \tag{19}$$

If the exposed interfacial surface is large enough so that practically every free radical produced enters the particles, then $\rho' = \rho$, the rate of production of free radicals per cc of water phase. Then there will be no advantage in having a large number of very small particles as the rate and lifetime will depend only on the total volume of polymer particles. This will simply be an oil phase type of polymerization in suspended particles which are supplied with free radicals from the water phase. If a substantial fraction of the free radicals are terminated in the water phase, then the system is an inherently inefficient one.

Regarding the relationships between the three cases discussed, it is evidently possible, under suitable conditions, to go progressively from one case to the next by increasing the rate of formation of free radicals. However, for case 2 two conditions must be fulfilled; i.e.,

$$k_0(a/v) \ll (\rho'/N) < (k_t/v),$$

so, obviously, for this case to be obtained, k_0a must be much smaller than k_t. If this condition is not fulfilled, then progressive increase in the rate of formation of free radicals will cause a transition from case 1 to case 3 without ever realizing case 2.

PART II. NUMBER OF POLYMER PARTICLES

The process considered in this development is based on the ideas originated by Harkins[2] regarding the formation of polymer particles by soap micelles. It is considered that originally most of the soap present is in the form of micelles containing dissolved monomer. When a free radical from the surrounding water phase enters a micelle, it initiates polymerization of the monomer in the micelle. When this polymerization starts, monomer from the surrounding medium diffuses into the polymerizing region until shortly this region is no longer identified as a micelle, but is now considered a growing polymer particle and is subject to the considerations given in Part I. As the area of the polymer particles increases because of growth and formation of new ones, the particles adsorb more and more soap from the surrounding micelles until a time is reached at which no soap remains in the micellar form. After this time, the soap is no longer effective in forming new particles.

To make the problem as simple as possible,

the soap dissolved in the water without forming micelles and the soap adsorbed on the emulsified monomer may be neglected; ordinarily this soap will represent only a small fraction of the total present.[2] Thus, if S is the total amount of soap associated with one cc of water phase, it will consist of S_m grams in micellar form and S_p grams adsorbed on polymer particles so that

$$S = S_m + S_p. \tag{20}$$

Also for simplicity, it will be assumed that the interfacial area, a_s, occupied by a gram of soap is the same in soap micelles as on polymer particles, so long as micelles are present. This is probably not true but is a good enough approximation for the present discussion. So if A, A_m, and A_p are the total interfacial area, area of micelles, and area of polymer particles, respectively,

$$A/S = A_m/S_m = A_p/S_p = a_s.$$

Now the question arises as to how effective a given interfacial area is in collecting free radicals from the solution. If the ordinary laws of diffusion hold, as they probably do in this case, then a given interfacial area on a very small particle will be more effective in collecting free radicals than the same area on a large particle (i.e., the number entering a particle will be proportional to the radius; hence, the number entering a given area will be inversely proportional to the radius). This introduces some difficult complications into the problem. However, one can solve the problem of the number of particles produced for two idealized situations which should give, respectively, more and fewer particles than the actual situation. Fortunately, the results obtained do not differ greatly so it is thus possible to approximate fairly closely the actual situation, without having to discuss the size distribution of particles.

The simplest idealized situation is that in which the very small micelles capture all the free radicals being generated as long as micelles are still present. Obviously, this will give too many particles, since actually some of the free radicals will enter polymer particles. If ρ is the rate of formation of free radicals per cc of water solution, the rate of formation of new particles, dN/dt, is assumed equal to ρ and constant as long as micelles are present. So

$$dN/dt = \rho. \tag{21}$$

To obtain the total number of particles formed, Eq. (21) must be integrated to the time t_1 at which the total area of the polymer particles, A_p, is just equal to the total area of the soap, a_sS.

The area of the polymer particles is the summation of the areas for all the particles produced from zero time to the time considered. To obtain the area at time t of a particle which was formed at time τ, it is necessary to know the law governing the rate of growth of a particle. For case 2 discussed in Part I, the rate of polymerization of a particle is a constant, independent of the size of the particle or of the rate of entrance of free radicals. Now if the ratio of monomer to polymer in the particle remains constant during the period in which new particles are being formed, the rate of increase in volume of a particle will be a constant which may be called μ, so if v is the volume of a particle

$$dv/dt = \mu.$$

Thus the volume, $v_{\tau,t}$, at time t of a particle formed at time τ is

$$v_{\tau,t} = \mu(t-\tau).$$

Assuming a spherical particle, the area, $a_{\tau,t}$, of this particle at time t is

$$a_{\tau,t} = [(4\pi)^{\frac{1}{3}}3\mu(t-\tau)]^{\frac{2}{3}}. \tag{22}$$

For convenience make the substitution

$$\theta = [(4\pi)^{\frac{1}{3}}3\mu]^{\frac{2}{3}}. \tag{23}$$

Then Eq. (22) becomes

$$a_{\tau,t} = \theta(t-\tau)^{\frac{2}{3}}. \tag{24}$$

The total area, A_p, of all the particles present at time t is given by the integration

$$A_p = \rho\theta\int_0^t (t-\tau)^{\frac{2}{3}}d\tau, \tag{25}$$

which gives

$$A_p = (3/5)\rho\theta t^{5/3}.$$

At time $t = t_1$, when the soap micelles disappear, $A_p = a_sS$ so

$$t_1 = (5a_sS/3\rho\theta)^{3/5}$$

and the total number of particles is

$$N=\rho t_1=\rho^{2/5}(5a_sS/3\theta)^{3/5}$$
$$=0.53(\rho/\mu)^{2/5}(a_sS)^{3/5}. \quad (26)$$

The other idealized situation is that in which a given interfacial area always has the same effectiveness in collecting free radicals regardless of the size of the particle on which it is situated. This will give too few particles since a given interfacial area on the very small micelles will be more effective than the same area on the larger polymer particles. (The diffusion current of free radicals through unit area of interface should be inversely proportional to the radius.) For this situation, the rate of formation of particles is given by

$$dN/dt=\rho A_m/A, \quad (21a)$$

instead of by Eq. (21). Substituting from Eq. (20) gives

$$dN/dt=\rho(1-A_p/a_sS). \quad (27)$$

The number of particles formed in the interval $d\tau$ at time τ may be expressed as $(dN/d\tau)d\tau$, and the area of one of these particles at some time, t, after τ is given by Eq. (24), so the total area at time t of all particles formed up to t is

$$A_p=\theta\int_0^t(t-\tau)^{\frac{2}{3}}(dN/d\tau)d\tau. \quad (25a)$$

Thus Eq. (27) may be written

$$dN/dt=\rho-(\rho\theta/a_sS)\int_0^t(t-\tau)^{\frac{2}{3}}(dN/d\tau)d\tau. \quad (28)$$

This integral equation is a form of Volterra's equation of the second kind[3] which may be written

$$\phi(x)=f(x)+\lambda\int_0^x K(x,z)\phi(z)dz.$$

The solution of this is given by the infinite series

$$\phi(x)=\sum_{n=0}^{\infty}\lambda^n\phi_n(x),$$

where

$$\phi_0(x)=f(x) \quad \text{and} \quad \phi_n(x)=\int_0^x K(x,z)\phi_{n-1}(z)dz.$$

Applying this to Eq. (28), the desired solution may be expressed by the infinite series

$$\frac{dN}{dt}=\rho\sum_{n=0}^{\infty}\frac{y^n}{\Gamma(1+n5/3)}, \quad (29)$$

where

$$y=-\frac{(4\pi)^{1/3}3^{2/3}\Gamma(5/3)\rho\mu^{2/3}t^{5/3}}{a_sS}.$$

Combination of the numerical constants gives

$$y=-\frac{4.36\rho\mu^{2/3}t^{5/3}}{a_sS}. \quad (30)$$

By using a method of successive approximation, the value, y_1, of y which gives $dN/dt=0$ in Eq. (29) is found to be

$$y_1=-2.13.$$

Thus the time t_1 at which the soap micelles disappear and after which no new particles are formed by them is (Eq. (30))

$$t_1=\left(\frac{2.13a_sS}{4.36\rho\mu^{2/3}}\right)^{3/5}=\frac{0.650}{\mu^{2/5}}\left(\frac{a_sS}{\rho}\right)^{3/5}.$$

Now for temporary convenience let

$$\xi=(4.36\rho\mu^{\frac{2}{3}}/a_sS),$$

so that (Eq. 30)

$$y=-\xi t^{5/3}.$$

Then the first few terms of Eq. (29), which are the only ones of importance, may be written out as

$$\frac{dN}{dt}=\rho\left(1-\frac{\xi t^{5/3}}{\Gamma(8/3)}+\frac{\xi^2t^{10/3}}{\Gamma(13/3)}\right.$$
$$\left.-\frac{\xi^3t^{15/3}}{\Gamma(18/3)}+\frac{\xi^4t^{20/3}}{\Gamma(23/3)}-\cdots\right).$$

To get the total number of particles produced by a given amount of soap, this may be integrated from $t=0$ to $t=t_1$, the time at which the soap micelles disappear. Carrying out term by term integration and substituting the limits gives

$$N=\rho t_1\left(1-\frac{3}{8}\frac{\xi t_1^{5/3}}{\Gamma(8/3)}+\frac{3}{13}\frac{\xi^2t_1^{10/3}}{\Gamma(13/3)}\right.$$
$$\left.-\frac{3}{18}\frac{\xi^3t_1^{15/3}}{\Gamma(18/3)}+\frac{3}{23}\frac{\xi^4t_1^{20/3}}{\Gamma(23/3)}-\cdots\right),$$

[3] H. Margenau and G. M. Murphy, *Mathematics of Physics and Chemistry* (D. Van Nostrand Company, Inc., New York, 1943), p. 506.

or

$$N=0.650\left(\frac{\rho}{\mu}\right)^{2/5}(a_sS)^{3/5}\left(1+\frac{3y_1}{8\Gamma(8/3)}+\frac{3(y_1)^2}{13\Gamma(13/3)}+\frac{3(y_1)^3}{18\Gamma(18/3)}+\frac{3(y_1)^4}{23\Gamma(23/3)}+\cdots\right)$$
$$=0.370(\rho/\mu)^{2/5}(a_sS)^{3/5}. \quad (26a)$$

This is identical with Eq. (26) except for the value of the numerical constant, and the constants are not greatly different. The actual situation should lie between that represented by Eqs. (26) and (26a). Thus

$$N=k(\rho/\mu)^{2/5}(a_sS)^{3/5},$$

where $0.37<k<0.53$. The application of this to experimental data will be discussed in a future paper.

APPENDIX I

Approximate Solution of Recursion Formula For No Transfer of Free Radical from Polymer Particle to Water Phase

For convenience, make the substitutions

$$x=N_{n-1}/N_n, \quad x_1=N_n/N_{n+1}, \quad x_2=N_{n+1}/N_{n+2},$$

then the recursion formula (12) may be written

$$x=1+\beta n(n-1)-(1/x_1x_2)\beta(n+2)(n+1). \quad (A1)$$

It is immediately evident that if x remains less than unity by a finite amount as $n\to\infty$ then the series $\sum_{n=0}^{\infty}N_n$ diverges and is therefore a physically unsatisfactory condition.

To examine the situation when $x\to1$ as $n\to\infty$ consider the ratio of the free radicals in the N_{n+2} particles containing $n+2$ free radicals each to those in the N_n particles containing n free radicals each. This ratio, from Eq. (A1) is

$$\frac{(n+2)N_{n+2}}{nN_n}=\frac{n-1}{n+1}-\frac{x-1}{\beta n(n+1)}. \quad (A2)$$

Making the substitution

$$n'=n/2,$$

so that n' will now give the number of the term in the series

$$S=N_1+3N_3+5N_5+\cdots(2n'-1)N_{2n'-1}. \quad (A3)$$

The ratio expressed by (A2) now becomes

$$\frac{(n+2)N_{n+2}}{nN_n}=1-\frac{1}{n'}+\frac{1}{n'(2n'+1)}\left[1-\frac{x-1}{2\beta}\right], \quad (A4)$$

which is the ratio of successive terms in the series of Eq. (A3). This is now in the form

$$a_{n+1}/a_n=1-\mu/n+\omega_n/n^k,$$

where $k>1$ and $|\omega_n|$ is finite. The series $\sum_{n=r}^{\infty}a_n$ has been shown[4] to diverge if $\mu\leqq1$. Therefore, the series in Eq. (A3) diverges so the condition $x\to1$ as $n\to\infty$ is physically unacceptable.

The one remaining possibility is for x to remain greater than unity by a finite amount as $n\to\infty$. To examine this, it is convenient to rewrite Eq. (A1) in the form

$$x=1+\beta n(n-1)\left[1-\frac{1}{x_1x_2}\frac{(n+2)(n+1)}{n(n-1)}\right]. \quad (A5)$$

Since $x>1$ as $n\to\infty$, then x_1 and x_2 must also remain greater than unity. Thus the term in brackets in Eq. (A5) must remain greater than zero. But since the multiplier, $\beta n(n-1)$, may become indefinitely large x, x_1 and x_2 will all become indefinitely large as $n\to\infty$. Thus the bracketed term will approach unity and the approximation

$$x\to1+\beta n(n-1), \quad (A6)$$

will be very good for large values of n; also it will remain a good approximation for small values of n if β is large enough.

---

[4] Frank and v. Mises, *Die Differential- und Integralgleichungen der Mechanik und Physik* (Friedrich Vieweg und Sohn Aktien-Gesellschaft, Braunachweig, 1930), p. 197.

Heats of Dissociation of Cyanogen

G. GLOCKLER
Department of Chemistry and Chemical Engineering, State University of Iowa, Iowa City, Iowa
(Received February 16, 1948)

Some arguments are presented which would indicate that the heat of dissociation of C_2N_2 into two CN radicals ($D(C_2N_2$ into 2CN)) is 5.52 ev and the heat of dissociation of CN radicals into atoms (D(CN)) is 6.52 ev.

THE heat of dissociation of the cyanogen molecule into two cyanogen radicals ($D(C_2N_2$ to 2CN)) and the heat of dissociation of the radical (D(CN)) are connected with the heat of formation from atoms of the cyanogen molecule (Q_a):

$$\begin{aligned} &CN(^2\Sigma^+)\rightarrow C(^3P)+N(^4S)-D(CN),\\ &\tfrac{1}{2}C_2N_2\rightarrow CN(^2\Sigma^+) \quad -D(C_2N_2).\\ &\tfrac{1}{2}C_2N_2\rightarrow C(^3P)+N(^4S)-Q_a \end{aligned}$$

The calculations of D(CN) made earlier[1] are shown in Table I. They depend on the heat of sublimation of carbon (L(C)) or the atomic heat of formation of carbon monoxide (D(CO)) and the heat of dissociation of nitrogen ($D(N_2)$). In cases *a*, *b*, and *c*, the values used at that time are indicated, while in cases *d* and *e* the value 9.608 ev for D(CO), suggested by Hagstrum,[1] is employed along with two different values for $D(N_2)$. In case *d*, the current value for $D(N_2)$ (=7.384 ev) is tried, and in case *e* the value of 9.764 ev suggested by Gaydon[2] is accepted. In case *f* Herzberg's value for D(CO) = 9.144 ev is used. The object of this note is to suggest that the higher value for $D(N_2)$ is preferable since cases *e* and *f* are the only ones to which no objection can be raised. The reasons are:

1. Cases a and b.—They can be excluded because $D(C_2N_2)$ from Kistiakowsky and Gershinowitz[1] is too low to account for the rate experiments of Robertson and Pease[1] and the results of a Born-Haber cycle discussed below.

2. Case c.—Here D(CN) (=6.37 ev), being nearly equal to $D(C_2N_2)$ (=6.34 ev), is unlikely on chemical grounds as mentioned by Herzberg.[3] It would be expected that the breaking of a carbon-carbon bond, even if it were almost a double bond since it is located between two triple bonds, would require less energy than the breaking of a triple bond between carbon and nitrogen as in the radical. However, the difference between bond energies and heats of dissociation in molecules more complicated than diatomic structures must not be lost sight of.

3. Case d.—Now D(CN) (=5.34 ev) is even less than $D(C_2N_2)$ (=5.52). Hence it can be excluded for the reason given under case c. Furthermore, D(CN) would be less than 5.5 ev, which can hardly be the case since any sort of Birge-Sponer extrapolation should yield a value greater than 5.5 ev, as mentioned by White.[1]

4. Case e.—It is based on the work of Robertson and Pease[1] and Hogness and Lui-Sheng.[1] D(CN) is greater than $D(C_2N_2)$, and the latter is also greater than 5.5 ev (see case d). The value of $D(C_2N_2)$ used agrees with the result of a Born-Haber cycle calculation shown below.

5. Case f.—It is also acceptable since it differs only from Case e by a somewhat lower D(CO) value.

Hence the present considerations point toward the higher value of the heat of dissociation of nitrogen ($D(N_2)$ = 9.764 ev).

Further evidence for the value of 127 kcal. for $D(C_2N_2$ to 2CN) can be obtained from a Born-Haber cycle involving potassium and sodium cyanides (Table II). While some of the energy values entering the calculation, such as the electron affinity of CN radical and the lattice energies of KCN and NaCN, are not well known, still the calculation suffices to show that values of 77 kcal. and 146 kcal. of Kistiakowsky and Gershinowitz[1] and White,[1] respectively, cannot be correct. The electron affinity of the CN radical is taken to be equal to the value for the bromine atom since both have very closely the same ionic radius. It is assumed that the CN radical is in

[1] See references, Table I.
[2] A. G. Gaydon, Nature **153**, 407 (1944).
[3] G. Herzberg, J. Chem. Phys. **10**, 306 (1942).

TABLE I. Heats of dissociation of cyanogen (ev).

	a	b	c	d	e	f
$\frac{1}{2}C_2N_2 \rightarrow CN$	−1.67	−1.67	−3.17	−2.76	−2.76	−2.76
$C+O \rightarrow CO$	9.14	9.61	11.05	9.61	9.61	9.14
$N \rightarrow \frac{1}{2}N_2$	3.69	3.69	3.69	3.69	4.88	4.88
$\frac{1}{2}N_2+CO \rightarrow \frac{1}{2}C_2N_2+O$	−5.20	−5.20	−5.20	−5.20	−5.20	−5.20[g, h, i]
$C+N \rightarrow CN$	5.96	6.42	6.37	5.34	6.53	6.06

[a] G. Herzberg, Chem. Rev. **20**, 145 (1937); $D(C_2N_2)$ from G. B. Kistiakowsky and H. Gershinowitz, J. Chem. Phys. **1**, 432 (1933) as 77 kcal. or 3.384 ev.
[b] H. D. Hagstrum, Phys. Rev. **72**, 947 (1947); same as a except $D(CO)=9.608$ ev.
[c] J. U. White, J. Chem. Phys. **8**, 459 (1940) finds $D(C_2N_2)=146$ kcal. or 6.384 ev and uses $D(CO)=11.054$ ev.
[d] T. R. Hogness and Lui-Sheng, J. Am. Chem. Soc. **54**, 123 (1932) give $D(C_2N_2)=127$ kcal. or 5.522 ev; accepted by N. R. Robertson and R. N. Pease, J. Chem Phys. **10**, 490 (1942).
[e] Same as d but $D(N_2)=9.764$ ev.
[f] Same as e but $D(CO)=9.144$ ev.
[g] From $D(O_2)=5.082$ ev; heat of combustion of $C_2N_2=256.4\pm5$ kcal. (reference h) and heat of combustion of $CO=2.902$ ev (reference i).
[h] F. R. Bichowsky and F. D. Rossini, *The Thermochemistry of the Chemical Substances* (Reinhold Publishing Corporation, New York, 1936).
[i] E. J. Prosen, R. S. Jessup, and F. D. Rossini, Bur. Stand. J. Research **33**, 447 (1944).

every respect halogen-like. Similarly, the lattice energy is obtained from a plot of lattice energies of halides of sodium and potassium as a function of their crystal spacing[4] and from the same quantity of CN radical. Other cyanides have also been considered, but their lattice energies are not known as accurately as the ones of the two alkali metals. It seems, therefore, that the value $D(C_2N_2 \text{ into } 2CN)=127$ kcals. mentioned by Robertson and Pease[1] and first determined by Hogness and Lui-Sheng,[1] is the correct heat

[4] R. W. G. Wyckoff, *The Structure of Crystals* (The Chemical Catalog Company, Inc., New York, 1931).

TABLE II. Heat of dissociation of cyanogen into cyanogen radicals $D(C_2N_2 \text{ into } 2CN)=120\pm8$ kcal.

Reaction	Na kcal.	K kcal.
$[M]+[C]+\frac{1}{2}N_2 \rightarrow [MCN]$	23.0[a]	28.5[a]
$E^-+M^+ \rightarrow [M]$	143.4[a]	120.9[a]
$CN^- \rightarrow CN+E^-$	− 84.3±3	− 84.3±3[b]
$[MCN] \rightarrow M^++CN^-$	−175.0±5	−159.0±5[a]
$\frac{1}{2}C_2N_2+O_2 \rightarrow CO_2+\frac{1}{2}N_2$	128.2±3	128.2±3[a]
$CO_2 \rightarrow [C]+O_2$	− 94.1	− 94.1[c]
$C_2N_2 \rightarrow 2CN$	−117.6	−119.6

[a] See reference 4.
[b] J. Sherman, Chem. Rev. **11**, 93 (1932); L. Helmholz and J. E. Mayer, J. Chem. Phys. **2**, 245 (1934); see reference 6.
[c] Reference 5.

of dissociation of the cyanogen molecule into cyanide radicals.

The high value of $D(CO)=11.04$ ev is excluded on the basis of another study[5] concerning carbon-carbon and carbon-hydrogen bond energies. No choice can be made in the present case between $D(CO)=9.14$ ev and 9.61 ev, but $D(N_2)=9.764$ ev seems indicated.

Appearance potentials[6–8] of C^+ and N^+ ions in HCN and C_2N_2 do not help in deciding between the two values of $D(N_2)$ discussed above. It simply means that the ions would have different amounts of kinetic energy, depending on the value of $D(N_2)$ used.

[5] Unpublished results.
[6] P. Kusch, A. Hustrulid, and J. T. Tate, Phys. Rev. **52**, 843 (1937).
[7] J. T. Tate, P. T. Smith, and A. L. Vaughan, Phys. Rev. **48**, 525 (1935).
[8] K. E. Dorsch and H. Kallman, Zeits. f. Physik **60**, 376 (1930).

Heats of Dissociation of the N_2 Molecule and the NH Radical

G. GLOCKLER
Department of Chemistry and Chemical Engineering, State University of Iowa, Iowa City, Iowa
(Received February 16, 1948)

A comparison made between certain radicals and molecules would indicate that the heat of dissociation of nitrogen molecules ($D(N_2)$) is 9.764 ev and the heat of dissociation of NH radicals ($D(NH)$) into atoms is 3.74 ev.

THE heat of dissociation (D) of nitrogen molecules (N_2, $^1\Sigma_g^+$) into normal nitrogen atoms (^4S) is given by Herzberg[1] as 7.384 ev. However, Gaydon[2] discussed the interpretation of a predissociation phenomenon in the nitrogen spectrum made by Van der Ziel[3] and suggested that Van der Ziel's consideration is not necessarily unique and that the value 9.764 ev for the heat of dissociation of nitrogen molecules is not necessarily excluded. It is of interest to point out that the higher value goes very well with the heat of dissociation of carbon monoxide as given by Herzberg[1] ($D(CO)=9.144$ ev) and by Hagstrum[4] ($D(CO)=9.608$ ev). While the latter's argument for $D(CO)=9.608$ ev rests on only one experimental value of the appearance potential of O^+ ions in CO gas, still his analysis of the band spectrum of carbon monoxide must be given weight. As far as the present discussion is concerned a choice need not be made between these two values.

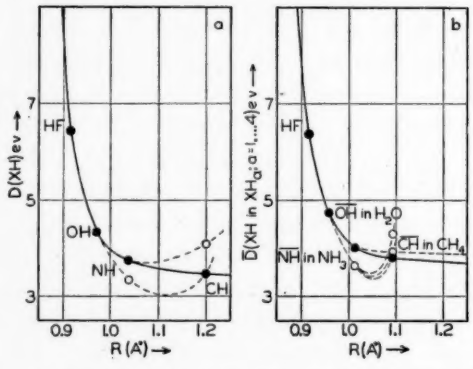

FIG. 1. Force constants of CH, NH, OH, and FH as radicals and in CH_4, NH_3, H_2O, and HF and the respective internuclear distances.

The comparison made here refers to the fact that $N_2(^1\Sigma_g^+)$ and $CO(^1\Sigma^+)$ molecules are isoelectronic and that it has been known for a long time that many of their physical properties are very closely alike.[5]

While considerations based on such comparisons are to be made with circumspection, as has been pointed out by Herzberg,[6] it may be permissible in the present stage of knowledge concerning heats of dissociation to bring the attention to any evidence which may contribute in the choice to be made of various values under consideration at this time.

A further bit of indirect evidence for the higher value of $D(N_2, {}^1\Sigma_g^+)$ can be gleaned from a study of the heats of dissociation of the first row hydride radicals (CH, NH, OH, FH). The force constants (k) of these diatomic molecules and their internuclear distances (R_e) are known.[7] In similar series it has been found by many investigators[8–13] that *the larger the internuclear*

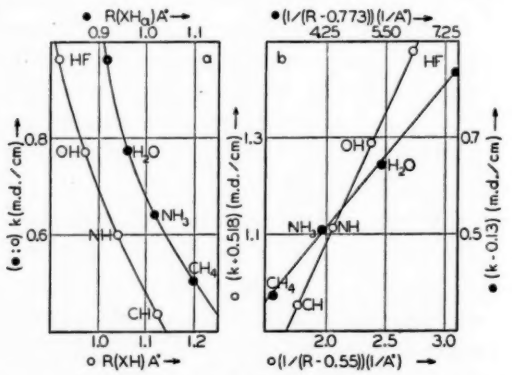

FIG. 2. Heats of dissociation of CH, NH, OH, and HF and average bond energies in CH_4, NH_3, H_2O, and HF and the respective internuclear distances.

[1] G. Herzberg, *Molecular Spectra and Molecular Structure, I. Diatomic Molecules* (Prentice-Hall, Inc., New York, 1939).
[2] A. G. Gaydon, Nature **153**, 407 (1944).
[3] A. Van der Ziel, Physica **4**, 373 (1937).
[4] H. D. Hagstrum, Phys. Rev. **72**, 947 (1947).
[5] I. Langmuir, J. Am. Chem. Soc. **41**, 868 (1919).
[6] See reference 1, p. 371.
[7] See reference 1, Table 36.
[8] R. M. Badger, J. Chem. Phys. **2**, 128 (1934); **3**, 710 (1935).

TABLE I. Force constants, heats of dissociation and internuclear distances (reference 1, Table 36).

		k(m.d./cm) (Expt.)	k(m.d./cm) (Calc'd) Eq. 1	R_e (A)	D(ev) (Expt.)	D(ev) (Calc'd) Eq. 2
CH	$^2\Pi_r$	0.435	0.436	1.120	3.47	(3.47)
NH	$^3\Sigma^-$	0.600[a]	0.597	1.038	3.40(?)	3.74
OH	$^2\Pi_i$	0.773	0.774	0.971	4.34[b]	(4.35)
FH	$^1\Sigma^+$	0.963	0.964	0.917	6.43[c]	(6.42)

[a] The frequency ($\omega_e \doteq 3300$ cm^{-1}) is only approximately known (reference d).
[b] R. J. Dwyer and O. Oldenberg, J. Chem. Phys. **12**, 351 (1944).
[c] $D(F_2)=2.8$ ev, reference 1.
[d] G. W. Funke, Zeits. f. Physik **96**, 787 (1935).

distance (R_e) the smaller is the force constant. The relation is shown in Fig. 1a (Table I). It can be expressed empirically as

$$k=0.544[1/(R_e-0.550)]-0.518 \qquad (1)$$

for the diatomic radicals (Fig. 1b). The force constants for the corresponding saturated molecules are also shown in Fig. 1a and as a straight line

$$k=0.12[1/(R_e-0.773)]+0.13 \qquad (2)$$

in Fig. 1b.

Similarly, it has also been found[14–21] that the *heat of dissociation (D) of diatomic molecules is greater for smaller internuclear distances* in certain series of molecules and radicals. The case for the hydrides CH, NH, OH, and HF is shown in Fig. 2a and as a straight line

$$D=0.12[1/(R_e-0.884)]+2.92 \qquad (2)$$

in Fig. 3 *where, however, $D(NH)=3.4$ ev has been omitted.* This empirical relation is used to interpolate a value for D(NH) of 3.74 ev. The value given by Bates[22] of 4.43 ev, and mentioned by Bichowsky and Rossini,[23] is only an upper limit. The value calculated by King[24] using Stehn's[25] formula also depends on an interpolation and may not deserve any more consideration than the value of 3.74 ev suggested here.

TABLE II. Average bond energies of hydrides of first row elements.

	Q_f ev	Q_a ev	$\bar{D}$(MH) ev	R_e[i] A	k[i] m.d./cm
CH_4	0.693[a]	15.07[d]	3.77	1.094	0.504
		15.54[e]	3.88		
		16.98[f]	4.25		
NH_3	0.476[b]	12.07[g]	4.02	1.014	0.642
		10.89[h]	3.63		
OH_2	2.49[c]	9.47	4.73	0.958	0.776
FH	2.78[b]	6.43	6.43	0.9166	0.963

[a] E. J. Prosen, K. S. Pitzer, and F. D. Rossini, Bull. Nat. Bur. Stand. **34**, 403 (1945).
[b] See reference 24.
[c] R. J. Dwyer and O. Oldenberg, J. Chem. Phys. **12**, 351 (1944).
[d] Based on $L(C)=5.424$ ev.
[e] Based on $L(C)=5.888$ ev.
[f] Based on $L(C)=7.334$ ev.
[g] Based on $D(N_2)=9.76$ ev.
[h] Based on $D(N_2)=7.38$ ev.
[i] G. Herzberg, *Infrared and Raman Spectra of Polyatomic Molecules* (D. Van Nostrand Company, Inc., New York, 1945).

It is next of interest to compare this value with the average bond energy of NH in ammonia ($\bar{D}$(NH in NH_3)). The calculation is made on the two assumptions: $D(N_2)=9.76$ ev *or* $D(N_2)=7.38$ ev:

$$\begin{aligned} N_2+3H_2 &\rightarrow 2NH_3 + 0.95 \text{ ev or } + 0.95 \text{ ev} \\ 2N &\rightarrow N_2 \quad + 9.76 \text{ ev or } + 7.38 \text{ ev} \\ 6H &\rightarrow 3H_2 \quad +13.44 \text{ ev or } +13.44 \text{ ev} \\ \hline N+3H &\rightarrow NH_3 \quad +12.07 \text{ ev or } +10.89 \text{ ev} \end{aligned}$$

$\bar{D}$(NH in NH_3) = 4.02 ev *or* 3.63 ev.

These two possible cases are now compared with the corresponding quantities $\bar{D}$(CH in CH_4),

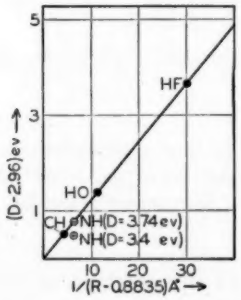

FIG. 3. Straight line relation between heats of dissociation and internuclear distance for CH, NH, OH, and HF.

[9] C. H. Douglas Clark, Phil. Mag. **18**, 459 (1934).
[10] G. M. B. Sutherland, J. Chem. Phys. **8**, 161 (1940).
[11] J. J. Fox and E. A. Martin, J. Chem. Soc. **180**, 2106 (1938).
[12] R. Cherton, Bull. Soc. Chim. Belg. **52**, 26 (1943).
[13] L. Pauling, *The Nature of the Chemical Bond* (Cornell University Press, Ithaca, 1940).
[14] A. H. Skinner, Trans. Faraday Soc. **41**, 645 (1945).
[15] A. H. Long and A. D. Walsh, Trans. Faraday Soc. **43**, 342 (1947).
[16] A. H. Long and R. G. W. Norrish, Proc. Roy. Soc. **A187**, 337 (1946).
[17] A. D. Walsh, Trans. Faraday Soc. **42**, 52, 779 (1946); **43**, 60 (1947).
[18] H. D. Springall, Trans. Faraday Soc. **43**, 177 (1947).
[19] J. L. Kavanau, J. Chem. Phys. **12**, 467 (1944); **15**, 77 (1947).
[20] W. Gordy, J. Chem. Phys. **15**, 81, 305 (1947).
[21] W. J. Bernstein, J. Chem. Phys. **15**, 284, 339, 688 (1947).
[22] J. R. Bates, Zeits. f. physik. Chemie Bodenstein Festband 329 (1931).
[23] F. R. Bichowsky and F. D. Rossini, *The Thermochemistry of the Chemical Substances* (Reinhold Publishing Corporation, New York, 1936).
[24] G. W. King, J. Chem. Phys. **6**, 378 (1938).
[25] J. R. Stehn, J. Chem. Phys. **5**, 186 (1937).

$\bar{D}$(OH in H_2O) and $\bar{D}$(HF in HF). As seen in Fig. 2b, the value $\bar{D}$(NH in NH_3) = 4.02 ev fits into this series. The needed information is collected in Table II. The heat of formation from atoms (Q_a) divided by the number of bonds gives the average bond energy ($\bar{D}$).

The lower value of 3.63 ev of $\bar{D}$(NH in NH_3) based on $D(N_2) = 7.38$ ev is *less than* D(NH, radical) (= 3.74 ev), whereas the corresponding distances are R(NH in NH_3) = 1.014A and R(NH, radical) = 1.038A. The higher value of 4.02 ev for $\bar{D}$(NH in NH_3) is therefore more acceptable.

With the higher value of $D(N_2) = 9.764$ ev, the appearance potential of N^+ ions[4] will then refer to the reaction

$$\begin{array}{ll} N_2(X\,^1\Sigma_g^+) \rightarrow N(^4S) + N(^4S) & -\ 9.764 \text{ ev} \\ N(^4S) \rightarrow N^+(^3P) + E^- & -14.480 \text{ ev} \\ \hline N_2(X\,^1\Sigma_g^+) \rightarrow N^+(^3P) + N(^4S) + E^- & -24.244 \text{ ev} \end{array}$$

rather than to

$$\begin{array}{ll} N_2(X\,^1\Sigma_g^+) \rightarrow N(^4S) + N(^4S) & -\ 7.384 \text{ ev} \\ N(^4S) \rightarrow N(^2D) & -\ 2.381 \text{ ev} \\ N(^4S) \rightarrow N^+(^3P) + E^- & -14.480 \text{ ev} \\ \hline N_2(X\,^1\Sigma_g^+) \rightarrow N^+(^3P) + N(^2D) + E^- & -24.245 \text{ ev} \end{array}$$

The only difference is the state of the nitrogen atom, which cannot be detected in a mass spectrograph. Hence no conflict is apparent with these impact experiments. The effect on the heat of dissociation of NO will be discussed at a later date.

The values for the carbon-hydrogen bond energies have been taken from a study[26] which indicates that the high value of the heat of sublimation of carbon (L(C) = 7.334 ev) is not acceptable, since the CH bond energy for the free radical would have to be 4.08 ev rather than the spectroscopic value of 3.47 ev (Table I). It is seen that this high value does not fit at all into the sequence of Fig. 2a nor does the average bond energy $\bar{D}$(CH in CH_4) as shown in Fig. 2b.

Wahrhaftig[27] determined that the heat of dissociation of F_2 should be somewhat less than the usually accepted value (2.8 ev). It has no great influence on the interpolation made here (Fig. 2). The constants of Eqs. (1) and (2) are slightly changed for a smaller value of $D(F_2)$, but the empirical value of D(NH) = 3.74 ev is not affected.

The comparison made here favors the higher value of the heat of dissociation of nitrogen ($D(N_2) = 9.764$ ev) and either of the lower values of the heat of sublimation of carbon (L(C) = 5.424 or 5.888 ev).

[26] Unpublished results.
[27] A. L. Wahrhaftig, J. Chem. Phys. **10**, 248 (1942).

THE JOURNAL OF CHEMICAL PHYSICS VOLUME 16, NUMBER 6 JUNE, 1948

The Heat of Dissociation of Nitric Oxide

G. GLOCKLER
Department of Chemistry and Chemical Engineering, State University of Iowa, Iowa City, Iowa
(Received February 16, 1948)

The heat of dissociation of nitric oxide (D(NO)) is considered to be 6.49 ev on the basis of a comparison of the series CO, NO, O_2, OF, its band spectrum, and its photo-chemical dissociation. Appearance potentials of N^+, O^+, and O^- can be interpreted on this basis.

IF the heat of dissociation of nitrogen is 7.384 ev,[1] then the heat of dissociation of nitric oxide must be 5.30 ev since the heat of dissociation of oxygen is known to be 5.082 ev. However, Gaydon[2] discussed the possibility that the higher value of 9.764 ev for the heat of dissociation of N_2 is more acceptable. The following considerations lend support to this view.

[1] G. Herzberg, *Molecular Spectra and Molecular Structure I. Diatomic Molecules* (Prentice-Hall, Inc., New York, 1939).

[2] A. G. Gaydon, *Dissociation Energies and Spectra of Diatomic Molecules* (John Wiley and Sons, Inc., New York, 1947).

SERIES COMPARISON

If the heats of dissociation of the oxides of the first row elements C, N, O, F are compared (Fig. 1 and Table I), it is seen that the relation between dissociation energy (D) and internuclear distance (R) shows the same trend as does the similar relation between force constant (k) and internuclear distance. Such comparisons have been made by other writers,[3] and they appear to have validity if the series of structures to be studied is chosen properly. In the present case the four elements belong to the first group of the periodic table, and their oxides are all diatomic molecules, with the exception of the OF radical, where the necessary information was obtained from fluorine monoxide, to be discussed below. The relation between force constants and internuclear distances follows the rule that a large force constant goes with a relatively small internuclear distance, even though the electron structures are disposed in a variety of ways.

Since the heat of dissociation of carbon monoxide is still in question,[2,4] two values have been included in Table I. However, the main point of the present argument is not affected. It is seen from Fig. 1 that *the lower value of 5.30 ev of the heat of dissociation of NO does not fit into this series*. If the attempt is made to include it, then a curve is obtained which is quite different from the corresponding $k-R$ curve. This finding is used for the assertion that the higher figure of D(NO) (=6.49 ev) is the correct value. The heat of dissociation of the OF radical was estimated to be 2.45 ev from the compound OF_2, using the heat of formation (Q_f) given by Bichowsky and Rossini.[5] The heat of dissociation of F_2 was taken as 2.6 ev.[6] Had the higher current value (2.8 ev)[1] been employed, then the average bond energy ($\bar{D}$(OF)) would have been 2.55 ev with no effect on the trend of the curve in the important region. The breaking of the first OF bond in OF_2 may, however, be quite different from the bond energy of the remaining OF radical. A study of similar cases (water, ozone) indicates that D(OF) would hardly be greater than about 3.5 ev and that R(OF) would not differ very much from R(OF in O_2F). In order

TABLE I. Force constants (k), dissociation energies (D), and internuclear distances (R) (reference 1, Table 36).

		k (m.d./cm)	R A	D(ev) [a]	[b]	[c]	[d]
N_2	$^1\Sigma_g^+$	2.286	1.095	7.384	7.384	9.764	9.764
CO	$^1\Sigma^+$	1.89	1.1284	11.054	9.608	11.054	9.608
NO	$^2\Pi_r$	1.59	1.150	5.30	5.30	6.49	6.49
O_2	$^3\Sigma_g^-$	1.18	1.2076	5.082	5.082	5.082	5.082
$\overline{OF}$	(OF_2)	0.56	1.41±.05	2.45	2.45	2.45	2.45[e]

[a] $D(N_2)=7.384$ ev; $L(C)=7.334$ ev.
[b] $D(N_2)=7.384$ ev; $L(C)=5.888$ ev.
[c] $D(N_2)=9.764$ ev; $L(C)=7.334$ ev.
[d] $D(N_2)=9.764$ ev; $L(C)=5.888$ ev.
[e] See text.

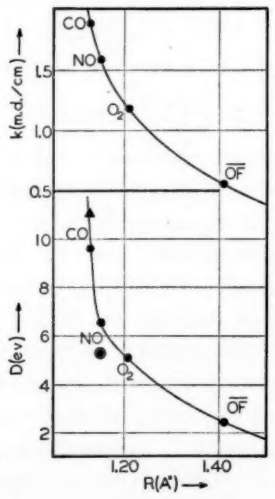

FIG. 1. Force constants and dissociation energies of CO, NO, O_2, and $\overline{OF}$.

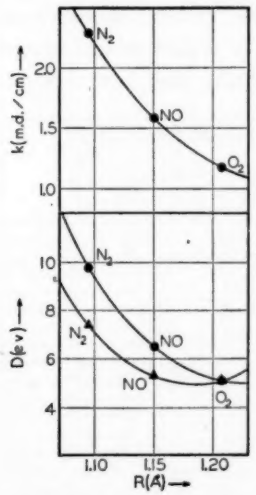

FIG. 2. Force constants and dissociation energies of N_2, NO, and O_2.

[3] For literature references see G. Glockler, J. Chem. Phys. **16**, 602 (1948).
[4] H. D. Hagstrum, Phys. Rev. **72**, 947 (1947).
[5] F. R. Bichowsky and F. D. Rossini, *The Thermochemistry of the Chemical Substances* (Reinhold Publishing Corporation, New York, 1936).
[6] A. L. Wahrhaftig, J. Chem. Phys. **10**, 248 (1942).

TABLE II. Beta-bands of nitric oxide.

1	2	3	4	5	6	7	8	9
	Band origins[a]		Band centers[b]		Intensity ob-			Reference
(v′, 0″)	cm⁻¹	diff.	cm⁻¹	diff.	2–4	served	F.C.	below
0′	45440					0	0	
		1023						
1′	46463					0	0	
		1008						
2′	47471		47369		+102	1	0	
		995		1006				
3′	48466		48375		+ 91	1	0	
		981		976				
4′	49447		49351		+ 96	2	0	
		969		984				
5′	50416		50335		+ 81	2	0	
		957		937				
6′	51373		51272		+101	?	0	e
		945		1068				
7′	52318		(52340)		− 22	?	1	d
		936		931				
8′	53254		(53271)		− 17	?	1	e
		925		859				
9′	54179		54130		+ 49	4	2	
		915		—				
10′	55094		—		—	0	1	f
		904		—				
11′	56008		55885		+123	1	2	i
		899		1150				
12′	56907		(57035)		−128	1	3	g,i
		892		778				
13′	57799		(57813)		− 14	1	8	h,i
		885		687				
14′	58684		58500		+184	1	10	i,j
		879		1105				
15′	59563		59605		− 42	8	10	k

[a] F. A. Jenkins, H. A. Barton, and R. S. Mulliken, Phys. Rev. **30**, 150 (1927), Eq. 8 (average values are used).
[b] S. W. Leifson, Astrophys. J. **63**, 73 (1926).
[c] On short wave-length side of $\gamma(3',0'')$; mentioned in Leifson's Table 5 (reference 2).
[d] Covered by $\delta(0',0'')$ with center at 52340 cm⁻¹.
[e] Covered by $\epsilon(0',0'')$ with center at 53271 cm⁻¹.
[f] Not mentioned by Leifson (reference 2).
[g] Near $\delta(2',0'')$ at 57035 cm⁻¹.
[h] Near $\epsilon(2',0'')$ or 57813 cm⁻¹.
[i] Allocation not certain.
[j] 1704A may be $\beta(16',1'')$.
[k] Strongest β-band in entire absorption spectrum.

that the value 5.30 ev for D(NO) should fit into the D–R curve, D(OF) would need to be about 4.5 ev. Such a value would mean that the removal energy for the first oxygen atom would

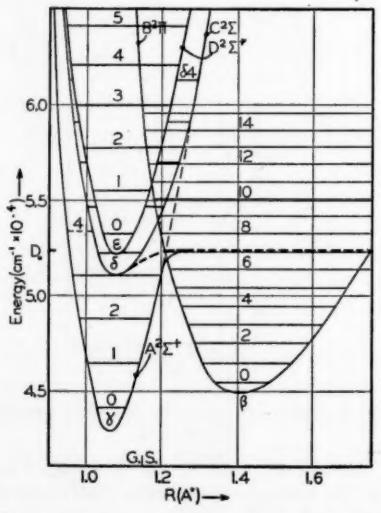

FIG. 3. Potential energy curves of NO.

TABLE III. Gamma- and epsilon-bands of NO.

1	2	3	4	5	6	7	8	9
	Band origins[a]		Band centers[b]		Intensity[c] ob-			Reference
(v′, 0″)	cm⁻¹	diff.	cm⁻¹	diff.	2–4	served	F.C.	below
0′	44198		44156		42	4	0	
		2342		2326				
1′	46540		46492		48	4	0	
		2310		2317				
2′	48850		48809		41	4	1	
		2278		2279				
3′	51128		51088		39	3	2	
0′	53293		53271		22	7	8	e
		2281		2297				
1′	55574		55568		6	10	8	
		2235		2245				
2′	57809		57813		−4	6	5	d
		2189		2187				
3′	59998		60000		−2	5	4	
		2143		2089				
4′	62141		62089		52	1		
		2097		2145				
5′	64238		64234		4	2		

[a] P. Migeotte, Bull. Soc. Roy. Sci. Liége **14**, 40 (1945) gives (0′,0″) =44120; (1′,0″) =46460; (2′,0″) =48780 and (3′,0″) =51060 cm⁻¹ (all values are averages); P. Migeotte and B. Rosen, *ibid.* **14**, 49 (1945); A. G. Gaydon, Proc. Phys. Soc. London **56**, 90, 160 (1944); B. Rosen, Phys. Rev. **68**, 124 (1945); R. Schmid, Zeits. f. Physik **49**, 428 (1928).
[b] S. W. Leifson, Astrophys. J. **63**, 73 (1926).
[c] $\beta(8',0'')$ at 53254 cm⁻¹.
[d] $\beta(13',0'')$ at 57799 cm⁻¹.

be only about 0.6 ev (5.1–4.5 ev). However, in the similar case of Cl_2O, Finkelnburg and Schumacher[7] give from spectral data

$$ClO_2 \rightarrow ClO + O(^1D) - 4.4 \text{ ev},$$

or

$$ClO_2 \rightarrow ClO + O(^3P) - 2.4 \text{ ev}.$$

Since[5]

$$Cl + 2O \rightarrow Cl_2O + 5.30 \text{ ev},$$

it follows that

$$ClO \rightarrow Cl + O + 2.9 \text{ ev}.$$

This is just about one-half of the atomic heat of reaction (5.30 ev). Hence it appears likely that D(OF) is about equal to $\bar{D}$(OF in OF_2).

Another comparison can be made for the three molecules N_2, NO, O_2. It is seen from Fig. 2 that the higher values for $D(N_2)$ and D(NO) give a $D-R$ curve which shows the same trend as the $k-R$ curve. It is interesting to recall that Mulliken[8] and Herzberg[1] give for the number of bonds, 3, 2.5, and 2, respectively. While such comparisons in themselves are not sufficient to render a decision in doubful cases, still they should be given some weight. Since heats of dis-

[7] W. Finkelnburg and H. J. Schumacher, Zeits. f. physik. Chemie Bodenstein Festband 704–16 (1931).
[8] R. E. Mulliken, Rev. Mod. Phys. **4**, 1 (1932).

sociation have been in question for so many years,[2] it seems appropriate to discuss any and all lines of argument which might help in settling the values of these important constants. It is believed that these *series comparisons* can be used as additional lines of argument to assist in determining magnitudes of force constants, internuclear distances, or bond energies.

BAND SPECTRUM

The higher value of $D(NO)$ must fit into the energy level scheme of the molecule. In this connection it is of interest to point out that. Herzberg and Mundie[9] make the suggestion that the ϵ-bands of NO are really a continuation of the γ-bands, as can be seen from their table of intervals. They base their remarks on the absorption spectra of Leifson[10] and derive a predissociation limit between 51088 and 53271 cm^{-1} (6.33 and 6.60 ev). Hence $D(NO)$ must be equal to or less than these values. There is quite a remarkable change in intensity of these bands at $v'=4$. It may be supposed that some of the so-called γ-bands ($v'=4$ to 7) are stronger than expected because some of them overlap certain β-bands, enhancing their appearance on the photographic plate. The band at 1877.2A (53271 cm^{-1}) could be $\gamma(4',0'')$ (53375 cm^{-1}) *and* $\beta(8',0'')$ (53254 cm^{-1}) *and* $\beta(10',1'')$ (53216 cm^{-1}). However, Gaydon[11] and Migeotte and Rosen[12] have shown that the ϵ-bands are really a band system apart from the γ-bands and $\gamma(4',0'')$ is really $\epsilon(0',0'')$, etc.

The band at 1799.6A (55568 cm^{-1}), however, is very likely only $\epsilon(1',0'')$ since other bands are about 400 cm^{-1} distant. The band at 1729.7A (53813 cm^{-1}) can be $\epsilon(2',0'')$ (57795 cm^{-1}) *and* $\beta(13',0'')$ (57799 cm^{-1}). The band at 1666.6A

TABLE IV. Delta-bands of nitric oxide.

Band origins[a–e]		Band centers[d]		Intensity		Reference
$(v',0'')$	cm^{-1}	cm^{-1}	diff.	observed	*F.C.*	below
0′	52287	52340		8	0	[e]
			2329			
1′		54669		10	5	
			2366			
2′		57035		6	10	[f]
			2127			
3′		59168		4	8	
			2518			
4′		61686		2	8	[g]

[a] A. G. Gaydon, Proc. Phys. Soc. London **56**, 90 (1944); P. Migeotte and B. Rosen, Bull. Soc. Roy. Sci. Liége **14**, 49 (1945); H. P. Knauss, Phys. Rev. **32**, 417 (1928).
[b] W. Jevons, *Band Spectra of Diatomic Molecules* (University Press, Cambridge, England, 1932).
[c] R. Schmid, Zeits. f. Physik **59**, 42 (1930); **64**, 279 (1930).
[d] S. W. Leifson, Astrophys. J. **63**, 73 (1926).
[e] $\beta(7,0)$ at 1911.4A or 52318 cm^{-1} is located here.
[f] $\beta(12,0)$ at 1757.2A or 56907 cm^{-1} is located here.
[g] Broad band.

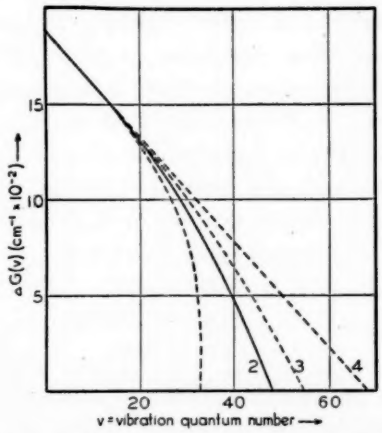

FIG. 4. Heat of dissociation of NO. 1. $D(NO)=5.30$ ev based on $D(N_2)=7.384$ ev. 2. $D(NO)=6.49$ ev based on $D(N_2)=9.764$ ev. 3. $D(NO)=7.02$ ev after Jenkins, Barton, and Mulliken (reference 10). 4. $D(NO)=7.92$ ev after Birge and Sponer (reference 18).

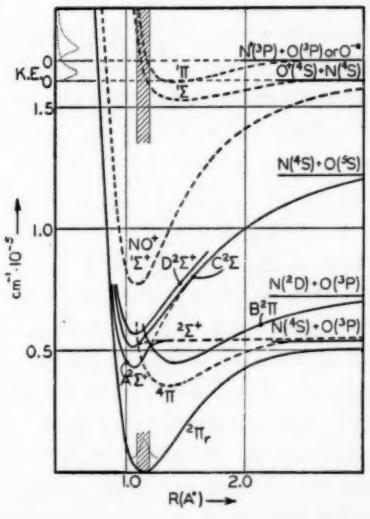

FIG. 5. Potential energy curves for NO and NO^+. $N(^4S)+O(^3P)=52380$ cm^{-1} or 6.49 ev; $N(^2D)+O(^3P)=71590$ cm^{-1} or 8.88 ev; $N(^4S)+O(^1S)=126150$ cm^{-1} or 15.64 ev; $O^+(^4S)+N(^4S)=161640$ cm^{-1} or 20.04 ev; $N^+(^3P)+O(^3P)$ or $O^{-*}=169140$ cm^{-1} or 20.97 ev.

[9] G. Herzberg and L. G. Mundie, J. Chem. Phys. **8**, 263 (1940).
[10] S. W. Leifson, Astrophys. J. **63**, 73 (1926).
[11] A. G. Gaydon, Proc. Phys. Soc. London **56**, 90, 160 (1944).
[12] P. Migeotte and B. Rosen, Bull. Soc. Roy. Sci. Liége **14**, 49 (1945).

(60000 cm^{-1}) can be γ (3′,0″) (59955 cm^{-1}) and no overlapping occurs. The band at 1957.4A (51088 cm^{-1}) is clear of β(6′,0″) (51373 cm^{-1}) and of β(8′,1″) (51376 cm^{-1}) by about 290 cm^{-1}. Hence considerable overlapping can be responsible for the actual intensity distribution of many bands on Leifson's photograph.

The details can best be seen in Tables II–IV. The band origins of the β-bands were calculated from an equation given by Jenkins, Barton, and Mulliken.[13] The similar quantities for the γ-, δ-, and ϵ-bands were obtained from Gaydon.[11] It should be noted that Knauss[14] recognized the band δ(0′,0″) on Leifson's photograph. The difference between his value for the band head (1915.7A) and Leifson's measurement (1910A) he ascribes to the fact that the latter's values were all for the middle of the bands. This latter fact must be kept in mind when comparison is made between calculated values and experimental absorption bands. Rough guesses of intensities based on visual inspection of Leifson's photographs[10] and a crude use of the Franck-Condon principle are given in columns 9 and 10 of his Tables II–IV. The principle is not applicable in a simple manner in the present case as has been mentioned by Kaplan[15] and Barton, Jenkins, and Mulliken.[16]

These considerations and the work of Gaydon[11] suggest that an upper $^2\Sigma^+$ state (from N(^{5}S) +O(^{3}P) at 6.49 ev) might cross the region near $\delta(1',0'')=54700$ cm^{-1} at 1.15A. However, the non-crossing rule would have to be violated three times ($A^2\Sigma^+$, $C^2\Sigma$, $D^2\Sigma^+$). It is therefore necessary to consider another scheme, shown in Fig. 3. Here $A^2\Sigma^+$ is perturbed by a flat $^2\Sigma^+$ state as above, so that γ(4′,0″) does not exist. These two states form C$^2\Sigma$. The $D^2\Sigma^+$ state lies above and is not affected. The non-crossing rule is not violated. $A^2\Sigma^+$ may have a maximum at about 1.2A. Two interesting facts are noticeable in this connection. β(10′,0″) is not mentioned by Leifson at all and certainly cannot be seen on the published photograph. This level seems greatly perturbed. Similarly, β(11′,0″) differs considerably from the calculated value. On the other hand, β(9′,0″) is very strong in comparison. Hence these three levels appear perturbed by the presence of a repulsive state. This point may be cited in favor of the crossing of the $^2\Sigma^+$ state at δ(1′,0″), as mentioned above. However, the main consideration, namely, that the higher value of D(NO)=6.49 ev, favored by Gaydon,[2] can be fitted into an energy diagram, seems acceptable. It is obvious that not all the points at issue have been resolved.

[13] F. A. Jenkins, H. A. Barton, and R. E. Mulliken, Phys. Rev. **30**, 150 (1927).
[14] H. P. Knauss, Phys. Rev. **32**, 417 (1928).
[15] J. Kaplan, Phys. Rev. **37**, 1406 (1931).
[16] H. A. Barton, F. A. Jenkins, and R. S. Mulliken, Phys. Rev. **30**, 175 (1927).

PHOTO-CHEMICAL DISSOCIATION

Flory and Johnston[17] state that they have observed photo-chemical dissociation at 1830A. However, this wave-length need not be taken too literally since spark sources usually have quite a continuous distribution in wave-length of radiation emitted.

BIRGE-SPONER EXTRAPOLATION

It is always of interest in a study of this kind to see how a suggested value for a heat of dissociation compares with the well-known Birge-Sponer extrapolation.[18] The usual plot is indicated in Fig. 4. It should be noted that the use of the equation of the origins of the β-bands given by Jenkins, Barton, and Mulliken[13] gives a value for D(NO) nearer to the presently suggested figure than the usually accepted one.

APPEARANCE POTENTIALS

Hagstrum and Tate[19] studied the ionization and dissociation processes in nitric oxide. In their interpretation of these collision processes they used D(NO)=5.30 ev. Gaydon[2] already remarks that the larger value of 6.49 ev can be reconciled with the impact experiments. A detailed study (based on Fig. 5) of the processes

$$\begin{aligned} NO+E^- &\rightarrow N+O^{-*} \\ NO &\rightarrow N^+ + O \\ NO &\rightarrow N^+ + O^{-*} \\ NO &\rightarrow N+O^+ \end{aligned}$$

indicates that merely different amounts of kinetic energy of the resulting products need be assumed in order to bring the experiments into line with the high value of D(NO)=6.49 ev.

[17] P. J. Flory and H. L. Johnston, J. Am. Chem. Soc. **57**, 2641 (1935).
[18] R. T. Birge and H. Sponer, Phys. Rev. **28**, 259 (1926).
[19] H. D. Hagstrum and J. T. Tate, Phys. Rev. **59**, 354 (1941).

THE JOURNAL OF CHEMICAL PHYSICS VOLUME 16, NUMBER 6 JUNE, 1948

The Energy of the C−H Bond in the Fluoro-Toluenes

M. SZWARC AND J. S. ROBERTS
Department of Chemistry, The University, Manchester, England

(Received January 21, 1948)

The pyrolysis of the three fluoro-toluenes was investigated, and it was shown that the mechanism of the decomposition is the same as suggested previously for the decomposition of toluene and the xylenes. The experimental results prove that the C−H bond energy in all fluoro-toluenes is nearly the same as the C−H bond energy in toluene, i.e., about 78 kcal./mole, thus showing that the field effect has very little influence on the bond energy. This conclusion definitely establishes the presence of hyperconjugation for para-xylene as the cause of the weakening of the C−H bond in the CH_3 groups. The difference in the effects of dipoles on ionic and radical reactions is pointed out.

THE investigation of the pyrolysis of toluene and the xylenes[1] has revealed that these processes are homogeneous, unimolecular gas reactions. Their rate determining step is the dissociation of the hydrocarbon into a benzyl (or xylyl) radical and a hydrogen atom, and the latter reacts with the excess of hydrocarbon producing either H_2 or CH_4. The unimolecular rate constant (measured by the quantity of H_2+CH_4 produced) is given by

$$k_u = \gamma \cdot e^{-E/RT},$$

where γ has a value of the order $2 \cdot 0.10^{13} - 2 \cdot 5.10^{13}$ for toluene, and twice as much for xylenes (because of the statistical factor 2), and E is the bond energy of the C−H bond in the methyl group.*

In further pursuit of this investigation we have now measured the rates of pyrolysis of the three fluoro-toluenes and compared them to the rate of pyrolysis of toluene. We hoped that this might reveal the effect which the fields of the dipoles have on the energy of C−H bonds.

We shall assume as the first approximation that the value of γ remains the same for the k_u of the pyrolysis of all substituted toluenes.**,[2-4] On this basis the change in the C−H bond energy caused by substitution can be calculated from the ratio of k_u of the pyrolysis of the substituted toluene to the k_u obtained for the pyrolysis of toluene itself at the same temperature.

EXPERIMENTAL

The apparatus and the technique have been described by one of us in a previous paper.[1] In the present work the reaction vessel and the furnace were changed slightly, thus improving the temperature distribution and reducing its variations in the reaction vessel from ±2°C to ±1°C. The reinvestigation of the pyrolysis of toluene gave the same products and in the same proportions as reported previously,[1] while the individual values for k_u were about 5 percent lower than in the earlier experiments. This small discrepancy is most probably due to the somewhat arbitrary method of fixing on a particular value for the temperature of the reaction—in view of the temperature gradient—and also to some uncertainty in estimating the volume of the reaction vessel. Such errors are, of course, eliminated in comparing the k_u for various similar compounds measured in the same apparatus as we do in this paper.

The fluoro-toluenes were prepared by the method of Balz and Schiemann[5] (through the tolyl-diazonium fluoborates) and purified by

[1] M. Szwarc, J. Chem. Phys. **16**, 128 (1948).

* It is assumed that the recombination of the benzyl radical and the H atom does not involve any activation energy, and therefore the energy of activation for the dissociation process is equal to the heat of dissociation, i.e., to the C−H bond energy.

** A review of the literature (see references 2 and 3) shows that in various reactions the substitution in para- or meta-position of the benzene ring causes but slight change in the entropy of activation. This seems to be true even in the case of ortho substitution by F atom (see reference 4).

[2] E. G. Williams and C. N. Hinshelwood, J. Chem. Soc. 1079 (1934).

[3] C. K. Ingold and W. S. Nathan, J. Chem. Soc. 222 (1936).

[4] D. P. Evans, J. J. Gordon, and H. B. Watson, J. Chem. Soc. 1430 (1937).

[5] G. Balz and G. Schiemann, Ber. **60**, 1188 (1927); *ibid.*, **62**, 1798 (1929).

TABLE Ia.

Extrapolated to T = 1077°K

Run	T°K	% Decomp.	$k_u \cdot 10^3$ sec.$^{-1}$	$k_{1077} \cdot 10^3$ sec.$^{-1}$		$\frac{k_{1077}}{\text{Average } k \text{ toluene}}$		Remarks
Toluene								
1	1082	0.180	4.8	3.8		0.99		
2	1082	0.168	4.5	3.6		0.95		
3	1081	0.167	4.4	3.7		0.97		
5	1080	0.161	4.3	3.8	average	0.99		
6	1080	0.165	4.4	3.9	for	1.02		
26	1075	0.084	3.4	3.6	1077°K	0.95		
27	1073	0.088	3.5	3.9	3.81	1.02		
28	1070	0.082	3.2	4.0		1.05		
29	1071	0.084	3.3	3.9		1.02		
30	1072	0.086	3.4	3.9		1.02		
Para-fluoro-toluene								
7	1080	0.158	4.0	3.5		0.92		not pyrolyzed
8	1082	0.159	4.0	3.3		0.87		not pyrolyzed
12	1084	0.161	4.2	3.2		0.84		once pyrolyzed
13	1090	0.210	5.4	3.4		0.89	average	once pyrolyzed
14	1077	0.105	3.6	3.6		0.95	0.906	not pyrolyzed
15	1078	0.098	3.5	3.4		0.89		not pyrolyzed
16	1080	0.108	3.9	3.5		0.92		not pyrolyzed
18	1076	0.102	3.6	3.7		0.97		once pyrolyzed
Meta-fluoro-toluene								
20	1079	0.095	3.5	3.2		0.84		not pyrolyzed
22	1078	0.090	3.3	3.1		0.81	average	once pyrolyzed
23	1076	0.082	3.0	3.0		0.79	0.812	once pyrolyzed
24	1078	0.086	3.3	3.1		0.81		once pyrolyzed

TABLE Ib.

Extrapolated to T = 1120°K

Run	T°K	% Decomp.	$k_u \cdot 10^3$ sec.$^{-1}$	$k_{1120} \cdot 10^3$ sec.$^{-1}$		$\frac{k_{1120}}{\text{Average } k \text{ toluene}}$		Remarks
Toluene								
31	1117	0.390	16.0	17.2		0.90		
32	1117	0.367	15.9	17.1		0.90		
33	1118	0.379	16.3	16.8	average	0.89		
46	1132	0.705	29.6	20.1	for	1.05		
47	1120	0.437	18.6	18.0	1120°K	0.94		
51	1130	0.695	31.3	22.6	19.1	1.18		
52	1124	0.550	25.2	21.7		1.13		
53	1118	0.419	18.7	19.6		1.02		
Para-fluoro-toluene								
34	1108	0.324	12.1	17.5		0.92		twice pyrolyzed
36	1124	0.495	18.2	15.7		0.80		twice pyrolyzed
37	1123	0.565	21.8	17.4		0.92	average	twice pyrolyzed
38	1119	0.495	18.9	18.9		0.99	0.920	twice pyrolyzed
44	1124	0.616	21.9	18.8		0.98		three times pyrolyzed
Meta-fluoro-toluene								
39	1121	0.465	17.8	16.8		0.88		not pyrolyzed
40	1122	0.430	16.2	14.8		0.78	average	not pyrolyzed
41	1117	0.342	13.5	14.5		0.76	0.805	once pyrolyzed
42	1121	0.455	16.3	15.4		0.80		once pyrolyzed

TABLE Ic.

Extrapolated to T = 1090°K

Run	T°K	% Decomp.	$k_u \cdot 10^3$ sec.$^{-1}$	$k_{1090} \cdot 10^3$ sec.$^{-1}$		$\frac{k_{1090}}{\text{average } k \text{ toluene}}$		Remarks
Toluene								
70	1090	0.18	8.0	7.75	average	0.99		
71	1091	0.19	8.6	8.02	for	1.02		
72	1091	0.18	8.3	7.74	1090°K	0.98		
					7.84			
Ortho-fluoro-toluene								
74	1090	0.22	7.25	7.2		0.92		once pyrolyzed
75	1093	0.21	7.7	6.9		0.88	average	once pyrolyzed
76	1091	0.22	7.1	6.8		0.87	0.860	twice pyrolyzed
77	1092	0.19	6.4	5.9		0.76		twice pyrolyzed
95	1089	0.19	6.6	6.9		0.88		three times pyrolyzed

distillation, using an efficient column (meta and para), or by vacuum distillation (ortho). Successive pyrolysis showed that in the case of meta- and para-fluorotoluenes these products were sufficiently pure for our purpose, while in the case of the ortho-compound a constant rate of decomposition was reached after the first pyrolysis.

The results of the pyrolysis of toluene and of the three fluoro-toluenes are summarized in Table I. In the last column are the ratios of the observed k_u to the average value of the k_u for toluene. The deviations of these ratios from their mean value indicate the magnitude of the experimental errors involved in these measurements. The following points should be emphasized:

(a) No C_2 hydrocarbons nor any HF were observed in the products of the pyrolysis.***

(b) The crystalline products of the pyrolysis of the fluoro-toluenes were isolated and identified as the corresponding di-fluoro-dibenzyls.[6] The quantities in which these compounds are formed during the pyrolysis indicate, as was expected if we apply here the reaction mechanism suggested for the pyrolysis of toluene, that their production corresponds to the stoichiometric proportion of one mole of dibenzyl derivative for one mole of H_2 or CH_4 produced.

(c) The analysis, recorded in Table II, of the gas produced in the pyrolysis shows that the H_2/CH_4 ratio for the para- and meta-fluoro-toluene is the same as for toluene,[1] while the gas produced in the pyrolysis of ortho-fluoro-toluene has a composition similar to that observed for ortho-xylene.[1]

(d) The rates of pyrolysis of all three fluoro-toluenes lie within a range 20 percent of the rate of pyrolysis of toluene at the same temperature.

In view of these results we have no hesitation in regarding the decomposition of the fluoro-toluenes as based on the same mechanism as that suggested for toluene.

DISCUSSION

The present results show that the C−H bond energy in all three fluoro-toluenes is nearly the same as the C−H bond energy in toluene, i.e., about 78 kcal./mole. If we assume the entropy of activation in the decomposition of all these compounds to be exactly the same, the small decreases in the k_u of the fluoro-toluenes, as compared with that of toluene, lead to changes

*** In a few cases the pyrolysis of ortho-fluoro-toluene produced products recorded as C_2 hydrocarbon. These results, however, were rare and probably due to traces of water.

[6] These compounds are not described yet in the literature. Our note describing their identification and properties will be sent elsewhere.

in the C−H bond energy of +0.2–0.4 kcal./mole only (experimental error is ±0.2 kcal./mole).* Calculations based on electrostatic interaction between the C−F and the C−H dipoles show that the energy lost by the breaking of the C−H bond is of the order 0.04–0.25 kcal./mole. The observed variations in k_u (10 percent for para-fluoro-toluene, 20 percent for meta-fluoro-toluene, and 15 percent for ortho-fluoro-toluene) could be amply explained as a result of these dipole interactions, as also by the small variations in the entropy of activation, which is obviously not exactly constant.

At any rate, the influence of the dipole interaction on the bond energy is very small, amounting to a mere fraction of a kcal./mole. The last conclusion is important for the problem of the C−H bond energy in para-xylene. It was reported by Szwarc[1] that the C−H bond energy in para-xylene is less by 2.5 kcal. than the C−H bond energy in toluene, and the observed decrease in the C−H bond energy was explained by hyperconjugation. There had been the possibility, however, to ascribe the decrease of bond energy to the effect of electrostatic interaction between the two CH_3 groups. This possibility is now ruled out and the presence of hyperconjugation definitely established.

THE INFLUENCE OF THE DIPOLE IN IONIC REACTIONS

The apparent absence of any influence of the field effect of the bond energy is in contrast to the well-known fact that dipoles affect strongly the equilibria and reaction rate in ionic reactions. The difference is due to the fact that the energy of the electrostatic interaction between a dipole and an electric charge is much greater than the energy of interaction between two dipoles. Using, for example, the previous method of calculation, we find that the replacement of the C−H dipole in para-fluoro-toluene by a one-electron charge in the *p*-fluoro-benzyl ion increases the energy of the electrostatic interaction about one hundred times. All the regularities which are summarized in Hammett's σ-factors are due not to the interactions between dipoles but to the much greater interactions between dipoles and electric charges of the ions produced in the final states (affecting equilibria), or in the transition states (affecting rates of reaction).

The same conditions prevail in aromatic substitution reactions. Substitutions caused by ionic reagents are governed by the charge distribution in the molecule, which is strongly influenced by the dipole action. On the other hand, substitution caused by radical reagents does not show any dipole effect, as is well known in the chemistry of free radicals.

The authors would like to express their gratitude to Professor M. Polanyi for his continued interest and encouragement. One of us (J. S. R.) is indebted to the Department of Scientific and Industrial Research for a grant.

TABLE II. Gas analysis.

Compound	$\%H_2$	$\%CH_4$
Toluene	60%	40%
Para-fluoro-toluene	59% 61%	41% 39%
Meta-fluoro-toluene	59% 60%	41% 40%
Ortho-fluoro-toluene	41% 47% 46%	59% 53% 54%

The Refractive Index of Several Hydrocarbons in the Near Ultraviolet Wave-Length Region*

JAMES L. LAUER**
Randal Morgan Laboratory of Physics, University of Pennsylvania, Philadelphia, Pennsylvania
(Received February 18, 1948)

Index of refraction measurements were carried out with twenty-one liquid hydrocarbons, paraffinic, naphthenic, olefinic and aromatic, in their respective transparent regions between 220 and 420 millimicrons, both at 20° and at 25°C, to an average accuracy and precision of ±0.0002 in refractive index. The data for each compound were fitted to an empirical equation relating frequency and index, and from these the constants in the Sellmeier-Drude equation were calculated wherever possible. Interesting variations in these constants were observed for compounds of related structures. The instrument used for the measurements was the same as the one described in an earlier article (see reference 4).

INTRODUCTION

VERY few data on the change of index of refraction with wave-length for liquids in the ultraviolet are available today. This is due to a large extent to difficulties of measurement and to the lack of very pure samples, because the influence of small impurities is very pronounced in this region of the spectrum. It had, therefore, frequently been assumed without sufficient experimental proof that the dispersion equations which had been found to hold for a few wave-lengths in the visible could be extrapolated into the ultraviolet, at least for compounds where no absorption bands were known to occur in the near ultraviolet. It should be realized, however, that in terms of frequency squared the region from 220 to 420 mμ is at least three times as long as the entire visible spectrum. This enables the investigator to make a much better analysis of dispersion data than where only measurements in the visible region are at his disposal. In most cases the important absorption bands of hydrocarbons fall into the far ultraviolet, a region which is very difficult to explore experimentally, and the measurements described here are one of the few ways of obtaining a clue to the optical behavior there. This behavior is in turn a function of the structure of the compounds. Thus it is often possible to decide between several proposed structural formulas for a given compound.[1-3]

In principle, the instrument used for the measurements was a cell consisting of two quartz plates and an airspace between them which was rotated in the liquid through which a parallel monochromatic beam of light was passing in a manner such that the critical angle at the quartz-air interface could be determined. Since this instrument has already been described in the literature,[4] no discussion of it is required here.[5]

The accuracy and precision of the measurements reported in this article are believed to be about ±0.0002 in refractive index.

Chiefly to test the consistency of the data, readings at two different temperatures were almost always taken, for a comparison of these values gives the best check on reliability. Besides this check there is also the test of internal consistency, which means that the data all satisfy empiri-

* The material in this paper is taken from a thesis by James L. Lauer, submitted to the Graduate School of Arts and Sciences of the University of Pennsylvania in partial fulfillment of the requirements for the degree of Doctor of Philosophy in Physics in January 1948. A limited number of copies of a more detailed account of this work are available in mimeographed form and may be obtained by writing to Professor P. H. Miller, Jr., Physics Department, University of Pennsylvania, Philadelphia, Pennsylvania.

** Present address: Sun Oil Company, Norwood, Pennsylvania.

[1] *International Critical Tables* (McGraw-Hill Book Company, Inc., New York, 1930), Vol. VII, pp. 1–109.

[2] H. Gilman, *Organic Chemistry—An Advanced Treatise* (John Wiley and Sons, Inc., New York, 1943), second edition, Vol. II, p. 381.

[3] N. Bauer and K. Fajans, *Physical Methods of Organic Chemistry*, ed. by B. Weissberger (Interscience Publishers, Inc., New York, 1946), Vol. I, p. 653.

[4] James L. Lauer and P. H. Miller, Jr., J. Opt. Soc. Am. **37**, 664 (1947).

[5] The full significance of the interference fringes which are quite noticeable at the longer wave-lengths was not realized at the time the earlier paper was written. An explanation of this effect is given in the Appendix.

cal equations, and the test of group consistency, which means that the empirical constants in a given group change in a reasonable manner from compound to compound. It is therefore believed that the results are actually within the limits stated.

THEORY

It is not intended to present a detailed discussion of dispersion theory in this report since a number of excellent reviews are available in the literature.[6-8] For the region of normal dispersion a very satisfactory expression has been derived by Sellmeier and Drude, which is based on classical electromagnetic theory. This has the form

$$f(n)=\sum_k (\rho_k/\nu_k^2-\nu^2), \qquad (1)$$

where ρ_k is a constant, ν_k is a "characteristic frequency" related to, but not identical with, the frequency of maximum light absorption, and ν is the frequency of the light used. For each absorption band anywhere in the spectrum there will be a term; for spectral regions far from absorption bands usually a single term is all that is required, and for spectral regions close to absorption bands the formula will not hold because of the apparent discontinuity at the point $\nu=\nu_k$. The sharp break there can be avoided, however, by introduction of another term into the denominator, and this is, in effect, what has been done by Helmholtz by his assumption of dispersion being caused by damped harmonic motion of quasielastically bound electrons. The "friction factor," as it is called, is quite insignificant for most compounds in the wavelength region studied in this paper.

The form of the function $f(n)$ had been the subject of much controversy, especially when the question of the connection between index of refraction and density (or pressure) was discussed. At present, most physicists have adopted the Lorenz-Lorentz expression, *viz.*,

$$f(n)=(n^2-1)/(n^2+2),$$

but some of the assumptions made in its derivation have given rise to serious doubts and the simpler form $f(n)=n^2-1$ (Sellmeier-Drude), which was thought applicable for gases only, has been given preference by others.[9] As far as this paper is concerned, this question is irrelevant, for the simpler form can be derived from the other by merely changing the value of the constants. This can be seen as follows: According to the classical theory $(n^2-1)/(n^2+2)=4\pi N\alpha/3$, where N is the number of dispersion electrons per unit volume (cubic centimeter, c.g.s.—Gaussian units are used throughout) and α is the polarizability; also $4\pi N\alpha=\sum_k (\rho_k/\nu_k^2-\nu^2)$, so that upon combining $n^2-1=(4/3)\pi N\alpha(n^2-1)+4\pi N\alpha$ or $n^2-1=12\pi N\alpha/(3-4\pi N\alpha)$ is obtained. If the number of characteristic frequencies ν_k to be considered is finite, then n^2-1 represents a rational function which can be decomposed into partial fractions. To do this one only has to determine the zeros of the denominator, *viz.*, the roots of the equation

$$3-4\pi N\alpha=3-\sum\rho_k/(\nu_k^2-\nu^2)=0.$$

Let these be $\tilde{\nu}_k$, then the dispersion formula becomes $n^2-1=\sum_k (\tilde{\rho}_k/\tilde{\nu}_k^2-\nu^2)$, which is exactly what one would have gotten had one started out with $f(n)=n^2-1$, the so-called Sellmeier-Drude form. For the important case with only one characteristic frequency

$$3-\rho_1/(\nu_1^2-\nu^2)=0,$$

whence $\tilde{\nu}_1^2=\nu_1^2-(1/3)\rho_1$ and $\tilde{\rho}_1=\rho_1$.

Dispersion measurements alone are thus inadequate to distinguish between the various forms proposed for $f(n)$; it is necessary to have available at least some crude data on the characteristic frequencies from other sources, such as the absorption spectrum or the dispersion of the Faraday effect.

It is important to note that the constant in the numerator is independent of the form assumed for $f(n)$ when one characteristic frequency only is dealt with. It is in the explicit expression for this constant that the classical electromagnetic theory gives a formula different from the one derived on the basis of quantum mechanics. According to the former, $\rho_k=e^2N_k/\pi m$, where e and m are the electronic charge and mass,

[6] S. A. Korff and G. Breit, "Optical dispersion," Rev. Mod. Phys. **4**, 471 (1932).
[7] G. Breit, "Quantum theory of dispersion," Rev. Mod. Phys. **4**, 504 (1932).
[8] R. Becker, *Theorie der Elektrizitaet* (Teubner, Leipzig, 1933), Vol. II, Section 25 *et al.*
[9] S. S. Kurtz and A. L. Ward, J. Frank. Inst. **224**, 583, 697 (1937).

TABLE I. Dispersion constants for a number of saturated hydrocarbons (the constants listed over those of the equation $(n^2-1)^{-1}=a-bx$).

Compound	a 20°C	b 0.0	a 25°C	Density 20°C 0.0	Density 25°C 0.0	*	**	***
n-pentane	1.2244	1312	1.2349	62624	62139	1.04	1.05	1.844
n-hexane	1.1594	1259	1.1686	65937	6548	1.00	1.01	1.890
n-heptane	1.1155	1217	1.1235	68568	6795	1.01	1.01	1.926
n-octane	1.0836	1191	1.0911	70260	6986	1.00	1.01	1.948
n-noname	1.0586	1162	1.0656	71770	7138	1.01	1.02	1.972
n-decane	1.0391	1139	1.0448	72993	——	1.01	——	1.99
2,2,3-trimethylpentane	1.0662	1165	1.0732	71605	7121	1.01	1.01	
2,2,4-trimethylpentane	1.1037	1233	1.1116	69193	6878	0.98	0.99	
cyclohexane	0.9965	1025	1.0038	7788	7739	1.08	1.08	
methylcyclohexane	1.0077	1110	1.0142	76939	7651	1.01	1.01	
ethylcyclohexane	0.9790	1033	0.9849	78792	7839	1.06	1.06	
dimethylcyclohexane								
1,1-	0.9895	1026	0.9956	78070	7766	1.07	1.08	
cis-1,2-	0.9709	1020	0.9770	79627	7922	1.06	1.06	
trans-1,2-	0.9955	1058	1.0015	77601	7720	1.05	1.05	
cis-1,3-	0.9861	1042	0.9912	78472	7806	1.05	1.06	
trans-1,3-	1.0068	1075	1.0131	76603	7620	1.04	1.05	
cis-1,4-	0.9880	1045	0.9942	78285	7787	1.05	1.06	
trans-1,4-	1.0125	1081	1.0190	76255	7584	1.04	1.05	

* Dispersion electrons per bond at 20°C.
** Dispersion electrons per bond at 25°C.
*** Dielectric constant at 20°C.

respectively, and N_k is the number of electrons in one cubic centimeter which are oscillating with frequency ν_k. The modern theory has instead $\rho_k=e^2N_bf_k/\pi m$, where N_b is the population of the stationary energy states and f_k is the transition probability between two states corresponding fo the frequency ν_k.

The dispersion equation is one of the great accomplishments of quantum mechanics, for through it one was able to derive the classical expression which had been shown to agree with the fact very closely, from entirely different assumptions. Failure of the old quantum theory to treat the phenomenon of the dispersion of light had been an important cause leading to its decline.[10]

If two different types of energy levels occur in the same molecule, the quantum-mechanical dispersion formula is to be written in the form

$$f(n)=(e^2/\pi m)\left[\frac{N_{b1}f_{1kl}}{(\nu_{1kl})^2-\nu^2}+\frac{N_{b2}f_{2kl}}{(\nu_{2kl})^2-\nu^2}\right], \quad (2)$$

when the transition between the energy states k and l is the only one determining the refractive index in the region considered. Since the f values are constants for certain types of energy levels, they also find application in the analysis of the electronic structure of molecules.[11]

All the characteristic frequencies that we have here to deal with are located in the ultraviolet, mostly in the vacuum ultraviolet region of the spectrum. The terms in the dispersion equation are therefore expected to be positive.

Since it can thus be assumed that $\nu_k^2\gg\nu^2$, the following expansion can be carried out:

$$\begin{aligned} f(n)&=\textstyle\sum_k \rho_k/(\nu_k^2-\nu^2)\\ &=A/(B-x)+C/(D-x)+\cdots(x\equiv(\nu^*)^2\cdot10^{-8})\\ &=(A/B+C/D+\cdots)(\nu^*\equiv\nu/c=1/\lambda)\\ &\quad+(A/B^2+C/D^2+\cdots)x\\ &\quad+(A/B^3+C/D^3+\cdots)x^2+\cdots, \end{aligned} \quad (3)$$

and the series will converge since $x^2\ll B^2$, $x^2\ll D^2$, etc. This equation gives the index as a function of frequency squared in the form of an ordinary

[10] Pauling and Wilson, *Introduction to Quantum Mechanics* (McGraw-Hill Book Company, Inc., New York, 1935), p. 48.

[11] R. S. Mulliken and C. A. Rieke, Reports on Progress in Physics 8, 231 (1941).

power series, i.e.,

$$f(n)=a'+b'x+c'x^2+\cdots, \quad (4)$$

which is linear in the coefficients and allows simple treatment by the method of least squares. From a knowledge of the empirically found coefficients a', b', c', and d', and from the assumption of a two term dispersion equation, the theoretically important constants A, B, C, and D could easily be calculated from the four simultaneous equations obtained by comparing coefficients in Eqs. (3) and (4).

As has already been pointed out, a one-term dispersion equation of the Sellmeier-Drude type is almost always satisfactory for spectral regions not too close to an absorption band. (This does not necessarily mean that there is only one characteristic frequency, because any number of such frequencies will produce an average effect.) P. Wulff[12] therefore advised plotting dispersion data in the reciprocal form

$$1/f(n)=B/A-(1/A)(\nu^*)^2=a-b(\nu^*)^2 \qquad (\nu^*\equiv 1/\lambda), \quad (5)$$

because $[f(n)]^{-1}$ and $(\nu^*)^2$ are linearly related. An increase in negative slope toward the shorter wave-lengths can be interpreted as being caused by either the presence of more than one Sellmeier-Drude term, or by the presence of a damping factor.

There is yet another way of writing the single-term dispersion equation which has to be mentioned here. Starting with $1/f(n)=a-bx$ and changing frequencies to wave-lengths yields

$$f(n)=1/a+b/a^2\cdot(\lambda^2-b/a). \quad (6)$$

Thus b/a is the characteristic wave-length and $1/a$ is the refractive index function for infinite wave-length which should be related to the dielectric constant by Maxwell's formula $n^2=\epsilon$. Assuming the Sellmeier-Drude form of $f(n)$, *viz.*, $f(n)=n^2-1$, the dielectric constant should be given by

$$\epsilon=1+1/a. \quad (7)$$

DESCRIPTION OF MATERIALS

It was intended to obtain refractive index data on a few groups of chemically closely related compounds in order that comparisons could be made. Obviously the purity and availability of the samples had to be considered first. The hydrocarbons which were selected are given in Tables 3, 4, and 6 and fall into the following classes: (a) The normal paraffins from pentane to decane, (b) Three isomeric octanes, (c) Cyclohexane and methylcyclohexane, (d) The isomeric C_8-cyclohexanes, (e) Cyclohexene, 1-heptene, and toluene.

TABLE II. Dispersion constants for a few hydrocarbons containing double bonds (the constants listed are those of the equation $(n^2-1)^{-1}=a-bx-cx^2$).

Compound	a	b	c	a
	20°C			25°C
cyclohexene	0.9439	0.00930	0.00021	
1-heptene	1.0777	0.01157	0.00018	1.0869
toluene	0.8469	0.01322	0.00035	

The samples of groups a to d are API-NBS hydrocarbons which have been made available by the American Petroleum Institute and the National Bureau of Standards through the A. P. I. Research Project 44 on the "Collection, analysis, and calculation of data on the properties of hydrocarbons." The samples were purified at the National Bureau of Standards by the A. P. I. Research Project 6 on the "Analysis, purification, and properties of hydrocarbons," under the supervision of Frederick D. Rossini, from material supplied by the following laboratories:

Pentane, hexane, heptane, octane, nonane, decane, and 2,2,4-trimethylpentane by the American Petroleum Institute Research Project 6 at the National Bureau of Standards, Washington, D. C.; 2,2,3-trimethylpentane by the General Mortors Corporation, Detroit, Michigan; cyclohexane by the Barrett Division of the Allied Chemical and Dye Corporation, New York, New York; ethylcyclohexane, 1,1-dimethylcyclohexane, and the *cis-* and *trans*-isomers of 1,2- and 1,3-dimethylcyclohexane by the A. P. I. Research Project 45 on "Synthesis and properties of hydrocarbons of low molecular weight" at the Ohio State University, under the supervision of Cecil E. Boord; *cis-* and *trans*-1,4-dimethylcyclohexane by the Standard Oil Development Company, Elizabeth, New Jersey.

The samples of class e are National Bureau of Standards spectroscopic samples which have

[12] P. Wulff, Zeits. f. physik, Chemie **B21**, 370 (1933).

been made available through the courtesy of the Sun Oil Company, Experimental Division, Norwood, Pennsylvania.

All these samples were certified to be at least 99 mole percent pure, and they are without doubt the best samples produced anywhere to this day. Every possible precaution was taken in handling them so as to preserve their high standard of purity.

RESULTS

The data obtained are represented by Tables I and II for wave-lengths of 220 to 420 mμ. The measurements for wave-lengths less than 250 mμ or greater than 400 mμ are probably less reliable than the others, chiefly because of the wider slit width and the interference effects, respectively. The comparison with literature data and the analysis of the apparatus errors show that the accuracy and precision in these regions vary from ± 0.0003 to ± 0.0010 in index. A comparison of the experimental data with the values calculated from the corresponding empirical equations showed that, except at the ends, these values agree with the observed ones well within the experimental error.

It was surprising at first that all the data for the saturated hydrocarbons, both paraffins and naphthenes, could be represented by an equation of the form

$$(n^2-1)^{-1}=a-bx \quad (\text{where } x\equiv(\nu^*)^2\cdot 10^{-8}) \quad (8)$$

or, what amounts to the same thing, that a plot of $(n^2-1)^{-1}$ *vs.* wave number squared yielded an essentially straight line. A more careful scrutiny of the data did show that there is a slight curvature in the plot which is probably real, although the deviations, except at the extremes, never exceed 0.0003 in the value of the index of refraction. It will also be noted from a study of Fig. 1, which is typical of all these materials, that at the upper and lower boundary regions more points lie on one side of the straight line than on the other so that the constants determining these lines as they are stated in Table I, and which were calculated by the method of least squares, are usually not the same as those which would have been obtained from a consideration of a shorter spectral region. In general, however, it was found that the empirical equations yield values which compare favorably with

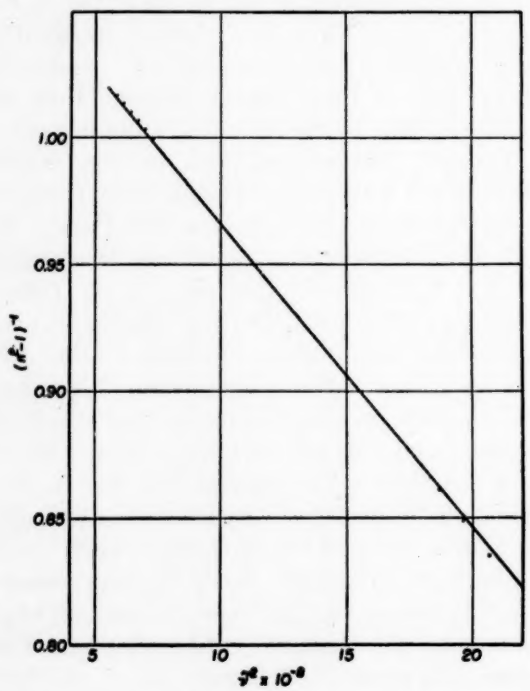

FIG. 1. $(n^2-1)^{-1}$ *vs.* $(\nu^*)^2\cdot 10^{-8}$ for *n*-octane. The straight line has been calculated from the single term Sellmeier-Drude equation.

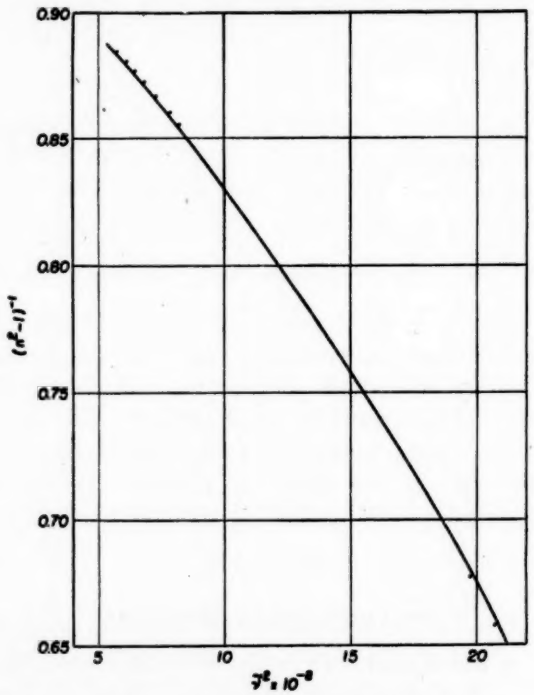

FIG. 2. $(n^2-1)^{-1}$ *vs.* $(\nu^*)^2\cdot 10^{-8}$ for cyclohexene. The curve was calculated from the equation $(n^2-1)^{-1}=a-bx-cx^2$, where $x\equiv(\nu^*)^2\cdot 10^{-8}$.

those reported in the literature for wave-lengths in the visible. Since a one-term Sellmeier-Drude equation is thus a satisfactory representation of the data for these compounds, down to 220 millimicrons wave-length, it is evident that their important characteristic wave-lengths must be quite far in the ultraviolet and probably around the value (in microns) which is obtained for $(b/a)^{\frac{1}{2}}$ according to Eq. (6). These characteristic wave-lengths are all about 1040 angstrom units.

The reader will note that for the normal hydrocarbons there is a slight tendency for the characteristic wave-lengths to increase with increasing molecular weight. If this is a real effect, it may be due to higher internal pressure at higher molecular weight.[13] For the isomeric dimethylcyclohexanes the characteristic wave-length is always longer for the *trans*- than for the *cis*-isomer.

In the same table are also listed the density (taken from the tables published by the American Petroleum Institute Research Project 44), the dielectric constant for reference, and the number of dispersion electrons per chemical bond, on the assumption that each bond corresponds to a type of energy levels.*** For the calculations involved there carbon-carbon and carbon-hydrogen bands were assumed to be equivalent, and the solution of simultaneous equations for a number of hydrocarbons with different carbon-carbon and carbon-hydrogen bond ratios shows that this is indeed true within our experimental limits; thus when the equations for hexane and octane are solved simultaneously for the number of oscillators per carbon and per hydrogen bond, one obtains for the former 0.99, for the latter 1.01. Of all the saturated hydrocarbons investigated, cyclohexane apparently has the largest number of dispersion electrons per bond, whereas 2,2,4-trimethylpentane has the smallest. Again a *cis-trans*-periodicity is noticeable with the dimethylcyclohexane isomers, the *cis*-isomer always having the larger dispersion.

Finally there are included in Table I interpolated values for the dielectric constant for a few of these hydrocarbons according to the excellent

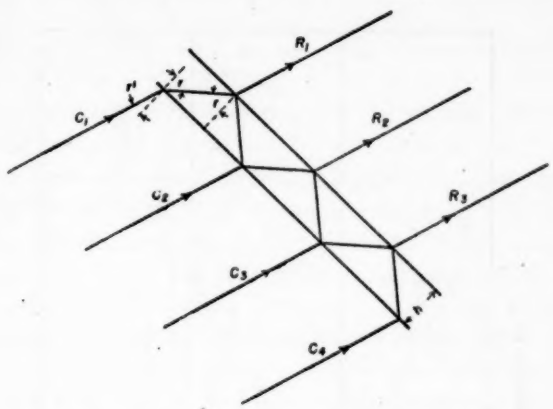

FIG. 3. Interference fringes between parallel plates.

data of Dornte and Smyth;[14] when these are compared with the values for $1+1/a$, one observes that, although generally higher, these constants are not unreasonably far off from the calculated ones, which fact may be taken to be an indication of the essential correctness of the one term formula.

Of the constants listed, only a changes with temperature, and in such a way that the characteristic wave-length decreases with increasing temperature, which is what one is led to expect on the basis of general principles.

An interesting fact that came out of this investigation is that the index of refraction *vs.* wave-length curves for cyclohexane and methylcyclohexane cross each other at about 240 millimicrons wave-length, or, in other words, that these two compounds have the same index of refraction at about 240 mμ. The probably correct explanation is that at this wave-length the effect of the higher molecular weight of methylcyclohexane which is to increase its refractive index is no longer large enough to overcome the index reducing effect of the side chain, so that from there on down its index is of smaller value than that of the lower homolog. Adding a paraffinic side chain to the cyclohexane ring brings the properties of the resulting compound into closer agreement with those of paraffins, but it is not until the third member of the cyclohexane homologous series is reached that the compounds have properties that follow the changes in molecular weight in a regular manner.

[13] T. W. Richards, Chem. Rev. **2**, 315 (1926); J. Frank. Inst. **198**, 1 (1924).

*** This assumption is made throughout the subsequent discussion; see reference 11.

[14] R. W. Dornte and C. P. Smyth, J. Am. Chem. Soc. **52**, 3546 (1930).

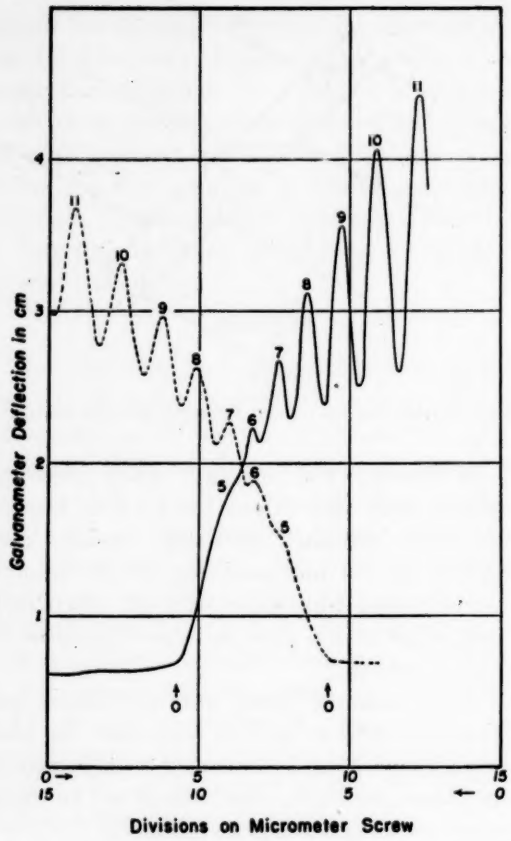

FIG. 4. A measurement of the index of refraction at 350-mμ wave-length. The spacing gasket had a thickness of only 12μ.

Relatively few data on hydrocarbon compounds of higher dispersion were taken, not only because the inherent limitations of the apparatus became more critical for this case, but also because many of these compounds had absorption bands with wings extending into the region that was studied. This decreased the light intensity so much that accurate readings became impossible. In addition, olefines are relatively easily oxidized by atmospheric oxygen and are unstable with regard to ultraviolet light. Nevertheless measurements were taken on three such compounds, chiefly for comparison with the paraffins and naphthenes. Plotting $1/(n^2-1)$ *vs.* $(\nu^*)^2\cdot 10^{-8}$ yielded lines of slight curvature for cyclohexane and 1-heptene and of a somewhat greater curvature for toluene (Fig. 2). These curves suggested that a parabolic fit should be tried, and it was actually found that the data are satisfactorily represented by an equation of the form

$$1/(n^2-1)=a-bx-cx^2 \quad (x\equiv(\nu^*)^2\cdot 10^{-8}), \quad (9)$$

The constants of this equation are then the constants which are listed in Table II. The third constants may be caused by one or more additional Sellmeier-Drude terms, by a damping factor, or by both of these effects combined. It was tried to represent the data by the power series of the form

$$n^2-1=a'+b'x+c'x^2+d'x^3 \quad (10)$$

in order to evaluate the constants of Eq. (3); however, these attempts have invariably met failure since c' turned out to be negative. According to the theory developed above, none of the constants can be negative since the absorption frequencies responsible for the dispersion in this wave-length region are in the ultraviolet. The contribution of the c' term is significantly greater than the experimental error, so this effect is probably real. The reader will note that also for these compounds a is the only constant which is temperature sensitive.

CONCLUSION

Measurements of the refractive index of hydrocarbons in the near ultraviolet wave-length region of the spectrum indicate that a single term Sellmeier-Drude equation is in good agreement with the facts throughout the region for paraffins and naphthenes. The apparent number of dispersion electrons per bond is greater for naphthenes than for paraffines and greater for *cis*- than for *trans*-isomers. The data for two olefines and one aromatic compound can be represented by a three-constant empirical equation of the form $(n^2-1)^{-1}=a-b/\lambda^2-c/\lambda^4$ at all wave-lengths not too close to absorption bands.

ACKNOWLEDGMENT

Acknowledgment is made to the American Petroleum Institute and the National Bureau of Standards for the loan of the samples measured in this investigation, to the Graduate School of Arts and Sciences of the University of Pennsylvania for granting the author a Harrison Fellowship for two consecutive years, to the Sun Oil Company, Experimental Division, for encouragement and material help, to the Physics Depart-

ment of the University of Pennsylvania, and particularly to Professor P. H. Miller, Jr., without whose continued help and advice this work would have been impossible.

APPENDIX

Transmission of Collimated Monochromatic Lightwaves through an Airspace between Parallel Plates near the Critical Angle of Incidence

If h is the thickness of the airspace (Fig. 3), the path length traversed by the light ray between successive reflections within the air film is $h \sec r$; in the neighborhood of the critical angle this distance will usually represent a quarter or a third of the diameter D of the parallel plates. Let T and R be, respectively, the fractional parts of the incident light intensity transmitted and reflected at each of the surfaces. Then the incident beam C_1 will give rise to a transmitted beam R_1' with an intensity T, to a transmitted beam R_2' with an intensity TR, etc., the incident beam C_2 will produce transmitted beams R_1'', R_2'', and so forth. The total intensity for the first bright fringe will therefore be given by the expression

$$I = \text{const.} T^2 \cdot [(D - h \sec r)/D + (D - 3h \sec r)R^2/D + \cdots + \{D - (2l+1)h \sec r\}R^{2l}/D],$$

where l is the number of interfering rays (all phase factors are unity for this case). Since all coefficients in this series must be positive, one can get a limit on l, *viz.*, $1 - (2l+1)h \sec r/D > 0$ or, since $\cos r = \lambda/h$, $2l < D \cdot \lambda/2h^2 - 1$.

Inserting typical experimental values ($D = 1$ cm, $h = 10\mu$) gives for $\lambda = 250$ millimicrons a value of $l < 1.05$. The first fringe should thus be hardly noticeable in this case, and this is in agreement with experiment. Only where one goes to longer wave-lengths is one able to distinguish lower order fringes (cf. Fig. 4). The position of the critical angle is indicated by an arrow. The order numbers given in the figure were determined from a consideration of the fact that the angular distances from the critical position are proportional to the squares of successive integers or, stated differently, that the angular deviations between successive maxima are small angles which are proportional to consecutive odd numbers.

The figure also shows differences in the sharpness of the interference fringes for the two critical positions. This effect changes from one side to the other at random, when the gasket which separates the two quartz plates forming the sandwich is replaced, and is believed to be caused by lack of parallelism of the bounding surfaces of the air space with respect to one another. A consideration of Fresnel's reflection equations shows that, especially in the neighborhood of the critical angle, reflection and refraction coefficients depend markedly on angle. Comparison of the results given here with data in the literature has shown, however, that this phenomenon has little, if any, influence on the measurements reported here within their limit of error determined from other causes.

Activation Energy for the Diffusion of Coupled Pairs of Vacancies in Alkali Halide Crystals*

G. J. DIENES**
Carnegie Institute of Technology, Pittsburgh, Pennsylvania
(Received March 3, 1948)

The theoretical activation energy for the diffusion of neutral combined pairs of positive- and negative-ion vacancies in alkali halides has been determined. Changes in Coulombic, repulsive, and polarization energies were taken into account with appropriate corrections for second-order effects. Calculations for the rigid and distorted lattice showed that distortion effects during diffusion are of appreciable magnitude. This energy contribution has been estimated as accurately as possible near the saddle point. An activation energy of 0.375 ev was obtained for diffusion in the KCl lattice. This activation energy value shows that migration of neutral combined pairs of positive- and negative-ion vacancies, rather than diffusion via single vacancies, may well be the predominant process. The experimental evidence for this type of migration is discussed. It is concluded that diffusion by means of neutral combined pairs of vacancies is supported rather than prohibited by the theoretical results.

INTRODUCTION

IT was first suggested by Frenkel[1] that in a crystal in thermodynamic equilibrium there exist a number of imperfections. The researches of Schottky,[2] Wagner,[3] and Jost[4] established the two types of imperfections of general interest, namely, interstitial atoms and lattice vacancies. The theoretical work of Schottky and Jost, more recently refined by Mott and Littleton,[5] showed on energetic grounds that only the formation and migration of lattice vacancies is of importance in alkali halides. The present study will be concerned with the migration of lattice vacancies.

The mobility of vacancies is of great importance in interpreting conductivity and diffusion data and in understanding the nature of *F*-centers.[6] Mott and Littleton[5] made a careful study of the energy of formation and migration of single positive- and negative-ion vacancies in NaCl. In the case of single vacancies long-range polarization and, therefore, the theory of the dielectric constant play very important roles. They obtained an activation energy of 0.51 and 0.56 ev for the migration of the positive- and negative-ion vacancies, respectively. Experimentally it is known[7,8] that in KCl at room temperature practically all the current is transported by positive ions. The experimental activation energy for diffusion from these conductivity measurements is about 0.82 ev.

It was shown recently by Seitz[8] that positive- and negative-ion vacancies have a tendency to combine into neutral pairs, or even larger clusters. For a neutral pair of vacancies the energy of combination in KCl is about 0.93 ev. The jump frequency of the negative ions is very low[7,8] but as a result of the high mobility of the positive ions isolated single vacancies would combine to form neutral pairs in less than a day at room temperature. At this temperature, then, the number of neutral pairs is expected to be considerably higher than the number of single vacancies. It is interesting to know how mobile the neutral pairs of vacancies are. It was pointed out by Huntington[9] that, because of the absence of ions of the opposite sign, as shown in Fig. 1A, ions of a given kind are less restricted in jumping into the corresponding vacancies than in the case of the single vacancy illustrated in Fig. 1B.

* This paper is from a dissertation submitted in May, 1947, by G. J. Dienes to the Committee on Graduate Instruction in partial fulfillment of the requirements for the degree of Doctor of Science. Presented at the January, 1948, meeting of the American Physical Society.

** Present address: Bakelite Corporation, Bound Brook, New Jersey.

[1] J. Frenkel, Zeits. f. Physik **35**, 652 (1926).

[2] W. Schottky, Zeits. f. physik. Chemie **B29**, 335 (1935).

[3] C. Wagner and W. Schottky, Zeits. f. physik. Chemie **B11**, 163 (1930).

[4] W. Jost, J. Chem. Phys. **1**, 466 (1933); Zeits. f. physik. Chemie **A169**, 129 (1934); *Diffusion und chemische Reaktion in festen Stoffen* (Theodor Steinkopf Verlag, Dresden, 1937).

[5] N. F. Mott and M. J. Littleton, Trans. Faraday Soc. **34**, 485 (1938).

[6] For recent surveys see: N. F. Mott and R. W. Gurney, *Electronic Processes in Ionic Crystals* (Oxford University Press, New York, 1940); F. Seitz, *Modern Theory of Solids* (McGraw-Hill Book Company, Inc., New York, 1940).

[7] C. Tubandt, *Handbuch d. Exp. Phys.*, Vol. XII.

[8] F. Seitz, Rev. Mod. Phys. **18**, 384 (1946).

[9] Private communication. See also reference 8, p. 403.

No quantitative study has been made of this process to the present time.

The most important experimental evidence in favor of diffusion mechanisms via neutral pairs comes from the work of Stern, Estermann, and Leivo (as discussed by Seitz[8]) on density changes accompanying heavy darkening of alkali halide crystals by x-rays. These measurements suggest very strongly that the major portion of the vacancies diffuse from the surface of the crystal. The low jump frequency of the halogen ions shows that at room temperature individual halogen vacancies diffuse extremely slowly from the surface into the lattice. Experimental evidence indicates, however, that under x-ray bombardment equilibrium darkening is established within a day, and the observed darkening extends to a depth of about 0.1 mm. The halogen ions would have jumped only a few lattice distances during this time and cannot, therefore, diffuse to the interior within the required time without assistance. Accordingly, Seitz[8] suggested that the vacancies migrate in the form of neutral pairs of positive- and negative-ion vacancies. To account for the experimentally observed diffusion the activation energy for the migration of neutral pairs should be about 0.5 ev or less.

It is evident that the magnitude of the activation energy for the diffusion of neutral pairs plays a critical role in the foregoing interpretation. It is the purpose of this study to determine theoretically this activation energy.

ACTIVATION ENERGY IN THE RIGID LATTICE

In order that a neutral pair may diffuse it is necessary that ions of both charges jump into their corresponding vacancies. Since the negative vacancy is much less mobile than the positive one, the rate-determining step in such a diffusion mechanism must be the migration of a negative ion as indicated in Fig. 1A. The negative ions immediately adjacent to the positive vacancy will be the more mobile ones since they are less restricted. Thus, the problem of determining the activation energy for the migration of the neutral pair reduces to the calculation of the activation energy for the negative jump shown in Fig. 1A. Since a great deal of experimental information for potassium chloride is available, the numerical

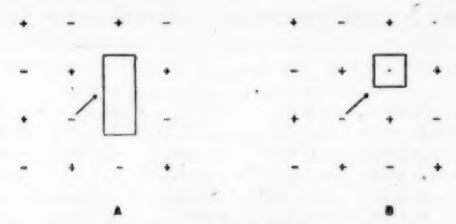

FIG. 1. A. Configuration of ions about a pair of vacancies. B. Configuration of ions about a single vacancy.

calculation will be carried out for this substance. The general techniques are applicable to all the alkali halides having the NaCl structure.

The calculation of the activation energy for the jump of a negative ion toward a neutral pair of vacancies will be carried out first for the rigid lattice. The surrounding ions will not be allowed to move away from their mean positions. They are polarizable, however, with polarizabilities α_- and α_+. The problem is to calculate the position and energy of the saddle point of the energy barrier as the configuration changes from state A through the activated state B to state C, as illustrated in Fig. 2. Most of the techniques applicable in the rigid lattice can also be used with minor modifications for calculations in the distorted lattice. As the negative ion moves from the (0 0 0) position toward the (1 1 0) position the activation energy is determined by changes occurring in the Coulombic, repulsive, and polarization energies of the system.

1. Coulombic Energy Contribution

The most general mathematical technique for calculating Coulombic potentials in ionic crystals has been worked out by Ewald.[10] The potential at any point in the lattice is given by a slowly converging series of the type

$$\phi(x, y, z) = \mathbf{S}_n \sum_k e_k / |\mathbf{r}_k^n - \mathbf{r}|, \qquad (1)$$

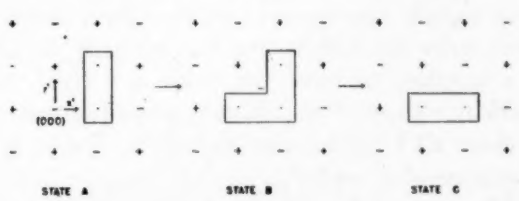

FIG. 2. Diffusion process in the rigid lattice.

[10] P. P. Ewald, Ann. d. Physik **64**, 253 (1921); see also M. Born, *Problems in Atomic Dynamics* (Massachusetts Institute of Technology, 1926), pp. 158–164.

TABLE I. Ewald potentials as a function of x' and y'.

	$V_E(r_0/e)$				
y'/x'	0.40	0.45	0.50	0.55	0.60
0.2	−0.4662	−0.2271	0.0000	0.2271	0.4662
0.3	−0.3051	−0.1501	0.0000	0.1501	0.3051
0.4	−0.1509	−0.0729	0.0000	0.0729	0.1509
0.5	0.0000	0.0000	0.0000	0.0000	0.0000
0.6	0.1509	0.0729	0.0000	−0.0729	−0.1509
0.7	0.3051	0.1501	0.0000	−0.1501	−0.3051

where $\mathbf{r}$ = vector from any origin 0 to any point in the cell, $\mathbf{r}_k^n$ = vector from any origin 0 to any lattice point, k = basis index, n = cell index, e_k = electrostatic charge at point k of the basis, and $\mathop{\mathbf{S}}_{n}$ = summation over n. With the help of the theory of theta-functions Ewald succeeded in expressing Eq. (1) in terms of two rapidly convergent series. The following formulas will be needed in the present calculations. The potential, ϕ, at any arbitrary point, $\mathbf{r}$, is given by

$$\phi(\mathbf{r}) = \sum_k e_k \psi(\mathbf{r}-\mathbf{r}_k), \tag{2}$$

where

$$\psi(\mathbf{r}) = \psi_1(\mathbf{r}) + \psi_2(\mathbf{r}), \tag{3}$$

$$\psi_1(\mathbf{r}) = (4\pi/\Delta) \mathop{\mathbf{S}'}_{n} \frac{\exp[-(1/4\epsilon^2)|\mathbf{q}^n|^2 + i\mathbf{q}^n\cdot\mathbf{r}]}{|\mathbf{q}^n|^2}, \tag{4}$$

$$\psi_2(\mathbf{r}) = \mathop{\mathbf{S}}_{n} \frac{G(\epsilon|\mathbf{r}^n-\mathbf{r}|)}{|\mathbf{r}^n-\mathbf{r}|} - \frac{\pi}{\Delta\epsilon^2}. \tag{5}$$

The symbols have the following meaning:

$\mathbf{r}^n = n_1\mathbf{a}_1 + n_2\mathbf{a}_2 + n_3\mathbf{a}_3$ = translation vector of the basis, n_1, n_2, n_3 are integers ($-\infty$ to ∞ including 0) and $\mathbf{a}_i$ are the vectors defining the unit cell.

$\Delta = \mathbf{a}_1\cdot(\mathbf{a}_2\times\mathbf{a}_3)$ = volume of the cell.

$\mathbf{q}^n = 2\pi(n_1\mathbf{b}_1 + n_2\mathbf{b}_2 + n_3\mathbf{b}_3)$ = translation vector in reciprocal lattice.

$\mathbf{b}_i$ = base vectors of the reciprocal lattice defined by $\mathbf{a}_i\cdot\mathbf{b}_k = \delta_{ik}$.

ϵ = arbitrary dividing value for expressing ψ as the sum of ψ_1 and ψ_2.

$$G(x) = (2/\sqrt{\pi})\int_x^\infty \exp(-\alpha^2)d\alpha.$$

The apostrophe over the summation sign in Eq. (4) means that the substitution $n_1 = n_2 = n_3 = 0$ is to be omitted.

For the purposes of this study these general expressions can be specialized for the sodium chloride type of lattice. The final equation for numerical computations, with the origin placed at a negative lattice point, as in Fig. 2A, is given by[11]

$$V_E(x,y,z) = \frac{e}{r_0}\left[-\mathop{\mathbf{S}}_{H_i} \frac{\exp[-(\pi^2/\epsilon^2a^2)\sum(2H_i-1)^2](8\cos\pi x'(2H_1-1)\cos\pi y'(2H_2-1)\cos\pi z'(2H_3-1))}{(\pi/4)\sum(2H_i-1)^2} \right.$$
$$\left. -\sqrt{\pi}\mathop{\mathbf{S}}_{n} \frac{G[\epsilon(a/2)[(n_1-x')^2+(n_2-y')^2+(n_3-z')^2]^{\frac{1}{2}}]}{\sqrt{\pi}[(n_1-x')^2+(n_2-y')^2+(n_3-z')^2]^{\frac{1}{2}}}(-1)^{n_1+n_2+n_3}\right], \tag{6}$$

where $x' = x/r_0$, $y' = y/r_0$, $z' = z/r_0$, r_0 = anion-cation distance, $a = 2r_0$ = lattice constant, and $V_E(x,y,z)$ = Ewald potential at any point $(x\,y\,z)$. It has been found in practice that the series are very rapidly convergent and that three terms of each series are sufficient in the majority of cases if ϵ is taken to have the value $\epsilon a = 2(\pi)^{\frac{1}{2}}$. Numerical values of the Ewald potential for the perfect KCl lattice are shown in Table I as functions of x' and y'.

The potential at any point in a lattice containing a pair of neutral vacancies (Fig. 2) is obtained by subtracting the Coulombic potential contribution of the missing ions.

As the negative ion is moved from the (0 0 0) position toward the (1 1 0) position the Coulombic potential energy of the whole system is changed. The total change in the Coulombic potential energy of the system, however, is equal to the change in the Coulombic potential energy of the moving ion.

This energy term is given by

$$E_- = -e[V_-(x',y',z') - V_-(0,0,0)]$$
$$= e[V_-(0,0,0) - V_-(x',y',z')]. \tag{7}$$

[11] For details see G. J. Dienes, thesis, Carnegie Institute of Technology, May 1947.

Here

$$V_-(0,0,0)=(e/r_0)[1.7476-(+\text{vacancy})+(-\text{vacancy})]$$
$$=(e/r_0)[1.7476-1+(1/\sqrt{2})]$$
$$=1.4547(e/r_0), \quad (8)$$

in which $1.7476(e/r_0)$ is the Ewald or Madelung potential at a negative lattice site. $V_-(x', y', z')$ is given by

$$V_-(x', y', z') = V_E(x', y', z') + \frac{e}{r_0}\Big[-\frac{1}{[(1-x')^2+y'^2+z'^2]^{\frac{1}{2}}}\ (+\text{vacancy}) + \frac{1}{[(1-x')^2+(1-y')^2+z'^2]^{\frac{1}{2}}}\ (-\text{vacancy}) + \frac{1}{[x'^2+y'^2+z'^2]^{\frac{1}{2}}}\ (\text{moving-ion})\Big], \quad (9)$$

where $V_E(x', y', z')$ is the Ewald potential in a perfect lattice given by Eq. (6).

The Coulombic potential energy changes, calculated according to Eqs. (7),. (8), and (9) as functions of x' and y' are shown in Table II. It will be shown later that because of the high degree of symmetry in the z direction the moving negative ion has no tendency to move out of the $x'y'$ plane. From symmetry it is clear that the energy terms have to be symmetrical about the diagonal line running from the positive ion at (0 1 0) to the positive vacancy at (1 0 0). This is related to the fact that the process of moving the negative ion at (0 0 0) into the negative vacancy at (1 1 0) is symmetrically equivalent to the process of moving the negative ion from (1 1 0) into a negative vacancy at (0 0 0). Symmetrically equivalent positions are given by $(x', y', 0)$ and $(1-y', 1-x', 0)$ for the coordinates employed. Thus, the energy barrier is symmetrical with respect to the diagonal, and the saddle point must occur somewhere along this line. The energy barrier is not symmetrical with respect to the diagonal from (0 0 0) to (1 1 0) because of the presence of a pair of vacancies rather than a single vacancy. Thus, the position of the saddle point on the (0 1 0) to (1 0 0) diagonal cannot be completely fixed by symmetry considerations. The calculated values of the Coulombic energy changes reflect, of course, the symmetry mentioned (compare, for example, positions (0.4 0.4 0) to (0.6 0.6 0) in Table II).

TABLE II. Coulombic potential energy changes in the rigid lattice.

Energies in electron volts.					
y'/x'	0.40	0.45	0.50	0.55	0.60
0.2	1.2069	1.4949	1.7902	2.0868	
0.3	0.7529	1.0373	1.3253	1.6133	1.8986
0.4	0.2075	0.4921	0.7905	1.0840	1.3616
0.5	−0.4853	−0.1447	0.1837	0.4957	0.7905
0.6			−0.4853	−0.1220	0.2075
0.7					−0.3837

2. Repulsive Energy Contribution

It is generally agreed that the exponential repulsive law is the best available at the present time. Following Born,[12] Born and Mayer,[13] and Pauling[14] the repulsive potential function

$$\phi = c_{12} b e^{(r_1+r_2-r)/\rho} \quad (10)$$

has been used in the present study. For potassium chloride the following values of the constants were employed[13]

$c_{++}=1.25$, $r_0=3.137\times10^{-8}$ cm,
$c_{--}=0.75$, $r_+=r_1=1.33\times10^{-8}$ cm,
$c_{+-}=1.00$, $r_-=r_2=1.81\times10^{-8}$ cm,
$\rho=0.345\times10^{-8}$ cm, $b=0.229\times10^{-12}$ ergs.

In calculating the repulsive energies, nearest (+ −interaction) and next nearest neighbors (− −interaction) surrounding the negative ion at the (0 0 0) position were taken into account. The expressions for the repulsive energies are (in ergs):

Nearest neighbors:

$$\phi_r(x', y', z') = be^{(r_1+r_2)/\rho}\Big[\sum_{n_1^2+n_2^2+n_3^2=1}{}' \exp[-(r/\rho)((n_1-x')^2+(n_2-y')^2+(n_3-z')^2)^{\frac{1}{2}}]\Big]$$
$$=0.229\times10^{-12}e^{9.1015}\Big[\sum_{n_1^2+n_2^2+n_3^2=1}{}' \exp[-9.0925((n_1-x')^2+(n_2-y')^2+(n_3-z')^2)^{\frac{1}{2}}]\Big]. \quad (11)$$

[12] M. Born and M. Goppert-Mayer, *Handbuch der Physik* **24**/2, 623 (1933).
[13] M. Born and J. E. Mayer, Zeits. f. Physik **75**, 1 (1932).
[14] L. Pauling, Zeits. f. Krist. **67**, 377 (1928).

In this expression the substitution (1 0 0) corresponding to the positive-ion vacancy is to be omitted.

Next nearest neighbors:

$$\phi_r(x', y', z') = 0.75be^{(2r_2/\rho)}\Big[\sum_{n_1^2+n_2^2+n_3^2=2}{}' \exp\big[-(r/\rho)((n_1-x')^2+(n_2-y')^2+(n_3-z')^2)^{\frac{1}{2}}\big]\Big]$$

$$= 0.17175\times 10^{-12}e^{10.4930}\Big[\sum_{n_1^2+n_2^2+n_3^2=2}{}' \exp\big[-9.0925((n_1-x')^2+(n_2-y')^2+(n_3-z')^2)^{\frac{1}{2}}\big]\Big]. \quad (12)$$

In Eq. (12) the substitution (1 1 0) corresponding to the negative-ion vacancy is to be omitted.

The equilibrium repulsive energies are obtained, of course, by letting $x'=y'=z'=0$, and the change in repulsive energy is given by

$$\Delta E_R = \phi_r(x', y', z') - \phi_r(0, 0, 0). \quad (13)$$

The contribution of ions further away is negligibly small.

The total energy changes caused by Coulombic and repulsive interactions are given in Table III. It will be noted that the energies are not completely symmetrical (compare (0.4 0.4 0) to (0.6 0.6 0)). The reason for this is that the calculations were made for the nearest and next nearest neighbors surrounding the (0 0 0) position which for simplicity were taken to be the same as those around the equivalent (1 1 0) position. The discrepancy is about 5 percent at the (0.6 0.6 0) position and is less than that near the saddle point. Such a small difference caused by asymmetry did not warrant any further calculations at this point. Asymmetry and distortion effects will be discussed later and have been included in the final energy values.

Interpolation along the diagonal gives a saddle point at $x'=0.55$, $y'=0.45$ with an energy of 1.324 ev. The position of the saddle point shows that the moving negative ion is attracted toward the vacancies. This is to be expected physically since the positive vacancy provides additional room for the passage of the negative ion (Fig. 2B).

Calculations were made in the $x'=0.5$ and $x'=0.6$ plane for $z'=\pm 0.10$. The results showed that the energy is a minimum in the $x'y'$ plane and, therefore, the moving negative ion has no tendency to move out of this plane. This result is as expected from the symmetry in the z' direction.

The Coulombic and repulsive energy changes were also calculated for the perfect lattice containing a single vacancy. The ion-jump under consideration is shown in Fig. 1B. The activation energy obtained was 1.75 ev. Thus, a lowering of about 0.45 ev can be expected in the Coulombic and repulsive energies as a result of the fact that two vacancies are present instead of one. It is known, of course, that polarization plays a very important part in this process. The problem of determining the polarization energy contribution (including distortion of the lattice) was solved by Mott and Littleton who found an activation energy of 0.56 and 0.51 ev for the motion of the negative- and positive-ion vacancies in NaCl, respectively. Since a pair of vacancies creates essentially a dipole field, it would be expected that the lowering caused by polarization would be smaller than in the case of a single vacancy where long-range polarization plays an important role. If the difference in polarization for the single and double vacancies is greater than the differences in the Coulombic and repulsive terms for the two cases, the single vacancy type of diffusion would be favored. It is clear, then, that polarization contributions are of crucial importance in this problem.

TABLE III.* Coulombic and repulsive energy changes in the rigid lattice.

Energies in electron volts					
y'/x'	0.40	0.45	0.50	0.55	0.60
0.2	1.0469	1.3501	1.6086		
0.3	1.0830	1.1983	1.3520	1.5400	
0.4	1.4939	1.3644	1.3115	1.3407	1.4208
0.5	2.7754	2.1318	1.6892	1.4159	1.2785
0.6					1.4259
0.7					1.8760

* The repulsive energy terms (ΔE_R) are not listed separately to conserve space. They are obtainable as the differences in the entries of Tables II and III.

3. Polarization Energy Contribution

The polarization energy contribution is conveniently separated into two parts; namely,

a part arising from the negative ions and a part arising from the rest of the lattice. The ions surrounding the vacancies become polarized since the field arising from the vacancies is finite at the positions these ions occupy. This polarization has associated with it a dipole field and a certain polarization energy. The polarization of the moving negative ion changes as it moves because the Coulombic and dipole fields vary from point to point. The problem is to calculate the difference in polarization energy between a configuration in which the negative ion is at $(x'\ y'\ 0)$ (Fig. 2B) and the equilibrium configuration in which it is at (0 0 0).

Klemm's[15] technique of calculating polarization energies in a lattice containing a pair of vacancies can be applied directly to the equilibrium configuration. Consider the configuration of Fig. 3 in which the origin of the coordinate system is for the purposes of this section chosen at the missing positive ion site, the negative ion vacancy being taken at (1 0 0). The dipole field, due to the pair of vacancies, is equivalent to that produced by a negative charge at (0 0 0) and a positive charge at (1 0 0). At any lattice point $(k\ m\ n)$ the electric field as the result of these charges is given by

$$\mathbf{E}_{kmn}=(e/r_0^2)\left[\frac{-(k,m,n)}{L_-^{\frac{3}{2}}}+\frac{(k-1,m,n)}{L_+^{\frac{3}{2}}}\right],$$

where

$$L_-=k^2+m^2+n^2,\quad L_+=(k-1)^2+m^2+n^2.$$

Using parenthetical notation for vectors the foregoing expression may be written

$$\mathbf{E}_{kmn}=\frac{e}{r_0^2}\left[\frac{k-1}{L_+^{\frac{3}{2}}}-\frac{k}{L_-^{\frac{3}{2}}},\frac{m}{L_+^{\frac{3}{2}}}-\frac{m}{L_-^{\frac{3}{2}}},\frac{n}{L_+^{\frac{3}{2}}}-\frac{n}{L_-^{\frac{3}{2}}}\right].$$

The energy of the dipole induced on the ion at $(k\ m\ n)$ is given by

$$\epsilon_P=-\tfrac{1}{2}\alpha\mathbf{E}\cdot\mathbf{E}, \qquad (14)$$

where α is the polarizability. Summing over the lattice points, Eq. (14) is easily transformed into

$$E_P=-\tfrac{1}{2}(e^2/r_0^4)[\alpha_-+\alpha_+][\sum_{k+m+n=\text{even}}\mathbf{E}_{kmn}^2]. \qquad (15)$$

This expression is applicable to the calculation of

[15] W. Klemm, Zeits. f. Physik **82**, 529 (1933).

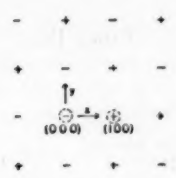

FIG. 3. Equivalent charges responsible for polarization. Rigid lattice, equilibrium configuration.

the polarization energy of a rigid lattice containing a neutral pair of vacancies. In numerical computations it is usually more convenient to carry out explicitly the dot product multiplications of Eq. (14) instead of using the summation formula of Eq. (15). This expression (Eq. (15)) includes the polarization energy of the negative ion which is eventually moved.

Klemm[15] found that the polarization of the nearest neighbors surrounding the vacancies gave a good approximation to the polarization energy. The contribution of more remote ions will be estimated and discussed later. Long-range polarization, which is very important in the case of a single vacancy,[5] is comparatively small in this case.

As the negative ion, which we shall assume is initially at (0 1 0), moves to a point $(x\ y\ 0)$ the polarization energy of the configuration illustrated in Fig. 4 is to be calculated. A method analogous to Klemm's technique can also be used in this case. The field responsible for polarization arises from four point charges which produce the following electric fields at any lattice point $(k\ m\ n)$:

Negative charge at (0 0 0):

$$\mathbf{E}_1=-[e/r_0^2][(k,m,n)/L_-^{\frac{3}{2}}],\quad L_-=k^2+m^2+n^2,$$

Positive charge at (1 0 0):

$$\mathbf{E}_2=[e/r_0^2][(k-1,m,n)/L_+^{\frac{3}{2}}],\qquad L_+=(k-1)^2+m^2+n^2.$$

Positive charge at (0 1 0):

$$\mathbf{E}_3=[e/r_0^2][(k,m-1,n)/L'^{\frac{3}{2}}],\qquad L'=k^2+(m-1)^2+n^2.$$

Negative charge at $(x\ y\ 0)$:

$$\mathbf{E}_4=-[e/r_0^2][(k-x,m-y,n)/R^{\frac{3}{2}}],\qquad R=(k-x)^2+(m-y)^2+n^2.$$

The polarization energy of the stationary ion at

TABLE IV.

	Change of polarization energy of stationary ions (units of electron volts) $\Delta E_P{}^s$			Dipole potential at x', y', 0 generated by polarized stationary ions $V_P(r_0/e)$		
y'/x'	0.4	0.5	0.6	0.4	0.5	0.6
0.3	−0.0590	−0.1646		0.2003	0.2274	
0.4	−0.0227	−0.0875	−0.1778	0.1998	0.2109	0.2325
0.5	−0.0308	−0.0376	−0.0875	0.2233	0.2075	0.2109
0.6		−0.0308	−0.0227		0.2233	0.1998

$(k\ m\ n)$ is, then, given by

$$\epsilon_P' = -\tfrac{1}{2}\alpha \mathbf{E}' \cdot \mathbf{E}', \tag{16}$$

where $\alpha = \alpha_-$ for $k+m+n=$odd, $\alpha=\alpha_+$ for $k+m+n=$even, $\mathbf{E}' = \mathbf{E}_1+\mathbf{E}_2+\mathbf{E}_3+\mathbf{E}_4$. We shall designate the sum of ϵ_P' over all stationary ions by E_P'. The change in the polarization energy of the stationary ions surrounding the vacancies is then from Eq. (16) and (14),

$$\Delta E_P{}^s = E_P' - E_P. \tag{17}$$

The energy $\Delta E_P{}^s$ is negative in the sense that the ions become more polarized during the jump of the negative ion, thereby lowering the activation energy. The numerical values of the energy are summarized in Table IV. The coordinates in this table are given in terms of the original system, $x'y'z'$, with the moving negative ion originally at (0 0 0).

The potential at $(x\ y\ 0)$ due to the dipole at $(k\ m\ n)$ is given by

$$v_P(x, y, 0) = (\alpha/r_0{}^2)\mathbf{E} \cdot [[-(k-x), -(m-y), -n]/R^3], \tag{18}$$

where

$$(1/r_0{}^2)[[-(k-x), -(m-y), -n]/R^3] = \text{radius vector from } (k\ m\ n) \text{ to } (x\ y\ 0).$$

Values of the total dipole potential at the position of the moving ion are given in Table IV. V_P is the sum of v_P over all k, m, n.

The most important change in the polarization energy of the system is caused by the polariza-

FIG. 4. Equivalent charges responsible for polarization. Rigid lattice, activated state.

TABLE V.* Sum of Coulombic, repulsive, and polarization energy changes in the rigid lattice.

	Energies in electron volts		
y'/x'	0.4	0.5	0.6
0.3	0.4294	0.6921	
0.4	0.4453	0.4834	0.7269
0.5	0.7077	0.4089	0.4504
0.6		0.7077	0.3776

* The total polarization energy changes are not tabulated but are obtainable as the differences in the entries of Tables V and III.

bility of the moving negative ion. Since the Coulombic potentials and the dipole potentials at any point $(x'\ y'\ 0)$ (in terms of the original coordinate system) are known, the field effective in polarizing the negative ion is easily obtained by graphical methods as the negative gradient of the total potential. Denoting this field by $\mathbf{F}(x', y')$ the polarization energy, E_P'', of the negative ion when at position $(x'\ y'\ 0)$ will be

$$E_P'' = -\tfrac{1}{2}\alpha_- \mathbf{F}(x', y')^2, \tag{19}$$

and the total change in polarization energy is given by

$$\Delta E_P = E_P' + E_P'' - E_P. \tag{20}$$

E_P'' was computed using the dipole field given in Table IV as well as the field $\mathbf{E}'$, arising from the four Coulomb charges. The total change in energy is finally given by

$$\Delta E_{\text{Total}} = \Delta E_C + \Delta E_R + \Delta E_P. \tag{21}$$

The values of ΔE_{Total} are shown in Table V.

The values of the ionic polarizabilities used in these calculations are those given by Pauling,[16] i.e., $\alpha_- = 3.66\times10^{-24}$ cm^3, $\alpha_+ = 0.83\times10^{-24}$ cm^3. In magnitude the total polarization energy changes are comparable to the Coulombic and repulsive energy contributions.

Interpolation of the data of Table V along the diagonal from (0 1 0) to (1 0 0) determines the position and magnitude of the activation energy. The total energy curve is constructed from ΔE_C, ΔE_R, and ΔE_P *versus* distance along diagonal plots and the minimum determined graphically. A value of 0.400 ev was obtained at $x'=0.514$, $y'=0.486$.

4. Second-Order Energy Terms

The most important second-order effects in the rigid lattice result from the approximations

[16] L. Pauling, Proc. Roy. Soc. **A114**, 181 (1927).

made in calculating the polarization energy changes. Energy contributions of the van der Waals type were neglected in this study. This will be estimated and discussed later.

We shall assume once again that the moving negative ion is at (0 0 0) and that the positive and negative ion vacancies are at (1 0 0) and (1 1 0), as in Fig. 2. The contribution of the next nearest neighbors to the polarization part of the activation energy was calculated near the saddle point, namely at $x'=0.5$, $y'=0.5$. This calculation included both the polarization energy of the next nearest neighbors and the change in the polarization energy of the negative ion at (0.5 0.5 0) arising from the change produced in the dipole field when the influence of next nearest neighbors is included. These two effects combine to decrease the activation energy by about 0.12 ev, which is about 10 percent of the total change in polarization energy.

There is also a dipole-dipole interaction term, which is rather difficult to calculate, arising from the strong dipole on the moving negative ion. An estimate can be made, however, of this energy contribution. Dipole-dipole interactions correspond to short-range forces, the energy of interaction falling off as $1/r^6$. Thus, it is reasonable to suppose that the most important contribution will come from the positive ion nearest the moving negative ion, i.e., the (0 1 0) position. This interaction was estimated for the case in which the negative ion is near the saddle point, namely, at $x'=0.5$, $y'=0.5$. The magnitude and orientation of the dipole on the negative ion is known. The field at (0 1 0), in the direction of decreasing r and θ (in this case θ is 180°), arising from a dipole of strength p on the negative ion at (0.5 0.5 0), is given by

$$E_r=2p\cos\theta/r^3=-2p/r^3,\qquad E_\theta=p\sin\theta/r^3=0, \tag{22}$$

where

$$p=1.49\alpha_-(e/r_0^2).$$

This field is found to decrease the polarization energy of the positive ion at (0 1 0) by 0.21 ev. Since this ion is subject to a higher moment the dipole field polarizing the negative ion is changed by about 3 percent, giving approximately a 6 percent change in the polarization energy of the negative ion, or $\Delta E\sim\pm0.07$ ev.

The contribution of ions further away is very small. Calculation for the negative ion at (1 −1 0) showed that its polarization energy was only changed by about one percent. If the other ions surrounding the vacancies contribute about the same amount, then the change in $\Delta E_P{}^s$, from all stationary ions except that at (0 1 0), would be about 0.004 ev. With this is associated a change in dipole potential of about 1.5 percent, which in turn changes the polarization energy of the moving negative ion by about 3 percent or 0.04 ev. Thus, the dipole-dipole energy contribution of ions other than the positive ion at (0 1 0) is estimated to be about ±0.05 ev.

The total dipole-dipole contribution is, therefore,

$$\Delta E=-(0.21\pm0.12)\text{ ev}.$$

Thus, a lowering in the activation energy of 0.09 ev or more is expected from this effect.

In other words, the combined contribution of the next nearest neighbors and of the dipole-dipole interactions will produce a lowering in the activation energy of about 0.21 ev or more. This lowers the activation energy for diffusion in the rigid lattice to about 0.20 electron volt.

Although the discussion of this and the previous sections is restricted to the rigid lattice, it is interesting to consider at this point the lowering of the activation energy which would result if the positive ion at (0 1 0) is allowed to move slightly outward along the line from (0 1 0) to (0.5 0.5 0). This would give more room for the passage of the negative ion. In order to calculate the energies involved in such a process the Coulombic, repulsive, and polarization energy changes for the negative ion at (0.5 0.5 0) and for the moving positive ion have to be taken into account. These calculations were carried out by procedures exactly analogous to those used previously. It was found that the positive ion would tend to move outward a distance of $0.014r_0$ and that the activation energy would be lowered by 0.027 ev as a result. The dipole-dipole interaction was neglected in this calculation and its inclusion might nullify the small displacement and energy change calculated above. It is concluded that only a very small displacement and lowering in activation energy can be expected from this effect.

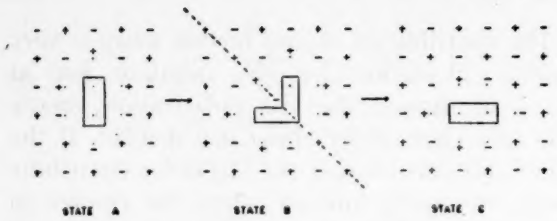

FIG. 5. Diffusion process in the distorted lattice. — — — Line of symmetry.

ACTIVATED ENERGY IN THE DISTORTED LATTICE

The diffusion process in the rigid lattice investigated in the previous sections represents an idealized case. In the actual crystal the ions around the vacancies are displaced, that is, the lattice is distorted before the diffusion process starts. Thus, the starting configuration resembles state *A* of Fig. 5. During the jump of the negative ion the distortion changes continuously (state *B* of Fig. 5) and must end in a symmetrically equivalent arrangement, as illustrated in state *C* of Fig. 5. The ions adjacent to the vacancies in the *z* direction are also understood to be displaced. The detailed investigation of this process is very difficult because of the continuous change in distortion. The activation energy can be calculated, however, in a simply distorted lattice and the effect of continuous distortion on the saddle-point energy estimated. The first step in this calculation is the determination of the equilibrium distortion around the vacancies.

1. Equilibrium Distortion Around a Pair of Vacancies

In order to make such a calculation feasible in practice it is convenient to assume that all the ions immediately adjacent to the vacancies are displaced by the same amount. The ions will be displaced directly outward as shown in state *A* of Fig. 5, as a result of the missing electrostatic attractive forces. The configuration actually will be more complex because of the missing electrostatic repulsive forces. The investigation of configuration *A*, however, will provide a fair picture of the magnitude of the displacements. The Coulombic, repulsive, and polarization energy changes have to be calculated for the distortion process. The calculations will be described for a displacement of $0.1r_0$.

The change in Coulombic energy is calculated as follows: The potential of any ion in a displaced position is given by

$$V_d = V_{\text{Ewald}} - (\text{ion at lattice site}) - (+\text{vacancy}) - (-\text{vacancy}) + (\text{ions in displaced positions}) - (\text{ions at ideal lattice sites}).$$

The equilibrium potential is given by

$$V = V_E - (+\text{vacancy}) - (-\text{vacancy}) + (\text{ions in displaced positions}) - (\text{ions at ideal lattice sites}).$$

The change in Coulombic energy is given by

$$\Delta E_C = ze(V_d - V), \tag{23}$$

where z is the valency. The ΔE_C terms were separately calculated for each displacement and summed up to give the total change in Coulombic energy.

The repulsive energy change was calculated directly as the difference between the total repulsive energy of state *A* (Fig. 5) and of the undistorted lattice, considering only the nearest neighbors of the displaced ions. The ion at $(-0.1\ 0\ 0)$, for example, has one neighbor at a distance of $1.0r_0$, one at $0.9r_0$, and three at $(1.01)^{\frac{1}{2}}r_0$, whereas in the undistorted lattice it has five neighbors at a distance of $1.0r_0$.

The polarization energy of displacement was calculated from Eq. (14) as the difference between the polarization energy of ions in the displaced position and the polarization energy of the ions at the lattice sites.

The results of these calculations are represented by the curves of Fig. 6. Construction of the total energy curve from the data of Fig. 6 shows that the maximum decrease in total energy occurs at a displacement of $0.1r_0$. Thus, a distortion of the order of magnitude of 10 percent is to be expected around a pair of neutral vacancies.

2. Energy Changes in the Distorted Lattice

Once the equilibrium distortion around the pair of vacancies is known one can proceed with the calculation of the activation energy for diffusion in the distorted lattice. Since no simplified technique is available for taking into account the continuous change in distortion, the most convenient procedure at this point is to calculate the

various energy contributions assuming that the equilibrium distortion around the vacancies remains unchanged during diffusion. The change in the saddle-point energy due to change in distortion will be estimated later.

The Coulombic energy change can be calculated by a technique analogous to the one used in the case of the rigid lattice. The potential at any point $(x'\ y'\ 0)$ is given by

$$\begin{aligned} V(x', y', 0) = V_E &- (\text{ion at } 0\ 0\ 0) \\ &- (+\text{vacancy}) - (-\text{vacancy}) \\ &+ (\text{ions in displaced positions}) \\ &- (\text{ions at ideal lattice sites}) \\ = V(&\text{rigid lattice}) \\ &+ (\text{ions in displaced positions}) \\ &- (\text{ions at ideal lattice sites}). \quad (24) \end{aligned}$$

The reference state will be $V(-0.1, 0, 0)$ and the Coulombic energy change is given by

$$\Delta E_C = e[V(-0.1, 0, 0) - V(x', y', 0)]. \quad (25)$$

The Coulombic energy changes calculated by Eq. (25) are considerably larger than the corresponding contributions in the rigid lattice. They are also obviously asymmetrical, the discrepancy becoming quite large (in such a direction as to raise ΔE_C) as x' and y' increase past the diagonal in the transition from (0 1 0) to (1 0 0). Thus, considerable error is introduced by neglecting the continuous change in ion displacement, and this error will tend to raise the activation energy. This effect will be discussed in detail later.

The repulsive energy contribution is calculated with the use of the principles described in the previous paragraph, that is, by adding the contribution of ions in the displaced position and subtracting it in the lattice site position. Both nearest and next nearest neighbors were taken into account. The repulsive energy contributions in the distorted lattice are considerably less than in the rigid lattice. The discrepancy due to asymmetry is in the direction of decreasing ΔE_R, that is, opposite to the one found for ΔE_C; however, the two discrepancies do not cancel since the repulsive terms contribute considerably less to the activation energy than the Coulombic terms.

The calculation of the polarization energy change represents a straightforward application of the method described for the rigid lattice. The position vector components k, m, n for the displaced ions, however, are no longer integers. The main difference between the two cases appears in the polarization energy of the moving negative ion. The change in this energy is derived principally from a decrease in the Coulombic field effective in polarizing the negative ion, since the dipole field is not appreciably altered. The net effect is an increase in the polarization energy and a corresponding increase in the activation energy. The asymmetry of the configuration under consideration tends to enhance this effect. As in the case of the rigid lattice, only nearest neighbors were taken into account in calculating

TABLE VI. Total energy change in the distorted lattice.

	Energies in electron volts				
y'/x'	0.40	0.45	0.50	0.55	0.60
0.25	0.577*				
0.30	0.5455	0.690*	0.8407		
0.35	0.570*	0.672*	0.792*		
0.40	0.6595	0.690*	0.7560	0.890*	1.0811
0.45		0.695*	0.725*	0.832*	
0.50	0.8630	0.719*	0.7264	0.805*	0.9856
0.55		0.820*	0.790*	0.815*	
0.60				0.850*	0.9033

* Interpolations from x' and y' plots of $\Delta E_{\text{electrostatic}}$ and $\Delta E_{\text{repulsive}}$.

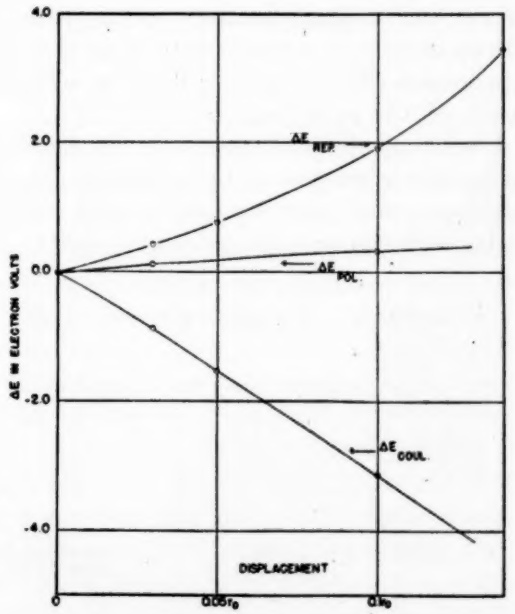

FIG. 6. Energy changes as a function of ion displacement around a pair of vacancies.

the change in polarization energy of the negative ion.

The total energy changes are summarized in Table VI. The starred values are interpolated quantities determined from plots of the electrostatic and repulsive energies *versus* x' and y'. Interpolation along the (0 1 0) to (1 0 0) diagonal from (0.45 0.55 0) to (0.55 0.45 0) fixes the position and energy of the saddle point. A value of 0.710 ev was obtained for the activation energy at $x'=0.507$, $y'=0.493$. The asymmetry of the configuration is clearly shown by the total energy values (compare, for example, (0.4 0.4 0) with (0.6 0.6 0)). The energy change near the saddle point may be too high by 0.1 ev or more because of this effect.

The second-order energy terms can be estimated by procedures analogous to the ones used in the case of the rigid lattice. The polarization energy contribution of the next nearest neighbors will be about the same since these ions are not displaced. This amounts to a lowering of the activation energy by about 0.12 ev.

Since the positive ion at (0 1 0) is now further away than in the rigid lattice, the dipole-dipole interaction will be somewhat less. The lowering of the dipole-dipole contribution is estimated to be

$$\Delta E=0.12\pm0.06 \text{ ev}.$$

Hence, the activation energy is decreased by 0.18 ev or more as a result of these second-order polarization effects. This leads to an activation energy of 0.53 ev or less.

A brief calculation showed the van der Waals energy contributions to be negligible. Nearest neighbors only were considered and the following equation and constants were used:[6]

$$E_{\text{v.d.w.}}=-C/r^6,$$
$$C=6.5952C_{+-}+1.8067((C_{++}+C_{--})/2);$$

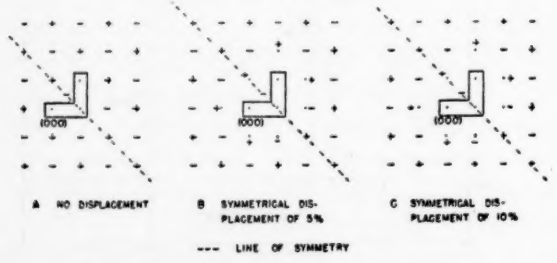

FIG. 7. Ion displacements around saddle-point configuration.

for KCl:

$$C_{++}=24.3\times10^{-60} \text{ erg cm}^{-6},$$
$$C_{+-}=48.0\times10^{-60} \text{ erg cm}^{-6},$$
$$C_{--}=124.5\times10^{-60} \text{ erg cm}^{-6},$$
$$r_0=3.137\times10^{-8} \text{ cm}.$$

The change in van der Waals energy was computed for the distorted lattice with the moving negative ion at the (0.5 0.5 0) position. A value of 0.014 ev was obtained, which is negligible in comparison with the other energy terms.

2. Effect of Change in Distortion at the Saddle Point

It was pointed out in the last section that considerable errors are introduced by disregarding the change that occurs in distortion during the diffusion process. The magnitude of this effect can be estimated near the saddle point. As the negative ion approaches the saddle point the ions redistribute themselves in a symmetrical manner, as was shown in Fig. 5B. The problem is to calculate the energy changes arising from the changing configuration.

To render the calculation feasible in practice it was assumed again that all the ions are displaced the same distance from their lattice sites. The calculations were carried out for three relatively simple configurations from which the distortion of minimum energy could be obtained by interpolation. The diffusing negative ion was assumed to be at (0.5 0.5 0) which is very close to the saddle point. The configurations are shown in Fig. 7. It should be emphasized that ions immediately adjacent to the vacancies in the z direction, as well as those shown, are displaced. States A and C represent the two extremes. In Case A the distortion is zero, whereas in Case C the distortional displacement is 10 percent and the configuration is symmetrical. In the first case all the ions originally displaced around the pair of vacancies (Fig. 5A) are moved in to their lattice positions. In the second case the ions around (0 0 0) are moved outward 10 percent to create a symmetrical configuration. The actual ionic displacement lies between these two extremes (subject to the assumption that all ions are displaced the same distance). The energies of these three configurations were calculated relative to the energy of the simply distorted

lattice considered previously. The configuration of minimum energy was then determined by interpolation.

The calculations are entirely analogous to those made in determining the equilibrium distortion around a pair of vacancies except that more ions are moved. In determining the repulsive energies only nearest neighbors of the displaced ions were taken into account. In calculating the polarization energies the change in the polarization of the moving negative ion was calculated in each case. The change in the polarization energy of the surrounding ions, which is small compared to the polarization of the moving negative ion, was estimated from existing data for states A and C and was interpolated for state B. The following energy changes were obtained:

	No displacement Fig. 7A	5% displacement Fig. 7B	10% displacement Fig. 7C
ΔE_C	1.9630 ev	0.4681 ev	−0.6019 ev
ΔE_R	−0.7260	−0.4470	0.4050
ΔE_P	−0.8717	−0.1747	0.2674
ΔE_{Total}	0.3653 ev	−0.1536 ev	0.0705 ev

If the various energy changes are plotted against the displacement and the total energy *vs.* displacement curve is constructed, a minimum is obtained at a displacement of 4.8 percent. The lowering of activation energy arising from this redistribution of the ions is 0.155 ev. Dipole-dipole interactions were neglected in these calculations. This effect would be very small; moreover, it would tend to lower the activation energy.

On the basis of these calculations the best estimate of the activation energy for the jump of the negative ion in the distorted lattice is 0.375 ev. The activation energy is made up as found in Table VII.

TABLE VII. Final composition of terms determining the activation energy for diffusion. (Energies in electron volts.)

Coulombic energy changes, ΔE_C	= +1.330 ev
Change in polarization energy (of moving negative ion+nearest neighbors around vacancies), ΔE_P	= −0.730
Repulsive energy changes, ΔE_R	= +0.110
Second-order polarization terms	= −0.120
Energy change arising from change in distortion around vacancies	= −0.155
Dipole-dipole interaction energy	= −0.060
Total energy change, ΔE_{Total}	+0.375 ev

DISCUSSION

It was shown in the previous sections that the activation energy for diffusion in the rigid lattice is 0.20 ev and in the distorted lattice it is 0.375 ev. In evaluating the contribution of second-order effects the estimates for both of these cases were made on the high side. It is recognized that the distorted lattice configurations treated here are somewhat idealized. The lattice distortion around a pair of vacancies and around the saddle-point configuration is undoubtedly more complex than assumed in this work. Any change in activation energy arising from a different distribution of ionic displacements would, however, be small. Moreover, since such a state would be of lower energy, the change would occur in the direction of lower activation energy. Thus, any second-order or distortion effect not sufficiently taken into account would lower the activation energy of 0.375 ev given above.

Our inaccurate knowledge of repulsive potentials is probably the most important source of error in this calculation. The agreement between the calculated and measured total energies for alkali halides is within about 2 percent. If all of this error is due to the repulsive terms, an inaccuracy of six percent in the activation energy can be expected from this source. Van der Waals type of interaction is unlikely to introduce an error larger than two to three percent. Thus, the activation energy may be higher by about ten percent (0.04 ev). On the other hand, all the second-order effects were estimated in such a way as to yield an activation energy on the high side, and the true energy may easily be lower by 0.1 ev or about 25 percent. Our estimate of the error in activation energy is, therefore, +10 percent and −25 percent. It must be admitted, however, that the value of ρ assumed in $\phi_{\text{repulsive}}$ may well vary with distance for such large displacement of ions. At our present state of knowledge there is no way of estimating this effect.

Although these results cannot be compared closely with the work of Mott and Littleton on

the diffusion of single vacancies in sodium chloride, the lower activation energy we have obtained for pairs of vacancies in contrast to their value for single vacancies (0.38 compared to 0.56 ev) shows that the migration of neutral pairs of vacancies may well be the preferred diffusion process when pairs are available. Mott and Littleton's value of 0.51 ev for the diffusion of the positive vacancies is to be compared with experimental activation energies of 0.8 to 0.9 ev. All details of Mott and Littleton's work have not been published and, therefore, the relative magnitude of the various energy terms is not available, but the investigators state that in their opinion the discrepancy is probably caused by the repulsive terms. It is unlikely that an error of such magnitude would be involved in the case of the combined vacancies considered here since the repulsive energy contributions amount only to 0.110 ev.

It will be recalled that the activation energy for the diffusion of the effective agent was estimated to be 0.5 ev or less from experimental studies of the darkening of alkali halide crystals by x-rays. Thus, as far as the experimental evidence is concerned, diffusion by means of neutral combined pairs of vacancies is supported rather than prohibited by these calculations.

SUMMARY

1. The activation energy for the diffusion of neutral combined pairs of positive- and negative-ion vacancies in potassium chloride has been calculated. The main energy contributions are due to Coulombic, repulsive, and polarization energy changes. The main contribution to the polarization part of the activation energy comes from the polarization of the diffusing negative ion. Second-order energy terms, such as polarization of next nearest neighbors, dipole-dipole interactions, and contributions caused by changes in the distortion of the lattice during diffusion have been estimated.

2. Calculations for the rigid KCl lattice show that in this case, when the ions are not allowed to move away from their mean lattice positions, the theoretical activation energy for diffusion is 0.20 ev.

3. In an actual crystal there is a ten percent lattice distortion around a neutral pair of vacancies. The distortion changes continuously during diffusion. The activation energy was calculated in two steps. The position and energy of the saddle point were determined in a lattice with fixed distortion (10 percent), then the lowering in activation energy at the saddle point, resulting from the redistribution of ionic displacements was calculated. An activation energy of 0.375 ev was obtained for diffusion in the distorted KCl lattice. The estimated error in this energy value is +10 percent and −25 percent. The activation energy is made up as follows:

$$\begin{aligned}
\Delta E_{\text{Coul.}} &= +1.330 \text{ ev}, \\
\Delta E_{\text{Pol.}} &= -0.730 \text{ ev}, \\
\Delta E_{\text{Rep.}} &= +0.110 \text{ ev}, \\
\Delta E_{\text{Second-order terms}} &= -0.335 \text{ ev}, \\
\Delta E_{\text{Total}} &= +0.375 \text{ ev}.
\end{aligned}$$

4. Comparison of these results with the work of Mott and Littleton on the diffusion of single vacancies in NaCl shows that the migration of neutral combined pairs of positive- and negative-ion vacancies may be the predominant process when pairs of vacancies are present in appreciable numbers.

5. Experimental evidence from heavy darkening of alkali halide crystals with x-rays indicates that the activation energy for diffusion should be 0.5 ev or less. As far as the experimental evidence is concerned, diffusion by means of neutral combined pairs of vacancies is supported rather than prohibited by the theoretical results.

ACKNOWLEDGMENT

The author is indebted to Professor Frederick Seitz and J. S. Koehler for suggesting this problem and for many helpful suggestions and stimulating discussions.

Letters to the Editor

THIS section will accept reports of new work, provided these are terse and contain few figures, and especially few halftone cuts. The Editorial Board will not hold itself responsible for opinions expressed by the correspondents. Contributions to this section should not exceed 600 words in length and must reach the office of the Managing Editor not later than the first of the month preceding that of the issue in which the letter is to appear. No proof will be sent to the authors. The usual publication charge ($4.00 per page) will not be made and no reprints will be furnished free.

Oriented X-Ray Diffraction Patterns Produced by Hydrous Liquid Crystals

S. S. MARSDEN, JR. AND J. W. MCBAIN
Stanford University, Stanford University, California
April 20, 1948

IN the course of an investigation of the fine structure of hydrous fibrous liquid crystals, we have been able to obtain some x-ray photographs having a relatively high degree of symmetry. These patterns were obtained from samples of the "middle soap" phase of the system dodecyl sulfonic acid-water which had been oriented by a special thermal "annealing" process, essentially as follows:

A sample of the system is sealed in a thin-walled Pyrex glass capillary by a method previously described;[1] the capillary, in turn, is sealed in a glass tube which also contains a small amount of water (to prevent the capillary from bursting in the following step). The entire ensemble is then heated in an air thermostat to a temperature at which the system is an isotropic solution according to the phase diagram of M. J. Vold.[2] It is then allowed to cool slowly so that the fibrous liquid crystalline phase is reformed under conditions which allow relatively large, uniformly oriented masses to be established.

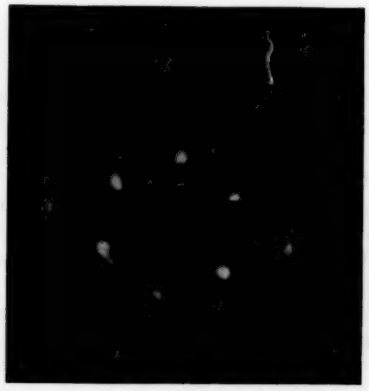

FIG. 1. 36.5 percent dodecyl sulfonic acid in water. "Middle soap" or hydrous fibrous liquid crystalline phase.

When the capillary was removed from the glass tube and viewed in the dark field of a polarizing microscope, most of the sample gave highly colored patterns, but small portions were observed to be light grey and uniform in texture. When these portions were photographed in an experimental set-up similar to that previously described,[1] they gave x-ray patterns similar to Fig. 1. The innermost set of six "spots" correspond to a Bragg spacing of 45.9A, the next to 26.4A, and the outer set to 23.0A; these are in the ratio of $1:\sqrt{3}:\sqrt{4}$, which is the requisite condition for the two dimensional hexagonal arrangement of particles, previously found by Bernal and Fankuchen[3] for certain aqueous systems of tobacco mosaic virus, and postulated by the authors for the middle soap phase of the system dodecyl sulfonic acid-water.[4]

A great similarity between the above photograph and the *electron* diffraction photographs of monomolecular films of soaps and fatty acids[5,6] is evident, both with respect to the number of spots and their orientation relative to each other. In the monomolecular films the long molecules are arranged laterally in a two-dimensional hexagonal lattice; in the hydrous fibrous liquid crystal it is believed that long soap fibers are arranged hexagonally with respect to each other, with water or an "ionic atmosphere" in between these fibers.

It may be pointed out that oriented samples of the "superneat" or non-expanding lamellar phase of this same system give an entirely different sort of x-ray pattern, as illustrated in Fig. 2 (96.0 percent dodecyl sulfonic acid in water). The Bragg spacings are in the ratio of $1:\sqrt{4}$, and the "maxima of intensity" (rather than spots) are oriented perpendicular to the axis of the capillary, indicating that the lamellar colloidal particles are oriented parallel to the long axis of the capillary.

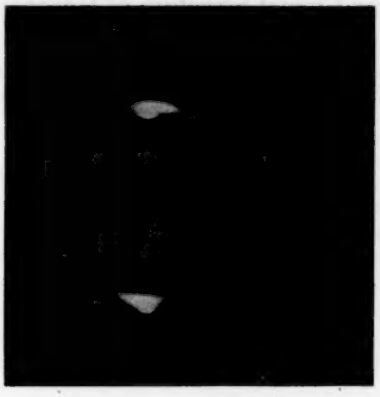

FIG. 2. 96.0 percent dodecyl sulfonic acid in water. "Superneat" or hydrous lamellar liquid crystalline phase.

[1] S. S. Marsden and J. W. McBain, J. Phys. and Coll. Chem. **52**, 110 (1948).
[2] M. J. Void, J. Am. Chem. Soc. **63**, 1427 (1941).
[3] J. D. Bernal and I. Fankuchen, J. Gen. Physiol. **25**, 111 (1941).
[4] S. S. Marsden and J. W. McBain, J. Am. Chem. Soc. (in press).
[5] E. Havinga and J. De Wael, Rec. Trav. Chim. **56**, 375 (1937).
[6] L. H. Germer, J. App. Phys. **9**, 146 (1938).

The Crystal Structure of Hexagonal Barium Titanate[1]

HOWARD T. EVANS, JR. AND ROBINSON D. BURBANK
Laboratory for Insulation Research, Massachusetts Institute of Technology, Cambridge, Massachusetts
April 15, 1948

TWO modifications of barium titanate have been described by Blattner, Matthias, and Merz[2] from studies on single crystals. The well-known cubic form (tetragonal and ferroelectric below the Curie point at 120°C) has the perovskite structure. We have now studied single crystals of the hexagonal form by x-ray diffraction and derived its structure. The results show that the two structures differ only in the manner of close-packed stacking of BaO_3 layers of atoms.

A series of Buerger precession photographs gave the following data for the hexagonal crystals.

Crystal class: hexagonal, 6/mmm
Cell dimensions: $a_0 = 5.735$A, $c_0 = 14.05$A
Space groups: $C6_3/mmc = D_{6h}^4$
Cell content: 6 formulas $BaTiO_3$.

The photographs show many systematic absences of reflections characteristic of the structure so that the space group is not immediately evident. The structure was therefore investigated on the basis of lattice and cell dimensions, exclusive of details of symmetry. There is a very close relationship between these dimensions and those of the cubic form, with a cube edge $a_{cub} = 4.02$A. The hexagonal cell fits almost exactly into the cubic lattice; thus, $a_{hex} = \sqrt{2}a_{cub}$; $c_{hex} = 2\sqrt{3}a_{cub}$. This means that the hexagonal structure must consist of close-packed BaO_3 layers of atoms as found in the cubic form lying parallel to the (111) planes. The structure problem, therefore, is one of finding all the possible ways of stacking these close-packed layers to give a six-layer repeat unit.[3]

There are only five such structures with a repeat unit of six layers or less. Using the conventional symbols *A*, *B*, and *C* to locate close-packed layers with respect to one another, these structures are: (I) *AB*, (II) *ABC*, (III) *ABCACB*, (IV) *ABCBCB*, and (V) *ABCB*. The titanium atoms will be located in the oxygen octahedral holes between the layers. The zero level *c* axis photograph shows that the reflections $(hk \cdot 0)$ occur only when $h - k = 3n$. This can only be true if there is an equal number of layers *A*, *B*, and *C* within the cell. Thus, structures I, IV, and V are ruled out. Structure II is cubic close-packed and corresponds to the perovskite structure of the cubic barium titanate. Therefore, the only structure remaining for the hexagonal form is structure III. The parameters for this structure give good agreement between calculated and observed intensities.

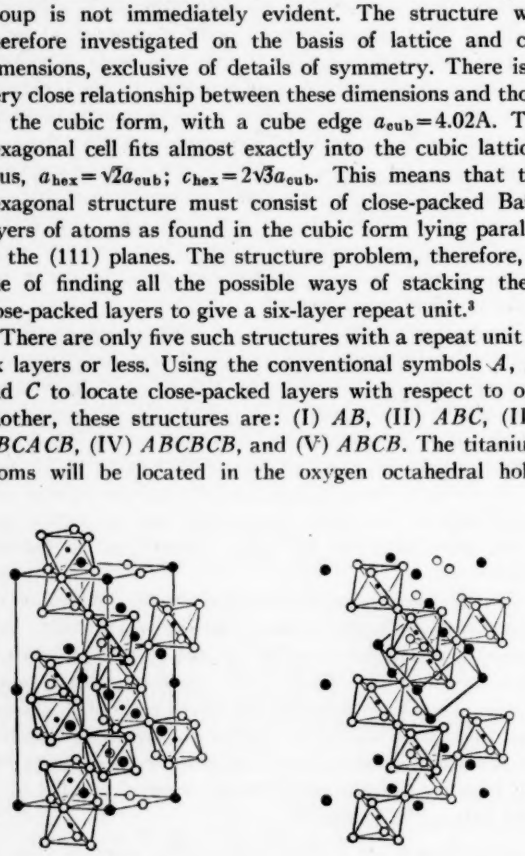

a b

FIG. 1. Barium titanate crystal structure: (a) hexagonal form; (b) cubic form. Large black circles, barium; small black circles, titanium; large open circles, oxygen.

The structures of the cubic and hexagonal forms are shown in Fig. 1. The cubic form contains TiO_6 octahedra linked to neighboring octahedra by corners throughout the structure. The hexagonal structure has the unusual feature of two TiO_6 octahedra sharing a face, forming a Ti_2O_9 group in the structure. The remaining third of the titanium atoms lies in single octahedra, linked by corners to these double groups. The two titanium atoms in the double group are strongly repelled by each other and are separated by about 2.96A (distance between octahedral centers, 2.35A). This Ti–Ti distance is almost identical with that found in rutile.

If these face-shared groups are allowed, there is no reason to suppose that there is not a large number of hexagonal polymorphs of barium titanate. Our crystals were prepared by Dr. B. Matthias from melts containing titanium dioxide, and barium, sodium, and potassium carbonates. Their x-ray powder patterns are identical with that given by Megaw[4] for a "rhombohedral" form. A search is being made for other polymorphs. The detailed investigation of atomic parameters in the hexagonal and other polymorphs of barium titanate will be reported in a later paper.

[1] This work is sponsored jointly by the Office of Naval Research and the Army Signal Corps, on Contract N5ori-78, T.O. 1.
[2] H. Blattner, B. Matthias, and W. Merz, Helv. Phys. Acta **20**, 225 (1947).
[3] This same problem was solved recently be Wells for the structure of $CsCuCl_3$: A. F. Wells, J. Chem. Soc. 1662 (1947).
[4] H. D. Megaw, Proc. Phys. Soc. **58**, 133 (1946).

On the Mercury Photo-Sensitized Reactions of Ethylene*

G. A. ALLEN AND H. E. GUNNING
Department of Chemistry, University of Rochester, Rochester, New York
April 22, 1948

IN order to determine quantum yields for certain mercury photo-sensitized reactions which were being investigated, the authors attempted to measure the intensity of the mercury resonance line, λ2537, entering their reaction cells by making use of the mercury photo-sensitized reactions of ethylene, for which LeRoy and Steacie[1] had reported the quantum yield of the initial stage as 0.37 at an initial ethylene pressure of 13 mm.

For the initial stage of this reaction, LeRoy and Steacie have proposed the following sequence:

$$C_2H_4 + Hg(^3P_1) \rightarrow C_2H_4^* + Hg(^1S_0),$$
$$C_2H_4^* \rightarrow C_2H_2 + H_2,$$
$$C_2H_4^* + C_2H_4 \rightarrow 2C_2H_4.$$

On the basis of this mechanism, the rate of formation of acetylene, the rate of formation of hydrogen, and the rate of pressure increase are all equal, in agreement with LeRoy and Steacie's data.

In the authors' first set of five runs, the ratio of the rate of formation of hydrogen to the rate of pressure increase, averaged over the five runs, was found to be 1.29 ± 0.01. The rate of pressure increase was determined from pressure measurements made with a McLead gauge. The hydrogen was determined by oxidation over oxide. Acetylene was not determined.

The second set of runs was carried out using a Hanovia Sc 2537 mercury resonance lamp. The incident intensity was varied over the range from 0.51×10^{-5} to 1.70×10^{-5} Einsteins per minute, as determined by uranyl oxalate actinometry,[2] by interposing oxidized bronze screens between the lamp and the cell. The pressure increase was measured to 0.01 mm by means of an automatic differential manometer of modified Pearson design.[3] Hydrogen was determined simply as the gas non-condensable over liquid nitrogen, appropriate corrections being made. Acetylene was determined by the method of Ross and Trumbull.[4] The average ratio, for six runs, of the rate of hydrogen formation to the rate of acetylene formation was 1.02, while the average ratio of the rate of hydrogen formation to the rate of pressure increase was 1.36. The quantum yield of hydrogen formation was 0.25.

All runs were carried out at an initial ethylene pressure of 13 mm. In all the experiments, the graph of pressure increase against time was linear, indicating that the data obtained referred only to the initial stage of the reaction.

The data given above indicate that in the authors' experiments, some pressure-reducing reaction, such as dimerization or polymerization, was present even in the initial stage of the reaction. The discrepancies between these data and those of LeRoy and Steacie may be due to differences in the characteristics of the lamps used, such as line breadth. Unpublished data from this laboratory suggest that for at least one substance the curve of initial rate of reaction against initial pressure of reactant was shifted and altered when one resonance lamp was substituted for another. Further work on the mercury photosensitized reactions of ethylene is under way in these laboratories in order to attempt to resolve the discrepancies reported.

* This work was supported by Contract N6onr-241, Task I, with the Office of Naval Research, United States Navy.

[1] D. J. LeRoy and E. W. R. Steacie, J. Chem. Phys. **9**, 829 (1941).
[2] G. S. Forbes and L. J. Heidt, J. Am. Chem. Soc. **56**, 2363 (1934).
[3] D. J. LeRoy, Ind. Eng. Chem. **17**, 652 (1945).
[4] W. H. Ross and H. L. Trumbull, J. Am. Chem. Soc. **41**, 1180 (1919).

Concentration of N^{15} in a Gaseous Exchange Column

T. I. Taylor and William Spindel
Department of Chemistry, Columbia University, New York, New York
April 7, 1948

In a previous communication[1] from this laboratory a concentration of C^{13} was reported using the reaction $C^{13}O + C^{12}O_2 \rightleftarrows C^{12}O + C^{13}O_2$ in a gaseous exchange column.

TABLE I. Pressure = 0.5 atmos. Filament temp. = 500°C (approx.).

Time (days)	Over-all separation	Time (days)	Over-all separation
0.33	1.48 ± .05	6.0	3.00 ± .10
0.90	1.93 ± .06	7.0	2.79 ± .10
2.0	2.18 ± .06	7.5	3.00 ± .10
4.9	2.90 ± .10	8.0	3.10 ± .10
5.2	2.78 ± .10	12.0	3.14 ± .10
Equilibrium over-all separation = 3.00 ± .10			

Using the exchange reaction[2] $N^{15}O + N^{14}O_2 \rightleftarrows N^{14}O + N^{15}O_2$ in an apparatus similar to that already described, enrichment of N^{15} has been effected. The exchange was first suggested by Urey[3] as a possibility for the concentration of isotopic nitrogen, and experiments by Leifer showed the rate of the exchange to be very rapid even at low temperatures. Calculations of the equilibrium constant using the spectroscopic data given by Leifer and the method of Bigeleisen and Mayer[4] gave values of 1.0146 at 200°C, 1.0075 at 400°C, and 1.0044 at 600°C.

The column constructed was 0.9 cm i.d. and 200 cm long. For the hot element a 0.64-mm Pt filament was used. NO_2 was circulated across the top from a 40-liter reservoir. The condition of reflux was satisfied by utilizing the reversible equilibrium $NO_2 \rightleftarrows NO + \frac{1}{2}O_2$.[5] With the wire temperature maintained at 500°C at a pressure of 0.5 atmos., an equimolar mixture of NO and NO_2 exists in the hot zone while recombination at the cold wall yields relatively pure NO_2. Since N^{15} preferentially concentrates in the NO_2 it is transported to the bottom by convective action in the cold stream. At the bottom of the column enriched NO_2 re-enters the rising hot stream where it is again dissociated into NO which undergoes further exchange with the descending stream of NO_2. In the cool region above the filament recombination of NO and O_2 occurs, yielding NO_2. Essentially, therefore, the gas in the system consists only of NO_2 except in the hot region where the decomposition into NO and O_2 is significant. The gases NO and NO_2 are readily interconvertible by a change in temperature. Thus a chemical converter which was necessary for the CO–CO_2 exchange is not required for the nitrogen exchange.

The data for an experiment at 0.5 atmos. is summarized in Table I. The isotopic abundances were measured to ±1.5 percent with a Nier type mass spectrometer. The NO_2 was reduced to N_2 by Fe powder at 400°C before isotopic analyses were made. The over-all separations shown in the table represent the ratio of the N^{15} abundance at the bottom of the column to that at the top.

Experiments at 0.25 atmos. and 1.0 atmos. gave values of 2.70 and 1.72, respectively, for the equilibrium separation. Calculation from the experiment at 0.5 atmos. gives a value of 1.1 cm for the H.E.T.P. using 1.006 for the equilibrium constant at 500°C.

Further study of this separation process is in progress.

[1] T. I. Taylor and R. B. Bernstein, J. Am. Chem. Soc. **69**, 2076 (1947).
[2] E. Leifer, J. Chem. Phys. **8**, 301 (1940).
[3] H. C. Urey and L. J. Greiff, J. Am. Chem. Soc. **57**, 321 (1935).
[4] J. Bigeleisen and M. G. Mayer, J. Chem. Phys. **15**, 261 (1947).
[5] D. M. Yost and H. Russell, *Systematic Inorganic Chemistry* (Prentice-Hall Inc., New York, 1944), p. 29.

The Electroviscous Effect with Measurements on Sodium Polymethacrylate Solutions

A. H. W. Aten, Jr.*
Institute for Nuclear Research, Oosterringdijk 18, Amsterdam, Holland
April 13, 1948

CERTAIN solutions of negative colloids, like agar,[1] gum arabic,[2] and starch,[3] show a very high viscosity, which is lowered greatly by the addition of electrolyte. This was discovered by Kruyt and Bungenberg de Jong. The authors explained this phenomenon by assuming rigid particles, surrounded by a double layer which influences the viscosity, according to calculations by Smoluchowski. It has often been said, however, that the observed changes are much larger than can be accounted for by this theory. Therefore, an alternative explanation may be suggested.

If a long chain molecule is dissolved in a medium by which it is not repelled, it will extend through an average volume of solvent which depends on the length and on the structure of the chain. If a number of negative charges are attached to this chain at regular intervals, the different parts of the chain will repel each other and the molecule will expand through a larger volume of liquid. This amounts to a swelling of the colloid particles. If an electrolyte is now added to the solution of this polymer, each negative charge on the chain will surround itself by a positive ion sphere, which lowers the electrostatic repulsion. This causes the particles to shrink again, but in no case to quite the same size as the uncharged molecule would have.

From these considerations the following facts are to be expected, if we take into account the fact that in a colloidal solution containing a certain number of particles, the viscosity increases with the volume pervaded by each particle.

1. Addition of electrolytes to a solution of a (negative) linear polymer causes a rapid decrease of the viscosity in the concentration range where the "radius" of the ion sphere is of the same order of magnitude as the distance between the nearest charges on the chain which can move fairly independently.

2. The efficiency of different salts in lowering the viscosity increases rapidly with the charge of the positive ions. The charge of the negative ions is without influence.

3. Even at high electrolyte concentrations the viscosity of the negative colloid is higher than that of the same polymer in the uncharged condition.

Table I. Viscosity of polymethacrylate and of polymethacrylic acid solutions (25°).

Polymethacrylic acid gram/liter	NaOH mole/liter	Added electrolyte mole/liter	$\eta/\eta H_2O$
0.320	0	0	1.009
0.340	0.00328	0	1.43
0.340	0.00328	0.00691 NaCl	1.123
0.340	0.00328	0.0345 NaCl	1.069
0.340	0.00328	0.173 NaCl	1.051
0.340	0.00328	0.00169 $MgSO_4$	1.139
0.340	0.00164	0	1.362
0.340	0.00164	0.00691 NaCl	1.097
0.340	0.00082	0	1.060
9.18	0.0886	0	4.523
4.59	0.0443	0	3.230
1.53	0.0148	0	2.135
0.510	0.00492	0	1.550
0.170	0.00164	0	1.243
0.0567	0.000547	0	1.087
0.0189	0.000182	0	1.016

These conclusions are in general agreement with the observations of Kruyt, Bungenberg de Jong, and their collaborators. However, it seemed desirable to check them with a polymer, the linear character of which was beyond doubt. Aqueous solutions of polymethacrylic acid and its sodium salt behave entirely as predicted (Table I).

In normal colloids $\eta/\eta H_2O-1$ is either approximately proportional to the concentration, or increases even more steeply. Table I shows that for sodium polymethacrylate the opposite is true, except at the very lowest concentrations. From our model this is easily understood. The increase of the number of Na^+ ions with increasing polymer concentration causes the colloid particles to shrink. In solutions of undissociated polymethacrylic acid, on the other hand, $\eta/\eta H_2O-1$ was found proportional to the concentration with a very satisfactory accuracy. Addition of NaCl did not affect the viscosity of these solutions.

It may be pointed out that in Staudinger's laboratory Kern and others observed a similar behavior in the case of sodium polyacrylate.[4] They found the behavior of polyacrylic acid itself entirely different from the results of our measurements on polymethacrylic acid.

I am deeply obliged to Mr. F. Langford, A.E.B., Plastics Division Research Manager, I.C.I., Welwyn Garden City, England.

[1] H. R. Kruyt and H. G. Bungenberg de Jong, Zeits. f. physik. Chemie **100**, 250 (1922).
[2] H. R. Kruyt and H. J. C. Tendeloo, Koll. Beih. **29**, 396 (1929).
[3] H. G. Bungenberg de Jong, Rec. **43**, 189 (1924). Kindly provided by Mr. F. Langford, Plastics Division Research Manager, I.C.I., Welwyn Garden City, England.
[4] H. Staudinger and H. W. Kohlschütter, Ber. **64**, 2091 (1931); H. Staudinger and E. Trommsdorff, Lieb. Ann. **502**, 201 (1933); W. Kern, Zeits. f. physik. Chemie A. **181**, 283 (1938).

A Note on Gaseous Thermal Diffusion: The Effect of a Third Component*

John Chipman and Minu N. Dastur
Department of Metallurgy, Massachusetts Institute of Technology, Cambridge, Massachusetts

IN his study of the kinetic theory of gases, Chapman[1] showed that a temperature gradient in a mixture of two gases results in establishment of a concentration gradient. His mathematical theory of thermal diffusion is based upon considerations of intermolecular force fields and upon relative molecular weights and diameters. More recently Gillespie[2] developed a simple theory of thermal diffusion based on elementary kinetic considerations. His treatment does not account for the dependence of the effect on the size of the molecules and their mutual forces, but is based solely on molecular weight which is the variable of major importance.

On the basis of his simplified treatment, Gillespie was able to show that in a mixture of any number of gases the

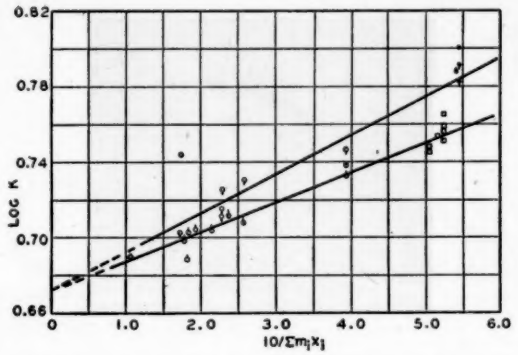

FIG. 1. Logarithm of the apparent equilibrium constant $p_{H_2O}/(p_{H_2} \times \%O)$ as a function of reciprocal mean root-molecular weight of the gaseous mixture.

Added gas	None	Helium	Argon	Mercury
No preheat	●		○	(mean of 7)
Low preheat	❣		○	
High preheat	●	□	○	Δ

relative separation of two gases is given by the equation

$$d \ln(x_1/x_2)/d \ln T = (m_2 - m_1)/(2\Sigma m_i x_i), \qquad (1)$$

where x_1 and x_2 are the mole fractions of the two gases, m_1 and m_2 the square roots of their molecular weights, and the summation is over all species present. According to this equation, the relative separation of two gases by thermal diffusion is inversely proportional to the mean root-molecular weight of the mixture, and it was therefore suggested that thermal separation of isotopes might be aided by addition of a third gas of low molecular weight.

An opportunity recently presented itself for testing the validity of this equation with respect to the addition of an inert gas to a mixture of water vapor and hydrogen in a thermal gradient at high temperatures. In an experimental study of equilibrium in the reaction of hydrogen with oxygen dissolved in molten iron, a controlled mixture of hydrogen and water vapor impinges upon the surface of the molten metal which is heated and also stirred by high frequency induction. It was shown some years ago[3] that under these conditions thermal diffusion occurs in the gas mixture near the hot metal surface, the result being a lower oxygen content of the metal than that which would correspond to equilibrium with the entrant gas. It was shown that strong preheating of the gas diminished the error due to thermal diffusion but whether or not the error was completely eliminated has remained undetermined. Equation (1) suggests the admixture of inert gas of high molecular weight as a means of minimizing thermal separation, and the results of such a study offer qualitative support for the validity of the equation.

It has been established[4] that the activity of oxygen in the melt is proportional to its percent by weight. It is therefore permissible to use the percentage of oxygen in the equilibrium constant as follows.

$$H_2(g) + O(\text{in Fe}) = H_2O(g); \quad K = p_{H_2O}/p_{H_2} \cdot \%O. \qquad (2)$$

Experiments were conducted at substantially constant steam-hydrogen ratios, the metal being held at 1563°C about twice as long as actually required to establish equilibrium. The oxygen content of the metal fell in the range 0.03–0.04 percent which is high enough for good analytical accuracy and low enough to avoid formation of a non-metallic phase.

The results are shown in Fig. 1 in which the logarithm of the apparent K is plotted against the reciprocal of the mean square root of the molecular weight of the gaseous mixture. The results fall into two groups with respect to intensity of preheating of the gas and include three early results without preheat. Previous results are confirmed in that preheating decreases the apparent value of K. Much more striking, however, is the effect of adding purified argon to the gas mixture. This decreased the apparent K by an amount proportional to the reciprocal of the mean root molecular weight. Addition of helium gave results approximately the same as those without admixture. In one series mercury vapor was added and here the apparent K was the lowest observed. Straight lines may be drawn through the two groups corresponding to the two degrees of preheat.

Each method of preheating was sufficiently reproducible to establish a constant temperature pattern within the apparatus. Thus $\int d \ln T$ of Eq. (1) was essentially constant for each condition. Figure 1 shows that under such circumstances $\int d \ln(x_{H_2O}/x_{H_2})$ is inversely proportional to $\Sigma m_i x_i$ as required by the equation. The constant of proportionality cannot be evaluated from the results but with this reservation these experiments confirm Gillespie's equations of thermal diffusion.

* This work was supported in part by the Office of Naval Research under Contract No. N5ori-78, Task Order XVI.

[1] S. Chapman, Phil. Trans. (London) **A217**, 115 (1917).
[2] L. J. Gillespie, J. Chem. Phys. **7**, 438(1), 530 (1939).
[3] J. Chipman and M. G. Fontana, J. Am. Chem. Soc. **56**, 2011 (1934).
[4] M. G. Fontana and J. Chipman, Trans. Am. Soc. Metals **24**, 313 (1936).

Erratum: The C—H Bond Energy in Toluene and the Xylenes

[J. Chem. Phys. **16**, 128 (1948)]

M. SZWARC
Department of Chemistry, The University of Manchester, Manchester, England

THE end of the sentence at the foot of p. 135 in the above letter should be amended as follows: Delete the word "xylene" and substitute "xylyl radical." The sentence should now read: ". . . hyperconjugation occurring for example in para xylyl radical as follows:

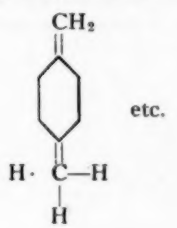

Erratum: Ultraviolet Absorption Spectrum of Hydrogen Peroxide

[J. Chem. Phys. 16, 225 (1948)]

R. B. Holt, C. K. McLane, and O. Oldenberg
Lyman Physical Laboratory, Harvard University, Cambridge, Massachusetts

THROUGH an error a wrong cut was used for Fig. 1 in this article. The following figure should have appeared in place of the one used.

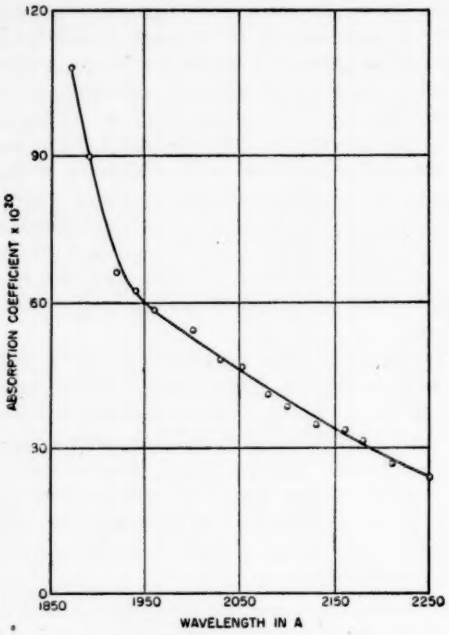

FIG. 1. Absorption coefficient for hydrogen peroxide vapor (average values).

Oscilloscope Scanning of Visible Spectra

W. E. Deal, William Bradshaw, and F. A. Matsen
The University of Texas, Austin, Texas

April 23, 1948

AN infra-red spectrograph with cathode-ray presentation has been developed by Daly and Sutherland and King, Temple, and Thompson.[1] On the vertical deflection system of a long-persistence tube was impressed the amplified output from a bolometer past which an infra-red spectrum was swept by means of a fourteen-second period rotation of the prism. A linear horizontal trace was employed.

In this laboratory the same principle has been applied in the visible region to obtain "instantaneous" spectra.[2] A glass prism was rotated at speeds from 1800 to 3600 r.p.m., the spectrum being detected by a photo-multiplier tube. A shutter attached to the prism table interrupts a beam of light producing a trigger pulse for a driven sweep circuit.

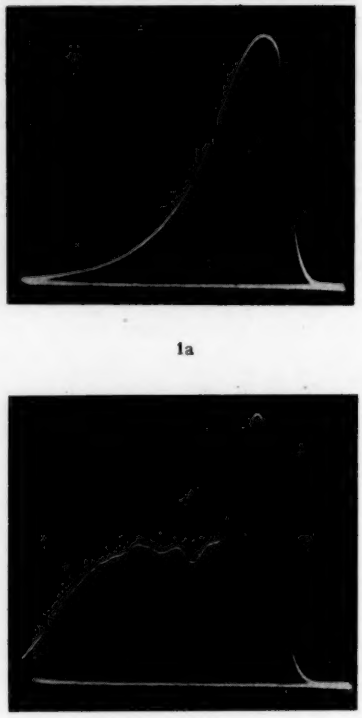

1a

1b

FIG. 1. Oscilloscope Trace: a—Emission spectrum of tungsten bulb; b—Dilute potassium permanganate in path. Gain for b twice that for a.

In Fig. 1a is reproduced the emission spectrum of a tungsten bulb; in Fig. 1b a cell containing dilute potassium permanganate solution has been placed in the optical path. These spectra were photographed from a P-11 phosphor tube with $\frac{1}{10}$-second exposure time on Eastman Super XX film. A movie camera will be used to study spectral sequences in rapid chemical reactions. A complete report will appear elsewhere.

Work is in progress extending the technique to the near infra-red region using photo-conductive detectors and to the ultraviolet using quartz optics.

[1] E. B. Baker and C. D. Robb, Rev. Sci. Inst. **14**, 362 (1943). E. F. Daly and G. B. B. M. Sutherland, Proc. Phys. Soc. (London) **59**, 77 (1947). See also J. King, R. B. Temple, and H. W. Thompson, Nature **158**, 196 (1946).

[2] See R. C. Herman and S. Silverman, J. Opt. Soc. Am. **38**, 209 (1948) for a photographic method involving translation of the spectrographic plate.